

PROBING THE EFFECT OF IKK ON FOXO3: A REGULATORY MECHANISM OF
APOPTOSIS AND AUTOPHAGY IN CHEMORESISTANCE

by
TUGSAN TEZIL

Submitted to Graduate School of Engineering and Natural Sciences
in partial fulfilment of the requirements for the degree of

Doctor of Philosophy

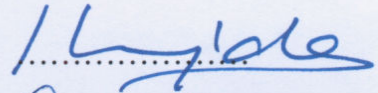
Sabanci University

July 2012

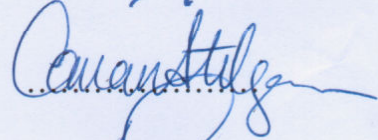
PROBING THE EFFECT OF IKK ON FOXO3: A REGULATORY MECHANISM OF
APOPTOSIS AND AUTOPHAGY IN CHEMORESISTANCE

APPROVED BY:

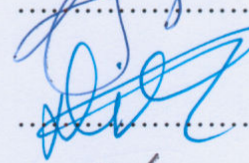
Prof. Dr. Hüveyda BAŞAĞA (Thesis Advisor)



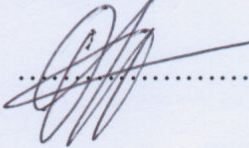
Prof. Dr. Canan ATILGAN



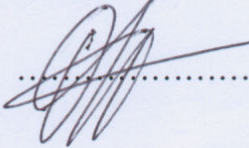
Assoc. Prof. Dr. Devrim GÖZÜAÇIK



Assoc. Prof. Dr. Dilek TELCİ



Assoc. Prof. Dr. Uğur SEZERMAN



DATE OF APPROVAL

26/07/2012

© Tugsan Tezil 2012
All Rights Reserved

PROBING THE EFFECT OF IKK ON FOXO3: A REGULATORY MECHANISM OF
APOPTOSIS AND AUTOPHAGY IN CHEMORESISTANCE

Tugsan Tezil

Ph.D. Thesis, 2012

Thesis supervisor: Prof. Dr. Hüveyda Başağa

Keywords: FOXO3, IKK, apoptosis, autophagy, breast cancer

ABSTRACT

Breast cancer chemotherapeutics are only 50% successful due to chemoresistance mechanism of cancer cells. FOXO3, a tumor suppressor protein, is involved in the regulation of several cell death-related genes; however, the extent of FOXO3 regulation in chemoresistance mechanism is not fully understood.

In this study our aim was to characterize the potential crosstalk between FOXO3 and NF-kappaB pathway with a special focus on IKK-FOXO3 interaction in relation to chemoresistance mechanism. For this purpose, we have used chemoresistant (MDA-MB-231) and chemosensitive (MCF-7) breast cancer cell lines treated with paclitaxel (20nM) or cisplatin (30uM). Administration of 30uM cisplatin induced FOXO3-dependent apoptosis in MCF-7 cells as indicated by RNA interference studies. Following the analysis of NF-kappaB pathway elements by immunoblotting and overexpression studies, we identified the physical interaction between IKK-beta and FOXO3 by co-immunoprecipitation. We have shown that IKK-beta sequesters FOXO3 in the nucleus promoting chemoresistance in MDA-MB-231 cells. Additionally, imbalance between FOXO3 and IKK-beta levels induced autophagy rather than apoptosis in FOXO3 overexpressing MDA-MB-231 cells. We have also studied the effect of p53 on FOXO3 levels and showed p53-dependent FOXO3 inhibition in colorectal cancer cells. This is the first study describing FOXO3 regulation by IKK-beta in detail and showing that FOXO3/IKK-beta ratio may influence the cellular decision of apoptosis or autophagy.

In view of the results obtained, NF-kappaB pathway-FOXO3 crosstalk has been discussed and the interaction between FOXO3 and IKK-beta is proposed as a target for therapeutic intervention.

IKK’NİN FOXO3 ÜZERİNDEKİ ETKİSİNİN ARAŞTIRILMASI: İLAÇ
DİRENCİNDE APOPTOZ VE OTOFAJİ DÜZENLEYİCİ MEKANİZMASI

Tuğsan Tezil

Doktora Tezi, 2012

Tez Danışmanı: Prof. Dr. Hüveyda Başağa

Anahtar Kelimeler: FOXO3, IKK, apoptoz, otofaji, meme kanseri

ÖZET

Kanser hücrelerinin ilaç direnci nedeniyle, meme kanseri tedavisinde kullanılan kemoterapi ilaçları yalnızca %50 başarı sağlamaktadır. Bir tümör baskılayıcı olan FOXO3, bir çok hücre ölümü ile ilişkili genin düzenlenmesinde yer almaktadır, ancak ilaç direncinde FOXO3’ün düzenlenmesi kapsamlı olarak tamamen anlaşılammıştır.

Bu çalışmadaki amacımız, ilaç direnç mekanizmasında IKK-FOXO3 ilişkisini ele alarak FOXO3 ve NF-kappaB arasındaki olası çapraz etkileşimi karakterize etmektir. Bu amaçla, ilaca dirençli (MDA-MB-231) ve hassas (MCF-7) meme kanseri hücre hatlarını 20nM paklitaksel ve 30uM sisplatin kullanarak tanımladık. RNA interferans çalışmalarına göre 30uM sisplatin tatbiki MCF-7 hücrelerinde FOXO3-bağımlı apoptozu tetiklemiştir. NF-kappaB yolak elementlerinin analizini takiben, ko-immünopresipitasyon yöntemiyle IKK-beta ve FOXO3 arasındaki fiziksel etkileşimi tespit etmiş ve IKK-beta’nın FOXO3’ü nükleus’ta tutarak MDA-MB-231 hücrelerinde ilaç direncini desteklediğini belirlemiş bulunmaktayız. Ek olarak, FOXO3 ve IKK-beta seviyeleri arasındaki dengenin bozulması da FOXO3’ün yüksek ifade ettirildiği MDA-MB-231 hücrelerinde apoptoz yerine otofajiyi teşvik etmektedir. Ayrıca p53’ün FOXO3 üzerindeki etkisinin de çalışarak, kolorektal kanser hücrelerinde p53-bağımlı FOXO3 inhibisyonunu göstermiş bulunuyoruz. Bu çalışma, IKK-beta tarafından gerçekleştirilen FOXO3 düzenlenmesini ayrıntılı olarak açıklayan ve FOXO3/IKK-beta oranının hücrenin apoptoz veya otofajiye karar vermesinde etkili olduğunu gösteren ilk çalışmadır.

Elde edilen sonuçlara bağlantılı olarak, NF-kappaB yolağı-FOXO3 çapraz etkileşimi tartışılmış ve ileride yapılması öngörülen çalışmalar sunulmuştur. Yayımlanan güncel veriler ışığında, FOXO3 ve IKK-beta arasındaki etkileşimin terapötik müdahalede hedef olacağı öngörülmektedir.

To my parents

*“Nothing in life is to be feared, it is only to be understood. Now
is the time to understand more, so that we may fear less”*

Maria Skłodowska-Curie

ACKNOWLEDGEMENTS

This dissertation would not have been possible without the guidance and the help of several individuals who in one way or another contributed and extended their valuable assistance in the preparation and completion of this study. It is a pleasure to convey my gratitude to them all in my humble acknowledgment.

First and foremost, my utmost gratitude to Prof. Dr. Hüveyda Başağa whose guidance, sincerity and encouragement I will never forget. Her good advice and support has been invaluable on both an academic and a personal level, for which I am extremely grateful. I gratefully thank Assoc. Prof. Dr. Devrim Gözüaçık, Assoc. Prof. Dr. Uğur Sezerman, Assoc. Prof. Dr. Dilek Telci and Prof. Dr. Canan Atılgan for the constructive comments on this thesis. I am thankful that in the midst of all their activity, they accepted to be members of my thesis jury.

I am also very indebted to Prof. Dr. David Fruman for giving me the opportunity to learn the details of FOXO signaling in his lab.

I would like to acknowledge the support of TÜBİTAK (109S340) and Turkish Association for Cancer Research and Control-Terry Fox Research Fund that provided the necessary financial support for this research. Additionally, I thank Yousef Jameel Scholarship for providing the financial support for my living expenses and tuition fees.

Many thanks go in particular to Dr. Çağrı Bodur and Dr. Özgür Kütük for their advice and their willingness to share their bright thoughts with me, which were very fruitful for shaping up my ideas and research.

I would also acknowledge Emel Durmaz for her patience, encouragement and priceless friendship. Işıl Çevik, for her sincere friendship, useful discussions and help in cloning. Pınar Önal, for being such a good friend even from a distance and making me smile all the time. Günseli Akçapınar, for a wide range of subjects we discussed. Batuhan Yenilmez, for all the coffee breaks. Cem Meydan, for sharing the most recent advances

on the world. Begüm Topçuoğlu, for her guileless friendship and Gözde Korkmaz for her friendship and helpful comments on autophagy.

My former and present lab partners; A. Can Timuçin, Beyza Vuruşaner, Ali F. Kısakürek, Ayça Tekiner, Bahriye Karakaş, Sinem Yılmaz and Gizem Karlı, for creating an enjoyable environment to work. Dr. Damla Arisan, for her desire to teach without expecting anything in return. Nalan Liv, for making the summer work fun. Deniz Saltukoğlu, for being the greatest roommate and a friend who I could discuss everything with. Alper Arslan, for coaching me in lab techniques in the very first year of my Ph.D.

Words fail me to express my appreciation to my parents, the reason of my existence, Sevim and Erdal Tezil whose infinite love and persistent confidence in me have taken the load off my shoulder. Last, but by no means least, I thank my friends in Turkey, Germany, Bulgaria, America and elsewhere for their support and encouragement, as well as expressing my apology that I could not mention personally one by one.

TABLE OF CONTENTS

	Page
1. INTRODUCTION	1
1.1. Cancer	1
1.1.1. Carcinogenesis	2
1.2. Cancer Therapy	4
1.2.1. Cisplatin	4
1.2.2. Paclitaxel	6
1.3. Programmed Cell Death	8
1.3.1. Type-I Cell Death: Apoptosis	8
1.3.1.1. Initiation	9
1.3.1.1.1. Mitochondrial outer membrane permeabilization (MOMP)	10
1.3.1.1.1.1. Mitochondrial permeability transition pore (PTP)	10
1.3.1.1.1.2. Protein Channels and Lipidic Pores	11
1.3.1.1.1.2.1 Bcl-2 family	11
1.3.1.2. Execution and removal of the cell remnants	15
1.3.2. Type-II Cell Death: Autophagy	16
1.3.2.1. Induction	16
1.3.2.2. Autophagosome formation	18
1.3.2.2.1. Ubiquitin-like conjugation system 1	21
1.3.2.2.2. Ubiquitin-like conjugation system 2	21
1.3.2.3. Autophagosome-lysosome fusion and degradation	23
1.4. Diminished Apoptosis/Autophagy in Cancer	23
1.5. NFκB Pathway	24
1.6. Forkhead Family and FOXO3	27
1.7. Aim of the Study	29
2. MATERIALS AND METHODS	31
2.1. Materials	31
2.1.1. Chemicals and media	31
2.1.2. Antibodies and enzymes	31
2.1.3. Molecular biology kits and reagents	31
2.1.4. Vectors	31

2.1.5. Oligonucleotides	32
2.1.6. Buffers and solutions	32
2.1.7. Equipment and computer software	32
2.2. Methods.....	32
2.2.1. Cell lines	32
2.2.2. Cell cycle analysis	32
2.2.3. Cell death, viability and proliferation assays.....	33
2.2.4. Cleaved caspase 3 staining	33
2.2.5. Fluorescent Microscopy.....	33
2.2.6. Transfections.....	34
2.2.7. RNA isolation	34
2.2.8. Semi quantitative and quantitative PCR.....	35
2.2.9. Total protein isolation.....	35
2.2.10. Subcellular protein extraction.....	35
2.2.11. Protein concentration determination.....	36
2.2.12. Immunoblotting	36
2.2.13. Densitometric analysis.....	36
2.2.14. Preparation of radiolabeled oligonucleotides	36
2.2.15. Electrophoretic Mobility Shift Assay (EMSA)	37
2.2.16. Co-immunoprecipitation.....	37
2.2.17. Statistical analysis.....	38
2.2.18. Illustrations	38
3. RESULTS	39
3.1. Effect of Cisplatin or Paclitaxel treatment on cell viability and cell death in MCF-7 and MDA-MB-231 cells	39
3.2. Effect of Cisplatin or Paclitaxel treatment on cell cycle arrest.....	41
3.3. Expression of Bcl-2 Family proteins in response to drug treatments	42
3.4. Transcriptional upregulation of DNA damage protein GADD45 α	45
3.5. Cisplatin induces apoptosis in MCF-7 and MDA-MB-231 cells.....	46
3.6. NF κ B pathway in response to cisplatin	47
3.7. Cisplatin induces nuclear translocation of FOXO3 in MCF-7 but not in MDA-MB-231 cells.....	48

3.8. Transfection of siFOXO3 decreases FOXO3 target gene expression and induces the proliferative activity of MCF-7 cells.....	50
3.9. FOXO3 silencing inhibits cisplatin-induced cell death in MCF-7 cells.....	51
3.10. Overexpression of FOXO3 potentiates cisplatin-induced cell death in MDA-MB-231 cells.....	52
3.11. Overexpression of IKK subunits and their effects on cell proliferation and viability.....	54
3.12. Differential interaction between FOXO3 and IKK β	56
3.13. IKK β sequesters FOXO3 in the cytoplasm.....	57
3.14. Chemical inhibition of IKK allows nuclear translocation of FOXO3 in MDA-MB-231 cells.....	59
3.15. Ser-644 residue on FOXO3 is essential for cisplatin resistance in MDA-MB-231 cells.....	61
3.16. FOXO3 overexpression induces autophagy in MDA-MB-231 cells after cisplatin treatment.....	62
3.17. Functional p53 is involved in sequestering FOXO3 in the cytoplasm.....	65
4. DISCUSSION AND CONCLUSION.....	70
4.1. FOXO3 Stability.....	71
4.2. DNA Damage and p53.....	72
4.3. FOXO3 Expression.....	73
4.4. Hormone Signalling.....	76
4.5. Future Studies.....	77
5. REFERENCES.....	78
APPENDIX A.....	100
APPENDIX B.....	103
APPENDIX C.....	104
APPENDIX D.....	105
APPENDIX E.....	106
APPENDIX F.....	107
APPENDIX G.....	112

TABLE OF FIGURES

	Page
Figure 1. 1. Lung and breast cancer mortality in Turkey and worldwide.....	2
Figure 1. 2. Main stages of carcinogenesis in somatic cells.....	3
Figure 1. 3. The structure of Cisplatin.....	5
Figure 1. 4. Mechanism of Cisplatin action.....	6
Figure 1. 5. The structure of Paclitaxel.....	7
Figure 1. 6. The mechanism of Paclitaxel action.....	8
Figure 1. 7. Dissociation of cytochrome-c following apoptotic stimuli.....	10
Figure 1. 8. Bcl-2 Family members.....	12
Figure 1. 9. Bax and Bak mediated MOMP.....	13
Figure 1. 10. Regulation of Bax and Bak in MOMP.....	14
Figure 1. 11. The execution phase of apoptosis.....	15
Figure 1. 12. Induction step of autophagy.....	18
Figure 1. 13. Autophagosome formation-I.....	19
Figure 1. 14. Autophagosome formation-II.....	20
Figure 1. 15. Ubiquitin-like conjugation systems in autophagy.....	22
Figure 1. 16. LC3-II recruitment and autophagosome formation.....	22
Figure 1. 17. NFκB Pathway.....	25
Figure 1. 18. Structure of FOXO3.....	27
Figure 1. 19. Mechanism of FOXO3 action.....	28
Figure 3. 1. The effect of paclitaxel/cisplatin on cell viability.....	40
Figure 3. 2. The effect of paclitaxel/cisplatin on cell death.....	41
Figure 3. 3. Cell cycle analysis in response to paclitaxel/cisplatin treatment.....	42
Figure 3. 4. The expression of Bcl-2 family members in response to paclitaxel/cisplatin.....	43
Figure 3. 5. Expression of FOXO3 in MCF-7 and MDA-MB-231 cells.....	44
Figure 3. 6. The effect of cisplatin treatment on GADD45α transcription.....	46
Figure 3. 7. Cisplatin-induced apoptosis in MCF-7 and MDA-MB-231 cells.....	47
Figure 3. 8. Effect of cisplatin on NFκB pathway.....	48
Figure 3. 9. Cisplatin-induced translocation of FOXO3.....	49

Figure 3. 10. Cisplatin-induced FOXO3 activation.....	50
Figure 3. 11. Silencing of FOXO3 expression in MCF-7 cells.	51
Figure 3. 12. Apoptotic response in siFOXO3 transfected MCF-7 cells.....	52
Figure 3. 13. Overexpression of FOXO3 in MDA-MB-231 cells..	53
Figure 3. 14. Overexpression of IKK subunits..	54
Figure 3. 15. Effect of IKK overexpression on cell proliferation and viability.....	55
Figure 3. 16. IKK β interacts with FOXO3.	56
Figure 3. 17. IKK β sequesters FOXO3 in the cytoplasm.	57
Figure 3. 18. Sequestering FOXO3 is limited to IKK β level.	58
Figure 3. 19. Inhibition of IKK activates FOXO3.....	60
Figure 3. 20. Transfection of mutant FOXO3 decreases cell viability in response to cisplatin.....	61
Figure 3. 21. FOXO3 overexpression diminishes cisplatin-induced apoptosis.....	63
Figure 3. 22. Cisplatin-induced autophagic cell death in FOXO3 overexpressing MDA-MB-231 cells.....	64
Figure 3. 23. The effect of functional p53 on FOXO3 subcellular localization in breast cancer cells.....	66
Figure 3. 24. The effect of functional p53 on FOXO3 subcellular localization in colorectal cancer cells.....	67
Figure 3. 25. Subcellular localization of FOXO3 in wild type and p53 ^{-/-} HCT116 cells.....	68
Figure 3. 26. Cell death response in HCT116 cells.	69
Figure 4. 1. The proposed mechanism with FOXO3-IKK β crosstalk.	75

LIST OF SYMBOLS AND ABBREVIATIONS

Akt	<i>Protein Kinase B</i>
AMPK	Adenosinemonophosphate activated protein kinase
ANT	Adenine nucleotide translocator
Apaf-1	Apoptotic protease activating factor 1
Bad	Bcl-2-associated death promoter protein
Bak	Bcl-2 homologous antagonist/killer protein
Bax	The Bcl-2-associated X protein
Bcl-2	B-cell lymphoma 2 protein
Bcl-w	(BCL2L2) Bcl-2-like protein 2
Bcl-xl	B-cell lymphoma-extra large protein
Bcl-xs	B-cell lymphoma-extra small protein
Beclin 1	autophagy-related gene (<i>Atg</i>) 6
Bfl1	BCL2-related protein A1
BH domain	Bcl-2 homology domain
Bid	BH3 interacting-domain death agonist protein
Bik	Bcl-2-interacting killer protein
Bim	Bcl-2-like protein 11
Blk	B lymphocyte kinase
Bmf	Bcl-2-modifying factor
Bnip3	BCL2/adenovirus E1B 19 kDa <i>protein-interacting protein 3</i>
Bok	Bcl-2-related ovarian killer <i>protein</i>
BSA	Bovine serum albumin
C. Elegans	Caenorhabditis elegans
CAD	Caspase Activated Dnase
Caspase	Cysteine-aspartic proteases
cDNA	complementary DNA
C-terminal	carboxy terminal
CyD	cyclophilin D
DAPI	4',6-diamidino-2-phenylindole
DEPTOR	DEP domain containing mTOR-interacting protein

DFCP1	double FYVE-domain-containing protein 1
DMEM	Dubecco's modified Eagle's medium
DN	Dominant negative
DNA	Deoxiribonucleic acid
Drosophila	Drosophila melanogaster
EMSA	Electromobility shift assay
ER	Endoplasmic reticulum
ERK	extracellular-signal-regulated kinase
FACS	Fluorescence-activated cell sorting
FAK	Focal Adhesion kinase
FBS	Fetal bovine serum
FIP200	focal adhesion kinase family interacting protein of 200 kDa
FITC	Fluorescein isothiocyanate
FOX	Forkhead box
FOXO	Forkhead box Class O proteins
FYCO1	FYVE and coiled-coil domain containing 1 protein
GADD45 α	Growth Arrest and DNA Damage protein 45 alpha
GAPDH	Glyceraldehyde 3-phosphate dehydrogenase
GFP	Green fluorescent protein
HOPS complex	Homotypic fusion and vacuole protein sorting complex
Hrk	Activator of apoptosis harakiri protein
HRP	Horse radish peroxidase
Htt	Huntingtin protein
IB	Immunoblotting
IGFBP	Insulin-like growth factor-binding protein 1
IgG	Immunoglobulin G
IgG H. Chain	IgG heavy chain
IgG L. Chain	IgG light chain
I κ B	Inhibitor of kappaB
IKK	I κ B kinase
IP	Immunoprecipitation
JNK	c-Jun N-terminal kinase

kDa	kilo Dalton (atomic mass unit)
LC3	Microtubule-associated <i>protein</i> light chain
mAtg	mammalian autophagy-related protein
Mcl-1	Induced myeloid leukemia cell differentiation protein
MDa	mega Dalton (atomic mass unit)
mLST8/G β L	Mammalian LST8/G-protein β -subunit like protein
MOMP	Mitochondrial outer membrane permeabilization
mTOR	Mammalian target of rapamycin
mTORC1	mTOR Complex 1
MTT	Dimethyl thiazolyl diphenyl tetrazolium salt
NES	Nuclear export signal
NF κ B	Nuclear Factor-kappaB
NLS	Nuclear localization signal
Noxa	phorbol-12-myristate-13-acetate-induced <i>protein</i> 1
NS	Non-silencing
p27KIP1	Cyclin-dependent kinase inhibitor 1B
p53	tumor protein 53
PAK2	p21-associated kinase
PARP	Poly (ADP-ribose) polymerase
PBS	Phosphate buffered saline
PCR	Polymerase chain reaction
PE	Phosphatidylethanolamine
PI3P	phosphatidylinositol (3)-phosphate
Pras40	Proline-rich Akt substrate of 40 kDa protein
PS	Phosphatidylserine
PTP	Mitochondrial permeability transition pore
Puma	p53 upregulated modulator of apoptosis protein
PVDF	Polyvinylidene fluoride
Rag GTPase	recombination activating gene Guanosinetriphosphatase
Raptor	Regulatory-associated protein of mTOR
Rheb	Ras homolog enriched in brain protein
RNA	Ribonucleic acid

RT-PCR	Reverse transcriptase PCR
SDS-PAGE	Sodium dodecyl sulphate- Polyacrylamide gel electrophoresis
SEM	standard error of the <i>mean</i>
SIRT1	Sirtuin 1
siRNA	Small interfering RNA
SMAC	Second Mitochondria-derived Activator of Caspase
SNARE	soluble N-ethylmaleimide-sensitive factor attachment protein receptor
ULK1	unc-51-like kinase
UT	Untransfected
VDACs	Voltage-dependent anion channels
Vps	Vacuolar <i>protein</i> sorting-associated <i>protein</i>
WIPI2	WD-repeat protein interacting with phosphoinoside
wt	Wild type

1. INTRODUCTION

1.1. Cancer

The term ‘cancer’, includes more than 200 different diseases. When we consider its incidence and mortality, while ignoring the biological and clinical differences, cancer can be divided into five major groups: *carcinoma*; cancers arising from epithelia, *sarcoma*; in supportive and connective tissues such as bones, tendons, cartilage, muscle, and fat, *myeloma*; in the plasma cells of bone marrow, *leukemia*; in bone marrow, *lymphoma*; in the glands or nodes of the lymphatic system (specifically spleen, tonsils, and thymus).

The most common type of cancer is carcinoma regarding the rate of death. Lung cancers are the most important problems in both genders with 18,2% mortality worldwide and 22,5% in Turkey (Figure 1. 1). Breast cancer for women, on the other hand, takes the first place in mortality in both Turkey and the rest of the world. Every year, more than a million people are diagnosed with breast cancer. Especially in Turkey, 25% of all cancers diagnosed in females are breast cancer [1]. Cancer incidence hardly changes in the century and shows variations between different populations in the different parts of the world reflecting different environmental effects [2-6].

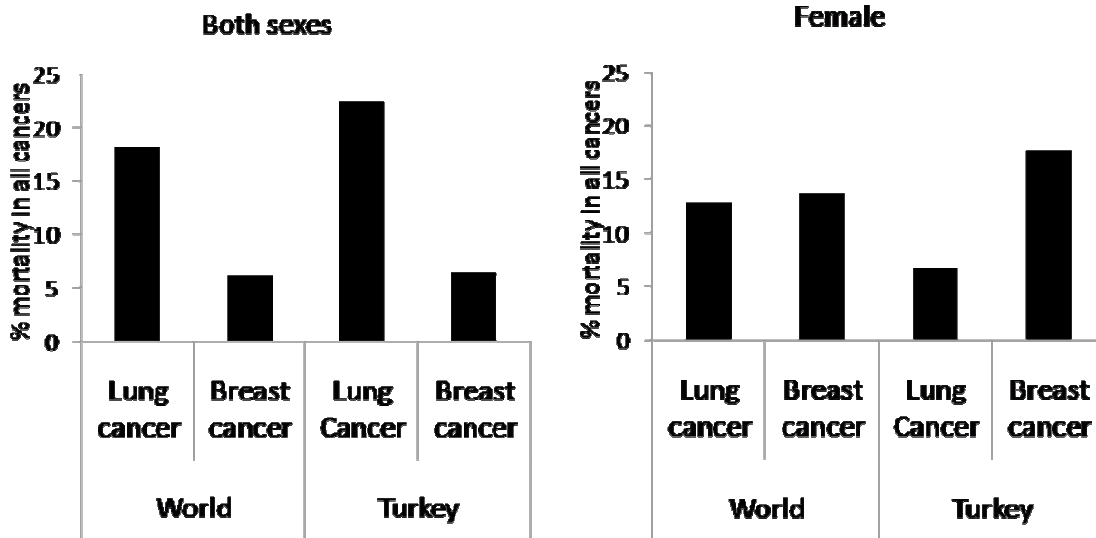


Figure 1. 1. Lung and breast cancer mortality in Turkey and worldwide (the data were obtained from the International Agency for Research on Cancer, Cancer incidence, Mortality and Prevalence Worldwide 2008, World Health Organization)

1.1.1. Carcinogenesis

Cancer is thought to be primarily an environment-related disease because of the fact that 90-95% of the cancer cases are based upon environmental factors and only 5-10% due to genetics. Environmental factors such as dietary habits (30-35%), tobacco usage (25-30%), infections (15-20%), ionizing and/or non-ionizing radiation (10%), lack of physical activity and environmental pollutants, can contribute to cancer [7].

The environmental pollutants or chemicals involved in cancer formation are generally called ‘carcinogens’. Since cancer have -in the beginning- ‘initiation’ and ‘promotion’ phases, sometimes those chemicals can be named as ‘co-carcinogen’ (initiative) or only ‘carcinogen’ (promoting). First, differentiated cells are initiated by mutagens, and then promoted by enhancer or/and suppressor agents which regulates proliferation-related signals. At this stage, cells are still differentiated with the uncontrolled proliferation ability which results in the formation of oversized and progressively disorganized tissue mass. Following that stage, dividing cells become unable to repair mutations occurred during unlimited cell divisions. This sequential

division causes genetic instability and disrupt the DNA repair mechanism as well as the regulation of genes responsible from cell differentiation. In the end, de-differentiated cells start to get apart from the tissue and disperse via blood or lymph into the different parts of the body (metastasis) (Figure 1. 2) [8].

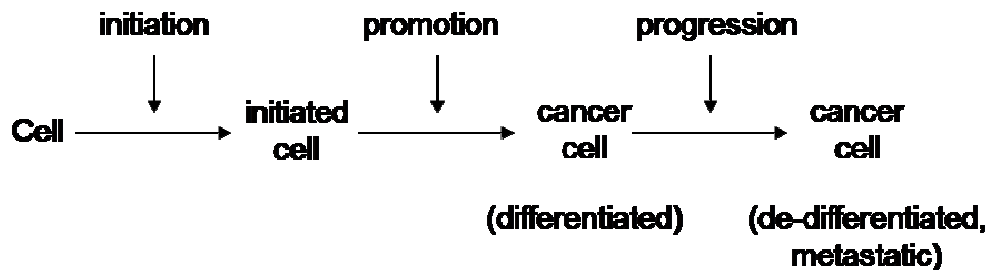


Figure 1. 2. The main stages of carcinogenesis in somatic cells.

The agents causing cancer act as either a mutagen that can cause DNA mutations, or a sensitizer of several endogenous/exogenous growth signals that can lead to uncontrolled cell proliferation. Cells, in the process ‘carcinogenesis’, generally comprise several changes at the molecular level: genetic instabilization, DNA deletions/mutations and accumulation of genetic and epigenetic differences. Those alterations generally cause the formation of complex and new protein signaling networks which represents the characteristics of human cancers. These characteristics are basically:

- Increased cell proliferation (often autonomous)
- Insufficient apoptosis
- Immortalization (growth beyond replicative senescence)
- Altered metabolism
- Genomic instability
- Altered cell and tissue differentiation
- Invasion into different tissues disturbing the tissue architecture
- Sometimes metastasis into local lymph nodes and/or distant tissues.

Cells that have those features are called as '*malignant neoplasia*' or '*malign cancer*' and usually fatal. On the other hand, '*benign cancers*' are generally neither invasive and metastatic nor immortalized. They are mostly well differentiated and unable to proliferate as much as malignant tumors.

1.2. Cancer Therapy

In order to prevent the progression of cancer; surgery, irradiation, drugs or their combinations can be employed. Choosing the appropriate therapy strongly depends on the stage/type of the cancer. Lymphomas, leukemias, metastatic or advanced carcinomas and soft tissue cancers mostly require chemotherapy.

As a matter of fact, the aim of the chemotherapy in this century mostly focuses on promoting cancer cells for cell death, especially 'apoptosis', instead of trying to transform them into their healthy form. The relationship between apoptosis and therapeutics is one of the most important fields of research in cancer therapy because understanding how therapeutics work in different cell types can help to design more efficient and specific drugs. The number of therapeutics has been designed for years and these drugs function by inducing apoptosis by changing the intracellular signaling pathways. Although breast cancer is one of the most important research topics both in Turkey and the rest of the world, therapeutics in use are only 50% successful. The main reason is therapeutic resistance (chemoresistance) mechanisms which can block the effect of drugs or/and desensitize the cells against cellular death signals. Cancer cells can build up chemoresistance either in the course of therapy or they already have innate resistance genotypically. Therefore, studies focusing on the resistance mechanisms have become more essential for the last decades [1, 9-11].

1.2.1. Cisplatin

Cisplatin (CDDP, $H_6Cl_2N_2Pt$, (*SP-4-2*)-*diamminedichloridoplatinum*) is an inorganic compound (Figure 1. 3) and one of the most effective drugs to treat testicular,

ovarian, breast, bladder, and neck cancers [12]. For therapeutic applications, the synthesis of Cisplatin starting with $K_2[PtCl_4]$ is a simple process in inorganic chemistry.

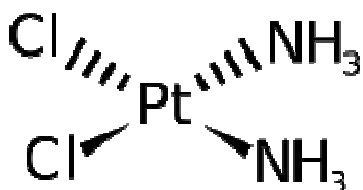


Figure 1. 3. The structure of Cisplatin

When Cisplatin is applied to the cells, only about 1% of the drug can reach the nucleus. Because of the low concentration of chloride ions in the cell, neutral cisplatin is hydrolyzed by the cytoplasmic hydrolases generating a positively charged agent. Charged Cisplatin attacks to the polar N7 nitrogen in the guanine nucleotides to form a covalent bond making 1,2 (GpG) intrastrand crosslinks (Figure 1. 4) [13-14]. Binding of Cisplatin to DNA induces a 60–80 degrees bend of the DNA in the direction of the major groove and causes a widening of the minor groove [15-16]. These DNA adducts are thought to be the primary cause of cisplatin cytotoxicity. The platinum center of cisplatin can also bind to the intracellular proteins and histones creating DNA-histone crosslinks which mainly prevent chromatin remodeling necessary for DNA transcription [17].

Although, cisplatin is widely used in chemoresistance studies *in vitro* and *in vivo*, cisplatin treatment has dose-limiting side-effects *in vivo* and cancer cells can develop a resistance to cisplatin [18].

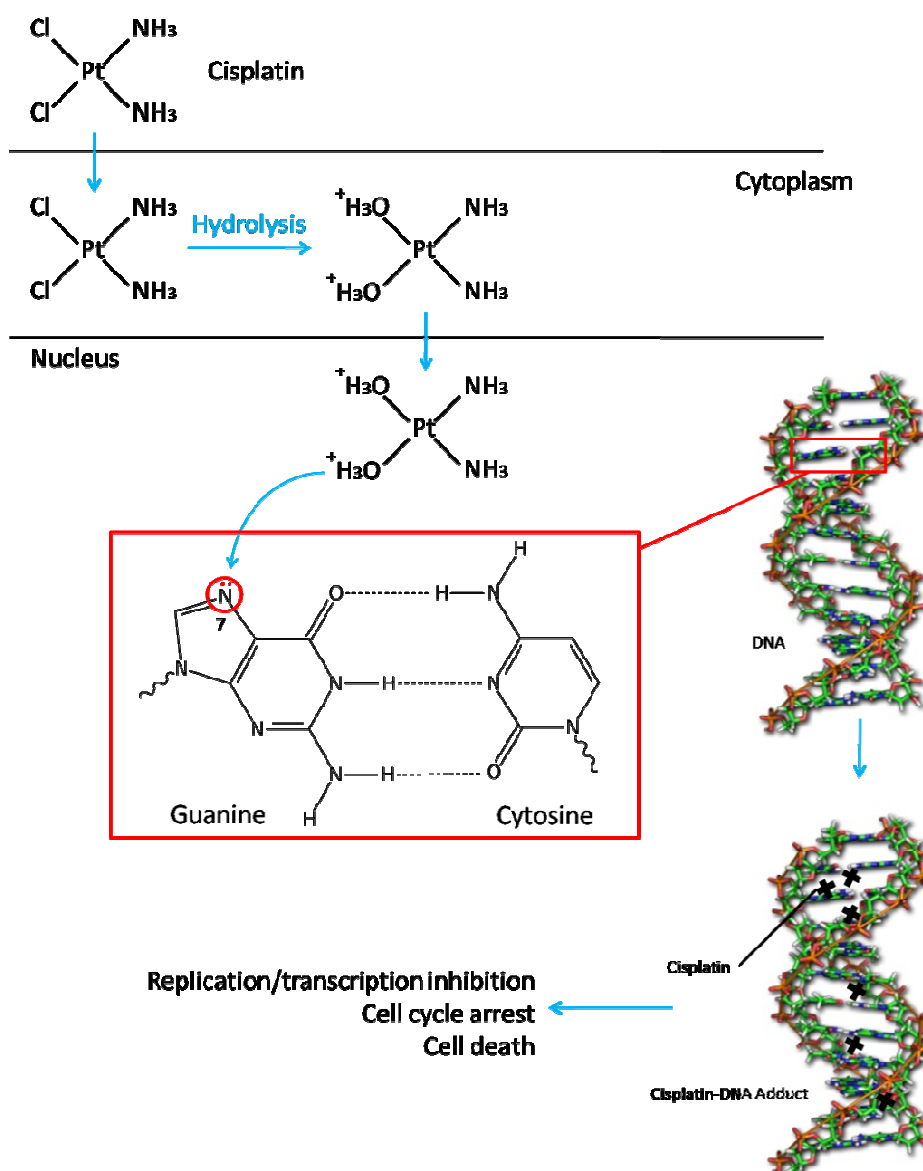


Figure 1. 4. Mechanism of Cisplatin action.

1.2.2. Paclitaxel

Paclitaxel (Taxol, $\text{C}_{47}\text{H}_{51}\text{NO}_{14}$, $(2\alpha, 4\alpha, 5\beta, 7\beta, 10\beta, 13\alpha)$ -4,10-bis(acetyloxy)-13- $\{[(2R, 3S)$ -3-(benzoylamino)-2-hydroxy-3-phenylpropanoyl]oxy $\}$ -1,7-dihydroxy-9-oxo-5,20-epoxytax-11-en-2-yl benzoate) is used to treat patients with ovarian, gastric, prostate, breast, head and neck tumors [19-22]. Paclitaxel is an organic compound (Figure 1. 5) and it was first isolated from the Pacific yew tree *Taxus brevifolia*. Now,

for therapeutic use, all paclitaxel compounds are produced by plant cell fermentation technology using a specific *Taxus* cell line and purified by chromatography.

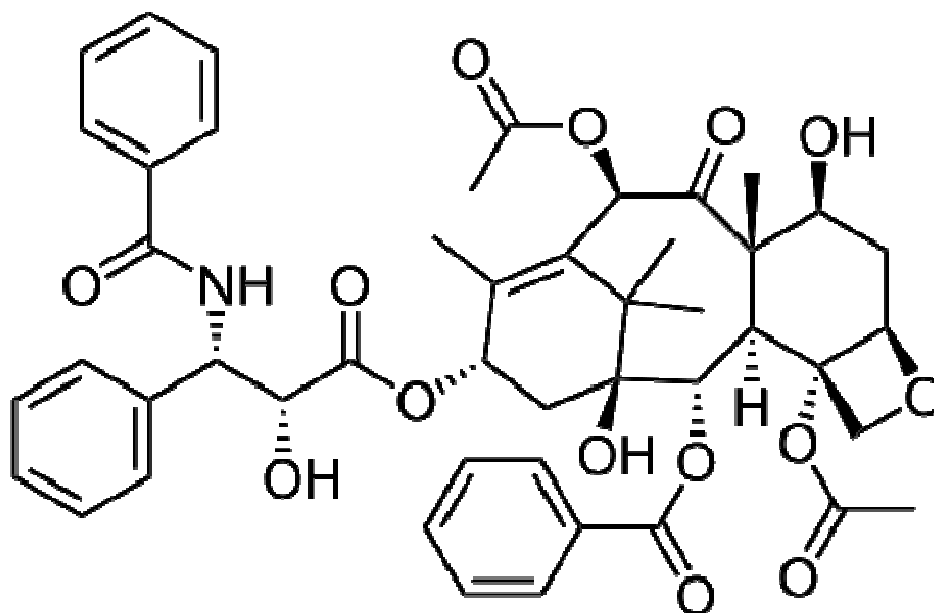


Figure 1. 5. The structure of Paclitaxel

When cells are treated with Paclitaxel, 5% of the drug can end up in the cytoplasm effectively [23]. Paclitaxel binds to the β -tubulin subunit of the microtubules and stabilizes the microtubule polymer structure leading to the prevention of its disassembly (Figure 1. 6) [24]. Additionally, it suppresses microtubule detachment from centrosomes which is essential to achieve the metaphase spindle configuration. This mechanism blocks the progression of mitosis and causes activation of the mitotic checkpoint proteins. Prolonged cell cycle arrest then triggers apoptosis [25-28].

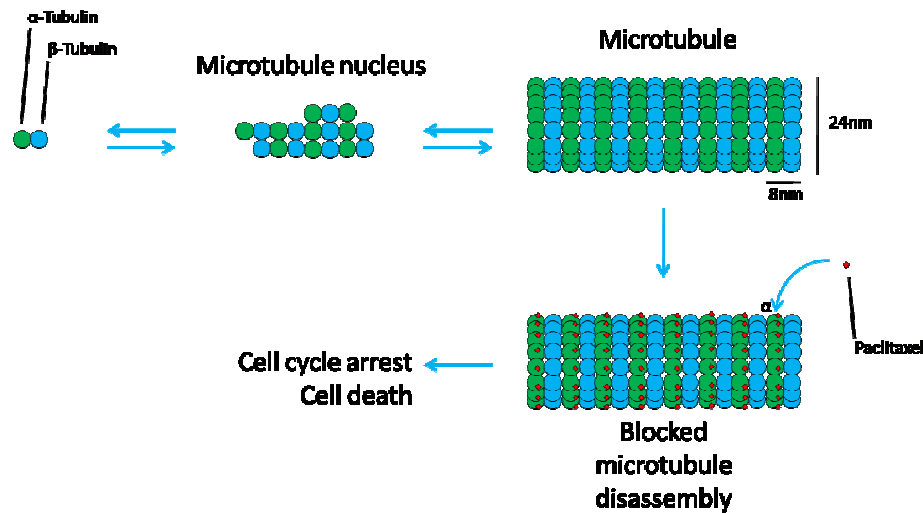


Figure 1. 6. The mechanism of Paclitaxel action.

1.3. Programmed Cell Death

Programmed cell death is the death of any cell in multicellular organisms that is mediated by an intracellular program. It confers fundamental functions for both plants and metazoa in their life cycle. Programmed cell death can be divided into three main subheadings: Apoptosis, Autophagy and Necrosis. As physiologic concentrations of chemotherapeutics do not cause necrotic cell death, we will be especially focusing on apoptosis and autophagy.

1.3.1. Type-I Cell Death: Apoptosis

In mammalian cells, the process “apoptosis” is involved in tissue sculpturing, immune system function, tissue homeostasis and deletion of damaged cells. It is regulated by a diverse range of extracellular- and intracellular-originated signals caused by various stimuli such as chemotherapy, toxins, growth factors, and cytokines. These signals may either trigger or repress the apoptotic cell death.

Apoptosis can be divided into several stages: initiation, execution and removal of the cell remnants. Basically, two separate pathways, often called ‘intrinsic’ and ‘extrinsic’, can start the initiation process. They then converge towards the execution

pathway. The intrinsic pathway can be activated by internal signals, such as DNA damage caused by a chemotherapeutic drug, whereas the extrinsic pathway responds to external signals such as death-related ligands. We will mostly emphasize the molecular mechanism of the intrinsic apoptotic pathway.

1.3.1.1. Initiation

Intracellular apoptotic signaling starts in response to a stress leading to cell death. These stresses, reported as “apoptosis inducers”, are: heat [29], radiation [30] infection [31-32] hypoxia [33] elevated calcium concentration [34-35] and DNA damaging agents [36].

Before the execution step is precipitated, apoptotic signals should promote regulatory proteins to initiate the apoptosis pathway. These regulatory proteins in the intrinsic pathway basically target the function of mitochondria [37-38]. Cytochrome-c, a small heme protein that is associated with the inner membrane of the mitochondria, is one of the most important intermediates for apoptosis induction [39]. It has a net charge of 8+ at the physiological pH which allows it to establish electrostatic interactions with the heads of anionic phospholipids. Under normal conditions, cytochrome-c is attached to cardiolipin, which is a type of diphosphatidylglycerol lipid, on the outer surface of the inner mitochondrial membrane. This attachment keeps cytochrome-c from releasing out of the mitochondria under normal conditions [40]. In response to apoptotic stimuli, cytochrome-c oxidizes cardiolipin which results in a conformational change in the structure of cardiolipin and consequently dissociation of cytochrome-c (Figure 1. 7) [41]. The dissociated form of cytochrome-c floating between the mitochondrion inner and outer membranes is not adequate to start apoptosis. To trigger the apoptotic signal, cytochrome-c is to be released from the mitochondria by permeabilization of its outer membrane. Therefore, there are several hypotheses explaining the mitochondrial outer membrane permeabilization.

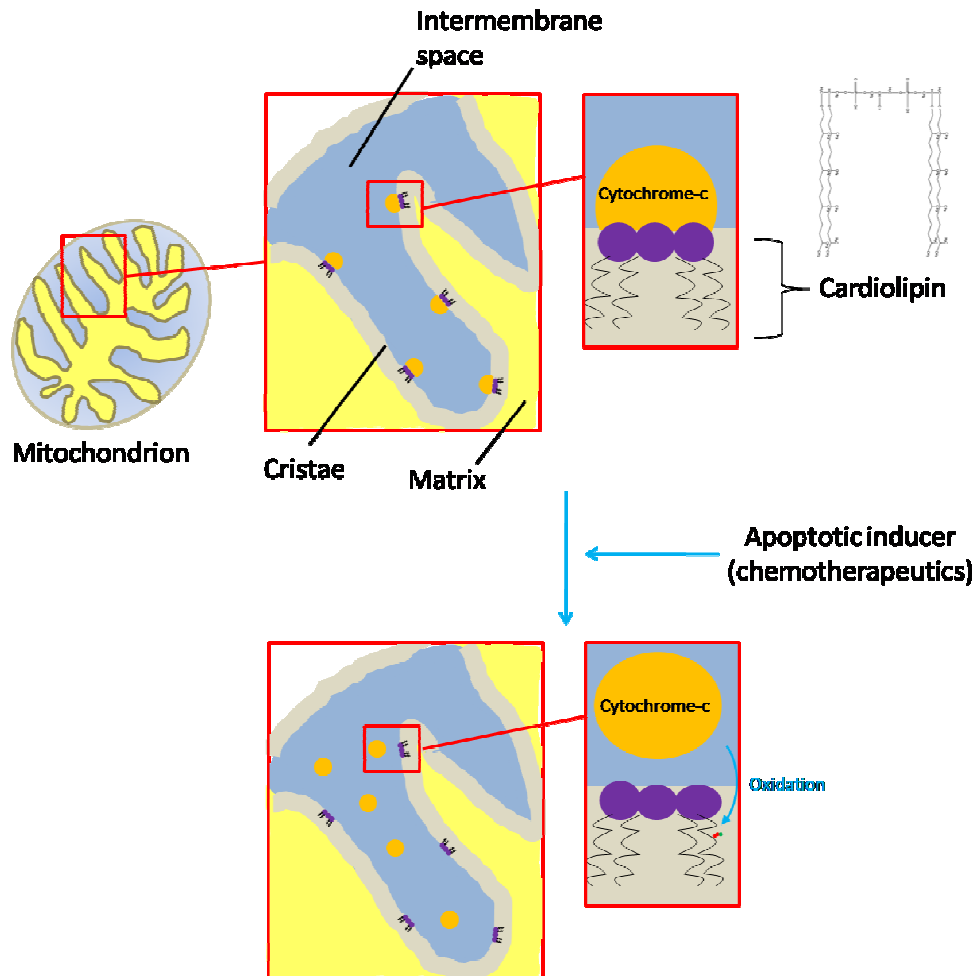


Figure 1. 7. Dissociation of cytochrome-c following apoptotic stimuli.

1.3.1.1.1. Mitochondrial outer membrane permeabilization (MOMP)

1.3.1.1.1.1. Mitochondrial permeability transition pore (PTP)

PTP is defined as an increased permeability of mitochondrial membranes to the proteins that are approximately 1,5 kDa in molecular weight [42-43]. In 1993, it was reported that pore opening on the outer membrane of mitochondria is associated with VDACs (voltage-dependent anion channels) which constitute the main pathway for metabolite diffusion through the mitochondrial membranes [44]. PTP is thought to be composed of three basic components: VDAC, inner membrane protein ANT (Adenine nucleotide translocator) and the matrix protein cyclophilin D (CyD). According to the

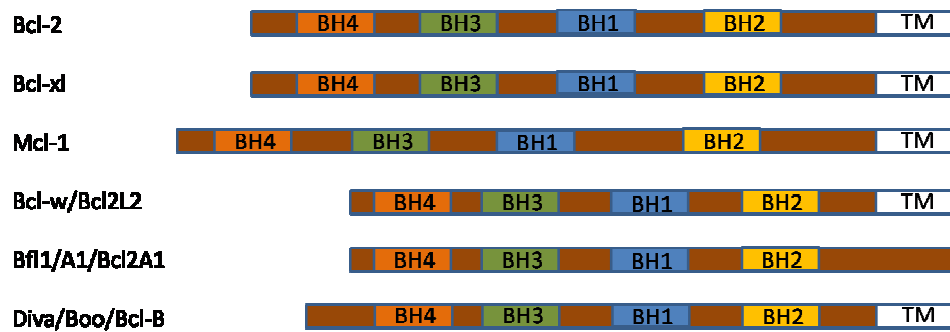
theory, an apoptotic stimulus causes elevated calcium levels and PTP opening, consequently mitochondrial swelling, cristae reorganization and outer membrane rupturing. This hypothetical process allows cytochrome-c and other intermembrane proteins to be released to the cytosol [45]. In contrary to this argument, another study showed that VDAC knockout cells can still release the equal amount of cytochrome-c during apoptosis indicating that cytochrome-c release is independent from VDACS [46]. Although several pieces of evidence exist for and against either model, the pore size of PTP alone is practically not adequate for cytochrome-c (12 kDa) to pass through if no membrane rupturing occurs. Hence, other hypotheses were raised proposing the involvement of Bcl-2 proteins in MOMP [47].

1.3.1.1.1.2. Protein Channels and Lipidic Pores

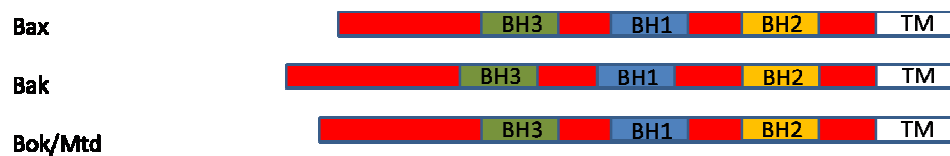
1.3.1.1.1.2.1 Bcl-2 family

Bcl-2 (B-cell lymphoma 2) is the first member of the Bcl-2 family, and encoded by the BCL2 gene [48]. Bcl-2 family members share at least one of the four characteristic homology domains; BH1, BH2, BH3, BH4 and can be divided into three major groups depending on their function: antiapoptotic Bcl-2 family proteins (such as Bcl-2, Bcl-xl, Bcl-w, Mcl-1, Bfl1, Diva), proapoptotic Bcl-2 family proteins (such as Bax, Bak, Bok and Bcl-xs) and a group of proteins that share only BH3 domain (such as Puma, Noxa, Bid, Bad, Bim, Bik, Blk, Hrk, Bnip3 and Bmf). Third group members are known to act as proapoptotic proteins by binding and inhibiting the effect of antiapoptotic Bcl-2 proteins (Figure 1. 8) [49-50].

Anti-apoptotic



Pro-apoptotic



BH3 Only

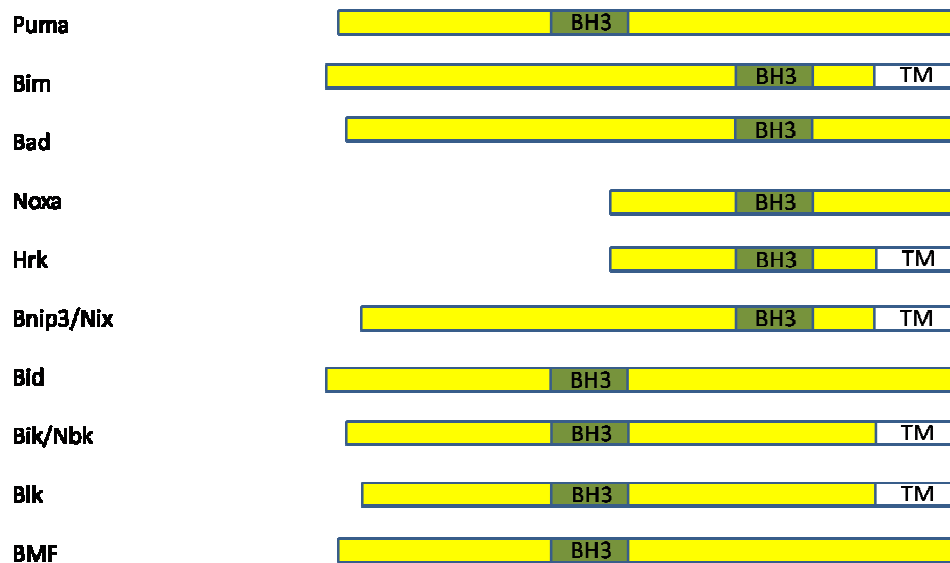


Figure 1. 8. Bcl-2 Family members. (BH: Bcl-2 Homology Domains, TM: Transmembrane domain)

Under normal conditions, proapoptotic member Bax is mostly localized in the cytosol (or loosely attached to the outer membrane of the endoplasmic reticulum (ER) and mitochondria) as a monomer and apoptotic signals induce Bax to translocate onto the mitochondria to form dimers, oligomers or high-order multimers [51-53]. Another

proapoptotic member: Bak constantly resides on mitochondria and/or ER and undergoes series of structural changes in response to apoptotic signals [54-56]. Structural changes on Bax and Bak are thought to be directly involved in MOMP. Studies showed that conformationally active forms of Bax and Bak can insert their transmembrane domains into lipid bilayers and be oligomerized through their exposed BH3 domains. Therefore, this oligomerization results in a lipidic pore opening or causes a proteinaceous channel formation whose size increases gradually over time [53, 57-60]. Bax-mediated lipidic pore opening allows the release of big molecules up to 2 MDa (Megadalton) *in vitro* and 100 kDa *in vivo* which allow the release of cytochrome-c from the mitochondria (Figure 1. 9) [61-62].

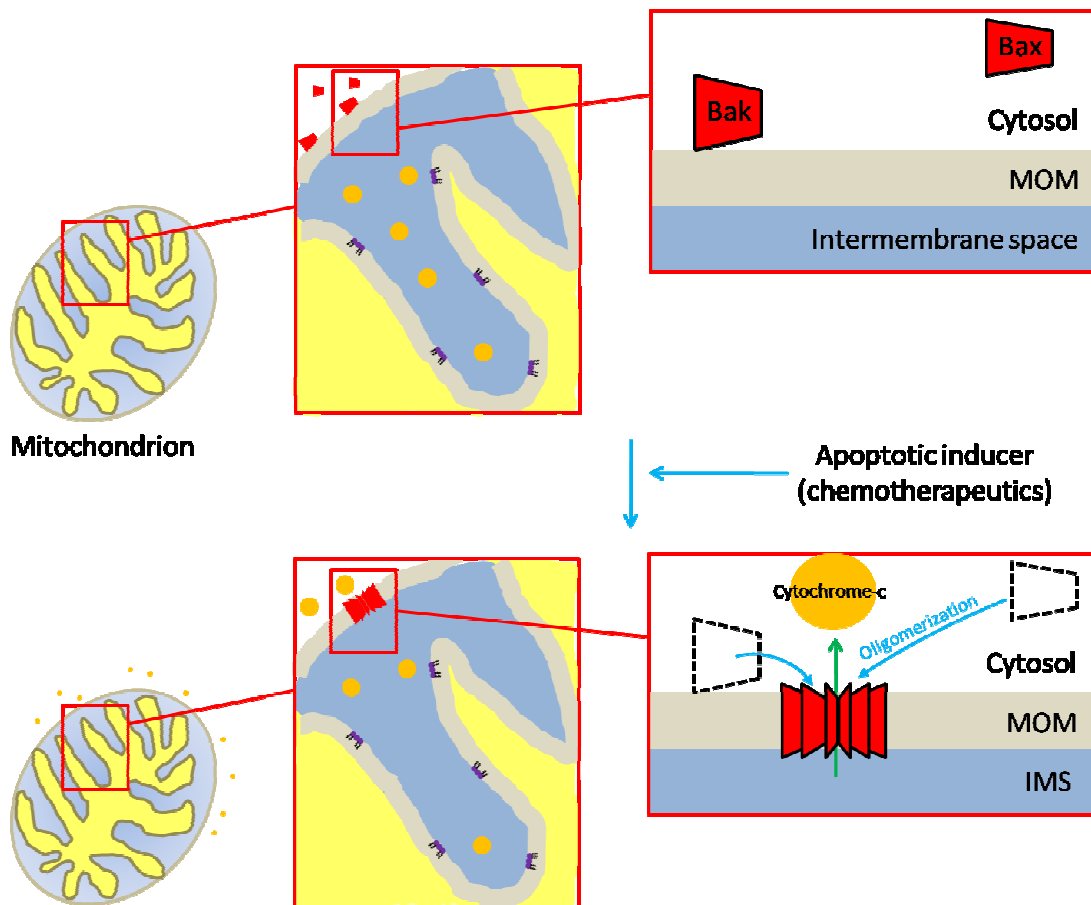


Figure 1. 9. Bax and Bak mediated MOMP. (MOM: Mitochondrial outer membrane, IMS: intermembrane space)

Although the exact mechanism explaining the cytochrome-c release from the mitochondria is still unknown, basically there are two models that are based on physical interactions among the Bcl-2 family members. The direct activation model (**Model 1**) proposes that Bim, Puma and Bid -called as “activators”- can directly activate Bax and Bak. Antiapoptotic proteins, on the other hand, may form stable complexes with activators to prevent Bax and Bak activation. Additionally, Bad, Noxa, Bmf, Bik/Blk and Hrk/DP5 –inactivators- can bind to the antiapoptotic proteins to displace Bim and Puma for apoptosis induction [63]. In the other model (**Model 2**), Bax and Bak can mediate apoptosis independent from Bim, Bid, and Puma. It is proposed that Bax and Bak are normally bound to antiapoptotic members. They become active when BH3-only proteins bind to antiapoptotic members with higher affinity leading to dissociation of Bax and Bak (Figure 1. 10) [64]. Recently it is thought that PTP opening and lipidic pore formation might be conjoint mechanisms depending on the apoptotic stimuli.

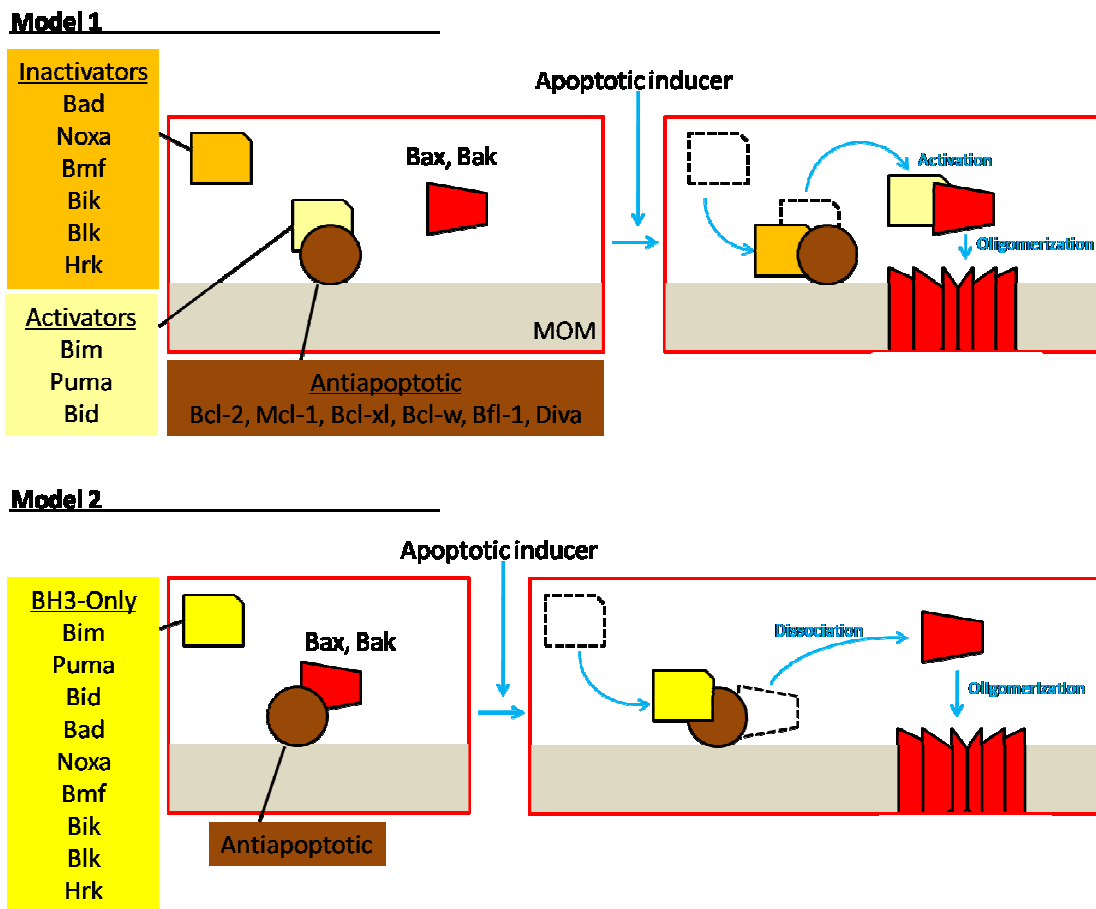


Figure 1. 10. Regulation of Bax and Bak in MOMP.

1.3.1.2. Execution and removal of the cell remnants

Following MOMP, cytochrome-c -and other proapoptotic signal molecules such as SMAC (Second Mitochondria-derived Activator of Caspase, DIABLO)- are released to the cytosol to activate Apaf-1. In the absence of cytochrome-c, oligomerization domain of Apaf-1 is folded onto the protein keeping Apaf-1 in an auto-inhibited state [65]. Cytochrome-c binding induces a conformational change on Apaf-1 leading to its oligomerization and the active apoptosome complex is formed with pro-caspase 9 recruitment [66-67]. For active apoptosome action, pro-caspase 9 should be cleaved and become active caspase 9. Two hypotheses propose that either apoptosome provides the location for caspase 9 dimerization causing its auto-cleavage, or the cleavage occurs while pro-caspase 9 is in monomeric form [68-69]. In each case, initiator caspase 9 cleaves and activates executioner caspases; caspase 3 and caspase 7 (Figure 1. 11).

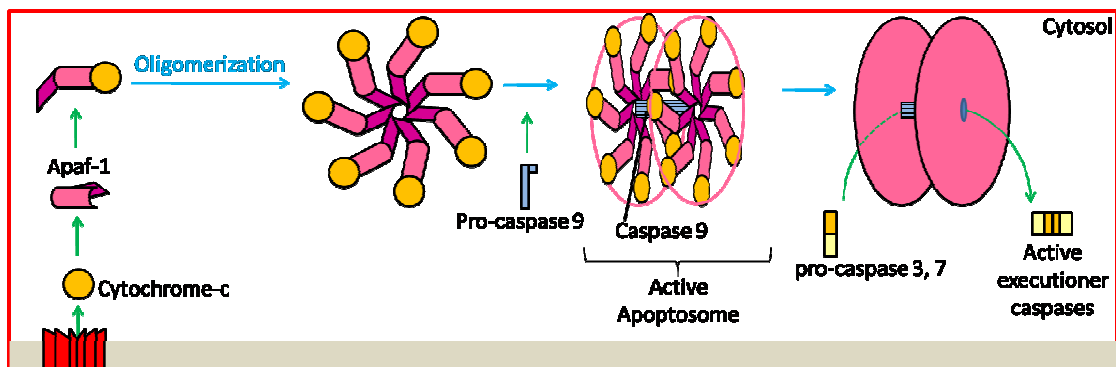


Figure 1. 11. The execution phase of apoptosis.

The multiple biochemical and morphological changes during the execution phase are caused by the proteolytic cleavage of more than 300 cellular proteins by caspase 3 and other executioner caspases. DNA fragmentation is mainly mediated by Caspase Activated DNase (CAD) [70-71]. CAD can only cleave the accessible sections of DNA in between nucleosomes because of the condensed chromatin structure in the cell [72]. The formation of these fragments is known as apoptotic DNA fragmentation, one of the characteristic features of apoptosis. Caspase cleavage of Focal Adhesion Kinase (FAK) and p21-associated Kinase (PAK2) causes loss of adhesion and

membrane changes [73-74]. Importantly, a phospholipid component; phosphatidylserine (PS) is normally restricted to the inner layer of the cell membrane by the enzyme “flippase”. In the presence of apoptosis stimuli, it is flipped to the outer layer of the cell membrane which provokes activated macrophages for the phosphatidylserine-dependent recognition. In addition to PS recognition, macrophages are further attracted by other chemotactic signals coming from the dying cell and perform phagocytosis for the removal of cellular debris [75].

1.3.2. Type-II Cell Death: Autophagy

Autophagy is an evolutionarily conserved self degradation system which degrades proteins, macromolecules, organelles and has an important role in development and differentiation [76-78].

Three types of autophagy have by now been identified: macroautophagy, microautophagy and chaperone-mediated autophagy. In macroautophagy, an “isolation membrane” sequesters a small portion of the cytoplasm which includes organelles and soluble materials to form autophagosome. Then, autophagosome fuses with lysosomes to degrade the materials within. In microautophagy, without an autophagosome formation, lysosome engulfs a small part of the cytoplasm by itself. On the other hand, chaperone-mediated autophagy does not have any membrane reorganization, proteins to be degraded translocate to the lysosome with the involvement of chaperone proteins [79]. Here in this thesis, macroautophagy is referred to as simply “autophagy”.

Autophagy, similar to apoptosis, also consists of sequential steps: induction, autophagosome formation, autophagosome-lysosome fusion and degradation.

1.3.2.1. Induction

Cellular stresses, such as amino acid starvation, are known to be strong autophagy inducers. One of the important components of amino acid signaling pathways is mTOR (mammalian target of rapamycin). mTOR is a serine/threonine protein kinase and involved in proliferation, motility, survival, transcription, protein

synthesis [80-82]. mTOR functions as a nutrient/energy/redox sensor within its complex: mTORC1 (mTOR Complex 1) which is composed of mTOR, Raptor (regulatory-associated protein of mTOR), mLST8/G β L (mammalian LST8/G-protein β -subunit like protein), Pras40 (Proline-rich Akt substrate of 40 kDa) and DEPTOR (DEP domain containing mTOR-interacting protein) [83-86]. Under normal conditions, mTORC1 inhibits autophagy with the help of Rag GTPase, Rheb and Vps34 [87-88]. Although mTORC1 inhibition is essential to induce autophagy, additional factors were reported as autophagy regulators, such as Bcl-2 [89], oxidative stress [90], calcium [91] and BNIP3 [92].

Under normal conditions, active mTORC1 interacts with “ULK1 kinase complex” which consists of ULK1 (unc-51-like kinase), mAtg13 (mammalian ortholog of Atg13 in yeast), FIP200 and Atg101. mTORC1 phosphorylates ULK1 and mAtg13 to inhibit the membrane targeting of ULK1 kinase complex. During starvation, changes in cellular energy levels activate AMPK (AMP-activated protein kinase), and then AMPK inactivates mTORC1 [93]. In addition to mTORC1 inactivation, it was shown that AMPK also phosphorylates ULK1 on several sites which causes ULK1 activation to induce autophagy signaling cascade [94]. Following the dissociation of mTORC1 from ULK1 kinase complex, active ULK1 starts to phosphorylate mAtg13 and FIP200 on the sites that cause their activation and consequently autophagy induction (Figure 1. 12) [95].

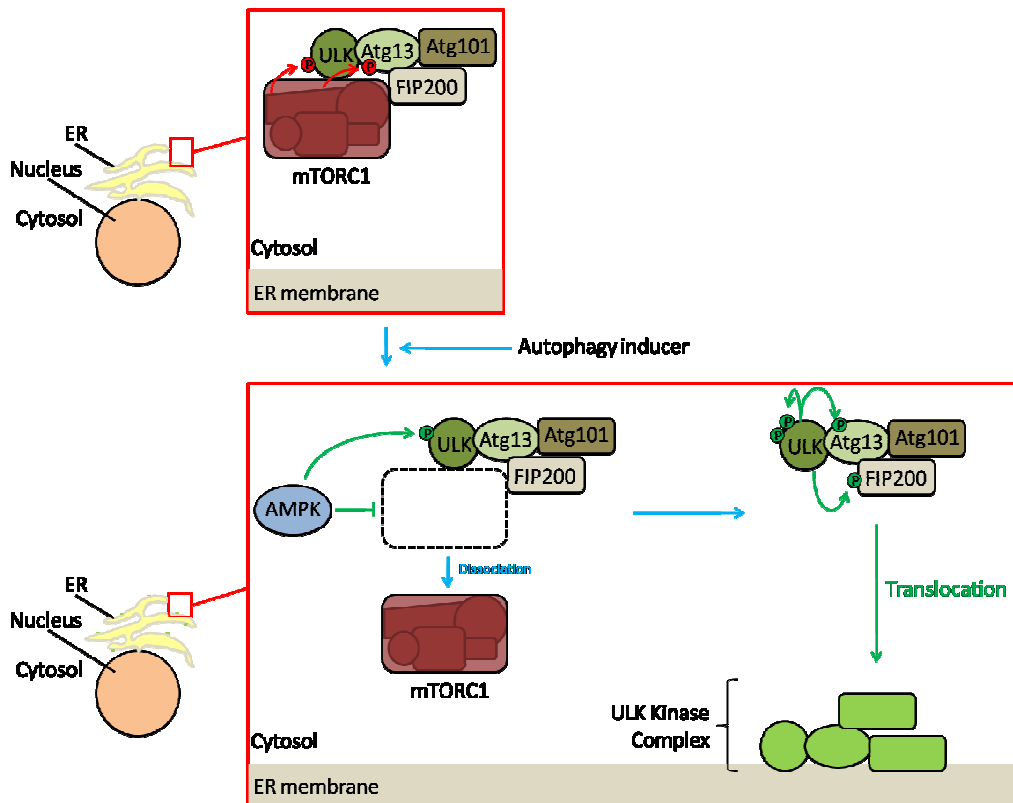


Figure 1. 12. Induction step of autophagy.

Some studies showed that under different stress conditions and/or in different cells, initiation of autophagy can follow ULK1-independent pathways [96-97]. These reports suggest that Atg13 and FIP200 may have a function to allow them to initiate autophagy independent from ULK.

1.3.2.2. Autophagosome formation

Vps34 (vacuolar protein sorting protein 34, Class III PI3K) is a phosphatidylinositol (PI) 3-kinase which can phosphorylate phosphatidylinositol to form phosphatidylinositol (3)-phosphate (PI3P). Under normal conditions, Bcl-2 sequesters Beclin1 through their BH3 domain and disrupts the interaction between Beclin1 and Class III PI3K (Vps34). Following the induction of autophagy, signaling proteins such as JNK, phosphorylates Bcl-2 and results in its dissociation from Beclin1 [98-99]. Beclin1 then binds to Vps34 and forms 'PI3K core complex' with PI3K adaptor protein p150. Then, Atg14L is recruited to the complex and directs PI3K core

complex to the local ER membrane since Atg14L has the high binding affinity to membrane curvature (Figure 1. 13) [100].

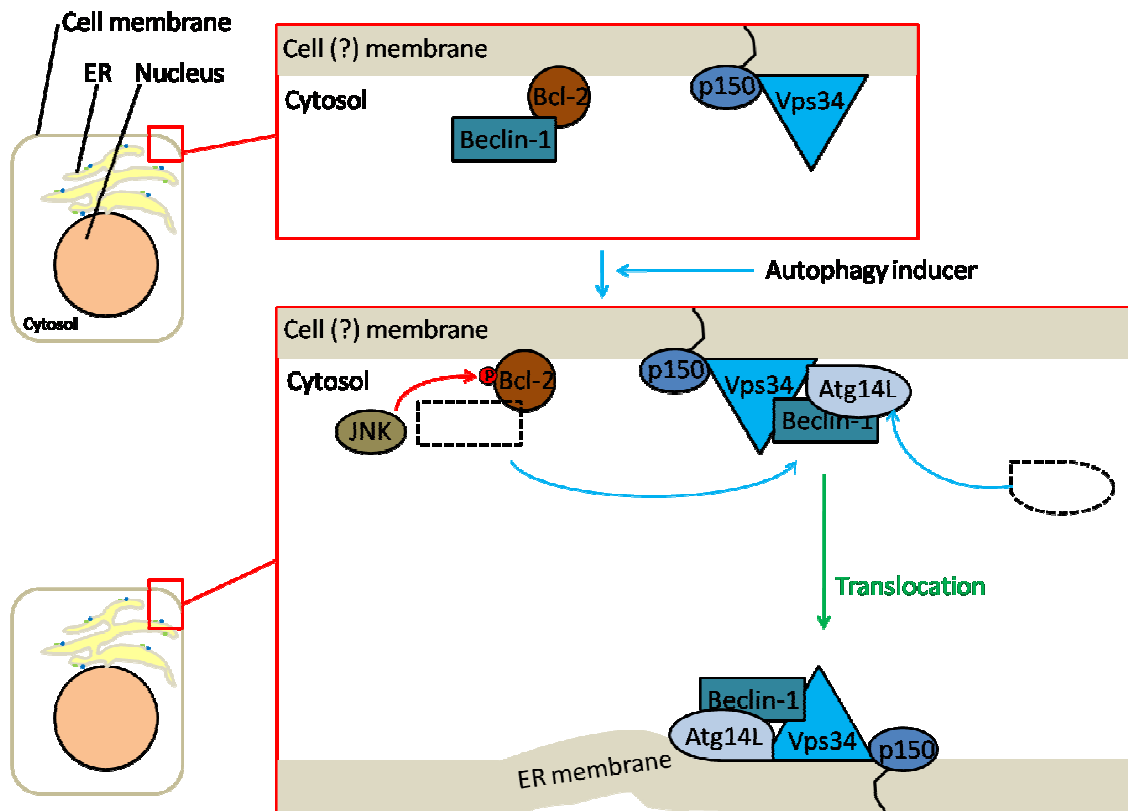


Figure 1. 13. Autophagosome formation–I

This localization and Atg14L enhance the activity of Vps34 and correspondingly PI3P production [101]. DFCP1 (double FYVE-domain-containing protein 1) binds PI3P promoting the omegasome formation (a platform of autophagosome formation). Additionally, the binding of WIPI2 (WD-repeat protein interacting with phosphoinoside) helps for the maturation of omegasome and isolation membrane. Although PI3P production by Vps34 may occur elsewhere in the cell, WIPI2 recognizes and localizes to the local pool of PI3P that is only produced by PI3K core complex (Figure 1. 14) [102].

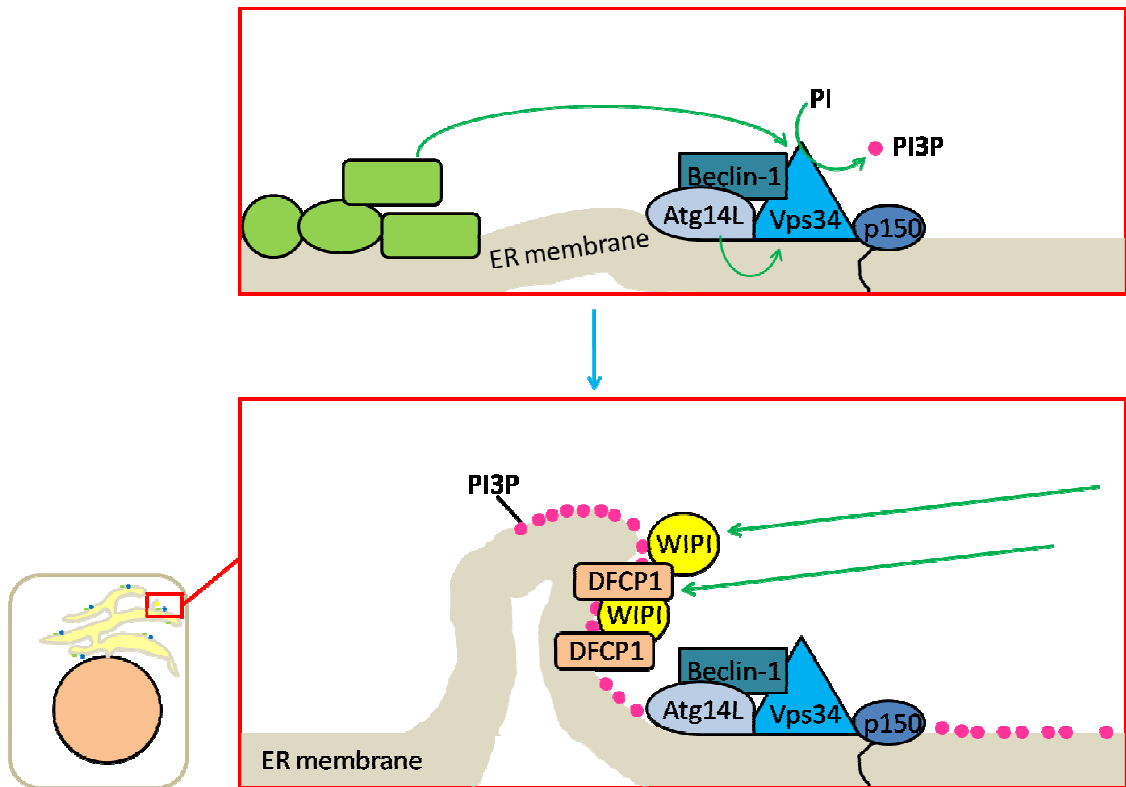


Figure 1. 14. Autophagosome formation-II

The molecular mechanisms that lie beneath the expansion of isolation membrane are still poorly understood. However, two ubiquitin-like protein conjugation systems are known to be involved.

Ubiquitin is a 76 amino acid long protein (8,5 kDa). The aim of the ubiquitin conjugation system is to transfer ubiquitin to a target protein via sequential reactions catalyzed by E1, E2 and E3 enzymes (specific proteases) [103]. The ubiquitin precursor is first processed by E1 enzyme for the exposure of C-terminal glycine residue. Then, ubiquitin is transferred to E2 enzyme forming a thioester bond. Another protease, E3, recognizes the target protein and catalyzes the binding of ubiquitin to the lysine residue of the target protein. The ubiquitin tag is a signal to direct target proteins to the proteasomal degradation. In autophagy, the conjugation of the autophagy-related proteins follows a similar strategy to the ubiquitin system.

1.3.2.2.1. Ubiquitin-like conjugation system 1

In the autophagy, the ubiquitin-like conjugation system is involved in the isolation membrane expansion. In the first conjugation system, C-terminal glycine residue of Atg12 is activated by Atg7 (E1-like enzyme) through a thioester bond in response to autophagic signals. After that, Atg12 is transferred to the lysine 149 residue of Atg5 by Atg10 (E2-like enzyme) involvement [104-105]. Atg12-Atg5 conjugate, further interacts with Atg16L and forms Atg12-Atg5/Atg16L1 complex. Through the homo-oligomerization of ATG16L, in mammalian cells it is thought that a 800 kDa multimer of Atg12-Atg5/Atg16L is formed (Figure 1. 15, Conjugation system I) [106-107].

Importantly, it is reported that autophagy may occur in an independent manner of Atg5 and Atg7 [108-110]. Atg12–Atg5/Atg16L complex is not sufficient to coat the autophagic vesicle in some cell types, but Atg16L complex specifies the accurate localization of LC3 and promotes its lipidation [111-112].

1.3.2.2.2. Ubiquitin-like conjugation system 2

In healthy mammalian cells, LC3 (Microtubule-associated protein light chain 3) is synthesized as pro-LC3. Atg4B (a cysteine protease, E1-like enzyme) immediately cleaves the C-terminal 22 residues for the exposure of its C-terminal glycine to form soluble cytosolic LC3-I [113]. Then, with the help of E2-like enzyme Atg7, LC3 is conjugated to another E2-like enzyme Atg3 [114]. In response to autophagic signals, it is proposed that LC3-Atg3 conjugate is recruited by Atg16L1 complex which resides on a yet undetermined membrane [111]. Thus, LC3-I is conjugated to the head group of a phospholipid: phosphatidylethanolamine (PE) by Atg3 (Figure 1. 15, Conjugation system II). Because Atg12–Atg5 in Atg16L complex acts as an E3 enzyme at the final step of this conjugation system, Atg12–Atg5 is proposed to be the E3-like enzyme [115]. The lipidated form of LC3 (LC3-II) then associates newly forming autophagosome membranes (Figure 1. 16) [116].

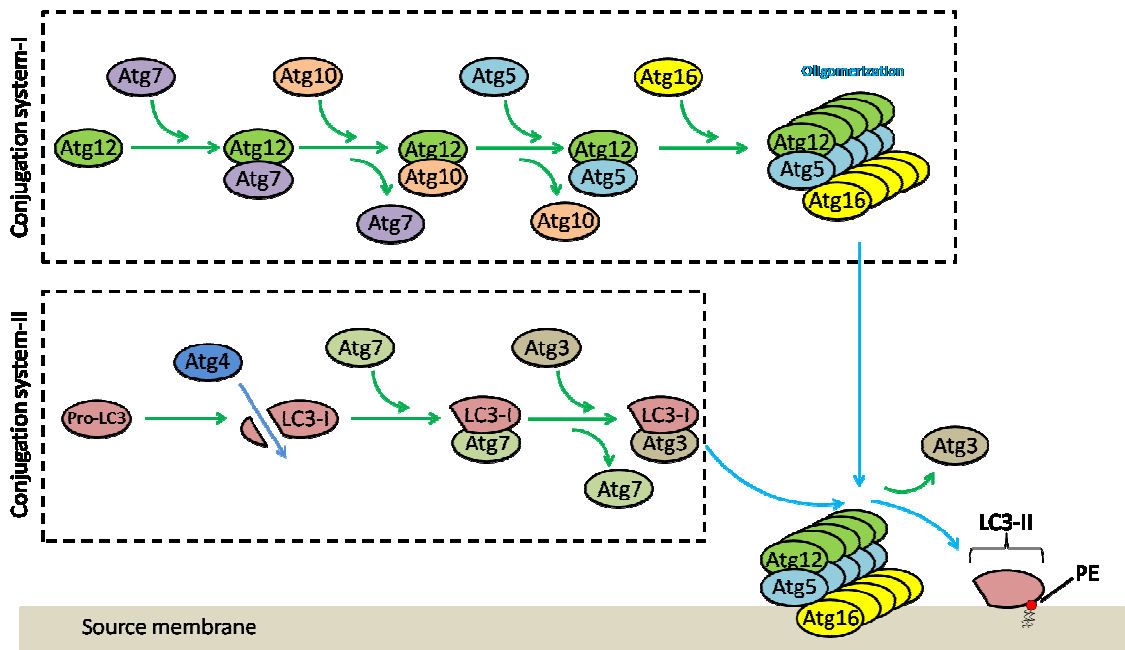


Figure 1. 15. Ubiquitin-like conjugation systems in autophagy

Although there are several studies proposing the omegasome as a platform of autophagosome formation, it must be said that it is still not clear whether only ER membrane is directly used in autophagy. Some studies showed that the membranes of autophagosome may also be derived from golgi, mitochondria or plasma membrane [117-123].

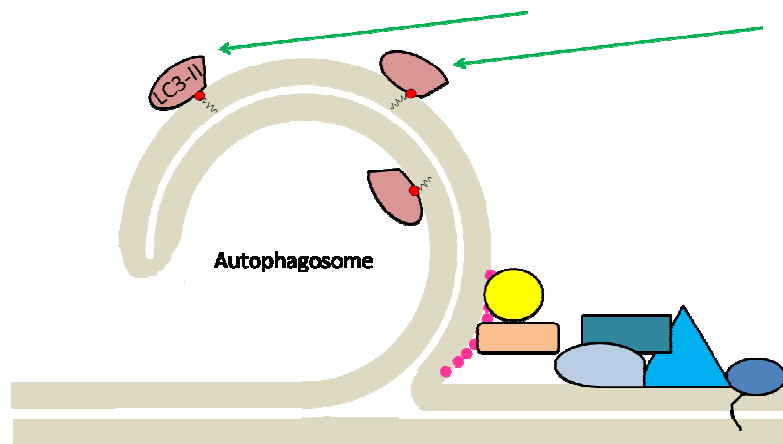


Figure 1. 16. LC3-II recruitment and autophagosome formation.

Once autophagosomes are formed, a novel protein FYCO1 (FYVE and coiled-coil [CC] domain containing 1) binds to LC3 and Rab7 (a GTPase) to form an adaptor complex. LC3 binds to microtubules and moves the autophagosome along microtubules toward lysosomes with the help of dyneins [124-127].

1.3.2.3. Autophagosome-lysosome fusion and degradation

The first contact between autophagosome and lysosome is mediated by a big protein complex called “HOPS complex” (homotypic fusion and vacuole protein sorting complex: Vps11, Vps16, Vps18, Vps33, Vps39, Vps41). Then, membrane anchored protein SNARE (soluble N-ethylmaleimide-sensitive factor attachment protein receptor) adjoins its transmembrane domain to fuse two lipid bilayers [128]. Following the fusion of lysosome and autophagosome, cytoplasm-derived proteins and the inner membrane of autophagosome are finally degraded by lysosome-derived hydrolases.

1.4. Diminished Apoptosis/Autophagy in Cancer

Decreased response to death related signals may lead to genomic instabilization. During the sequential divisions, the diminished rate of cell death causes hyperproliferation and serious tumor characteristics like metastasis. As mentioned before, many cytotoxic drugs used in chemotherapy induce –mostly apoptotic- cell death. Although some degree of apoptosis may occur within the cancer tissue, it is not at the same rate as in normal cells. Thus, further decrease in apoptotic response in cancer cells contributes to drug resistance. Diminished apoptosis is often caused by the overactivity of survival signaling pathways rather than the primary alterations in apoptotic pathways. Bcl-2, for instance, is over-expressed in a wide range of carcinomas such as breast and prostate cancers. Alternatively, cancers mostly have high levels of Bcl-xl protein. On the other hand, Beclin 1 was reported as deleted in many cancers suggesting that autophagy might be another tumor suppressor mechanism –similar to apoptosis- in cancers [129-130].

To understand the chemoresistance and mechanism of cell death, identifying the upstream events of the cell death signaling is essential. Cell death inducing stimuli (chemotherapeutics) first activates various transcription factors to start protein signaling cascade leading to cell death or survival. In this thesis, two transcription factors, their main pathways and possible intersections of two pathways were examined.

1.5. NF κ B Pathway

NF κ B (Nuclear Factor-kappa B) consists of five cellular proteins: p50/p105 (NF κ B1), p52/p100 (NF κ B2), p65 (RelA), RelB and c-Rel. These proteins function as homo- or heterodimers and the most prevalent complex among the combinations is p65:p50 heterodimer. The subunits p50 and p52 are derived from the proteolytic cleavage following mono-ubiquitination of the C-terminal domains from the precursor molecules p105 and p100 respectively [131]. Cleaved p50 or p52 binds to p65, c-Rel or RelB to form the active NF κ B complex. p50 and p52 do not have transactivation domains, unlike p65, RelB and c-Rel. Nevertheless, they play critical roles in modulating the specificity of NF κ B function.

In unstimulated, healthy mammalian cells, Rel subunits predominantly reside in the cytoplasm, bound to I κ B family proteins (I κ B- α , I κ B- β , I κ B- ϵ) which function by masking the nuclear localization signal (NLS) found on NF κ B subunits. I κ B- α is partially effective for blocking NLS meaning that it can enter the nucleus with NF κ B subunits. However, it contains a nuclear export signal (NES) that causes the rapid export of the complex back to the cytoplasm [132]. I κ B- β can also bind NF κ B in the nucleus without displacing it from DNA. Some studies propose that I κ B- β may have a function for the stabilization of DNA-NF κ B complex by preventing the displacement of NF κ B [133-134]. Other studies, on the other hand, point out that loss of I κ B- β prolongs NF κ B activity in certain cells [135-136]. These studies indicate that the inhibition of NF κ B is highly tissue and stimuli specific.

In response to activators of the NF κ B pathway, I κ B is phosphorylated at Ser32 and Ser36 residues by I κ B kinase (IKK) (Figure 1. 17). IKK consists of three subunits: IKK α , IKK β , and IKK γ (NEMO). IKK α and IKK β have the serine/threonine kinase activity, on the other hand IKK γ is known as the regulatory protein of the complex [137]. Besides I κ B proteins, IKK complex has other important cellular targets such as FOXO3 and Htt (Huntingtin) [138-140].

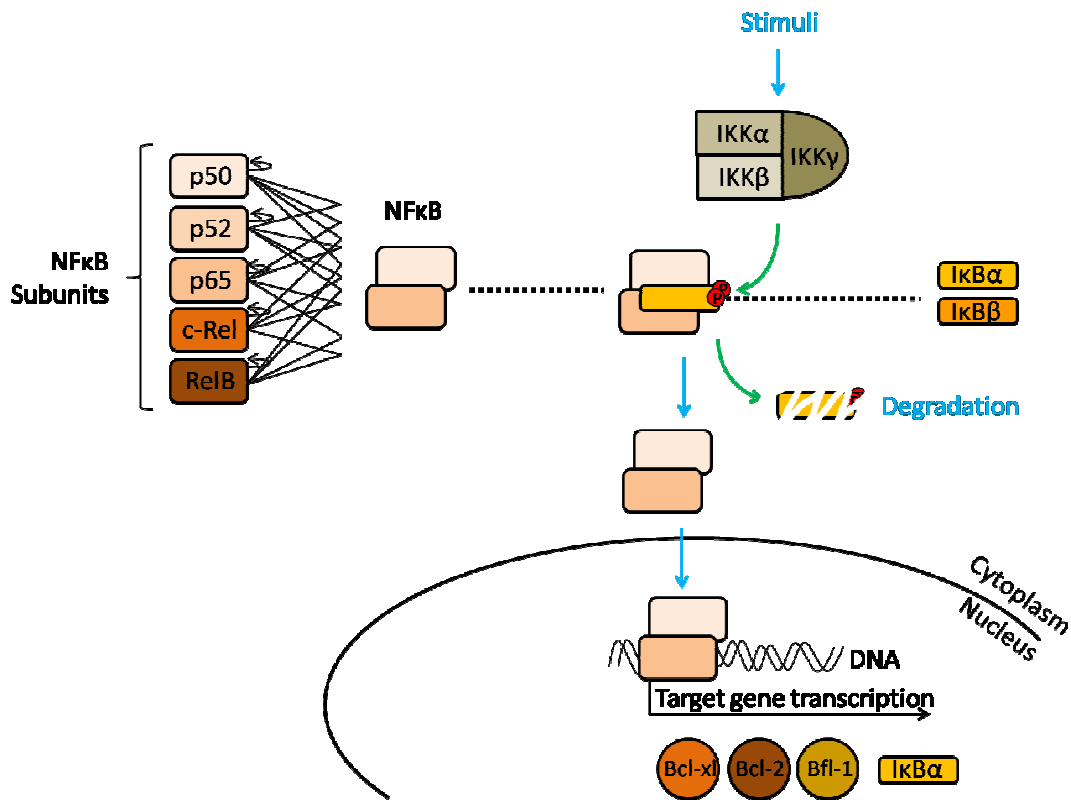


Figure 1. 17. NF κ B Pathway

After I κ B is phosphorylated by IKK, it is subjected to proteosomal degradation following ubiquitination [141-142]. The exposure of the NLS on NF κ B recruits nuclear transporter proteins importin- α 3 and importin- α 4 to bind to its NLS and to transport NF κ B into the nucleus via dynein and dynactin complex [143-144]. In the nucleus, NF κ B binds to its consensus sequences on DNA, known as “ κ B sites” (5’-GGGR N W YYCC-3’, R; a purine base, N; any base, W; adenine or thymine and Y; pyrimidine base) [145-146]. After the interaction between NF κ B and DNA takes place, DNA (κ B

site) slightly bends towards the major groove to be recognized by other transcription activators [147].

Theoretically, there are 15 possible dimers of NF κ B subunits and each couple may have some preference for different κ B sites depending on their affinities [148]. However, transcriptional specificity is not necessarily conferred by affinity differences of the subunits because each dimer can undergo conformational changes to interact with DNA. This suggests that different NF κ B dimers can bind to the same κ B site with comparable affinities [149]. This flexibility allows NF κ B to regulate the transcription of a wide range of genes. NF κ B itself is involved in the regulation of more than 300 genes of various biological processes including immune response, inflammation, cell growth, survival, and development [150].

While NF κ B has a basal level activity in normal cells, the activity of NF κ B pathway in cancer cells may vary and frequently causes increased expression of pro-survival genes. For instance, NF κ B-mediated increase in Bcl-2 and/or Bcl-xl expression allows these proteins to gain anti-apoptotic function in addition to basal pro-survival functions they have in normal state.

Pro-apoptotic Bcl-2 members Bax and Bim are also regulated by NF κ B but in a different way. In mammalian cells, heterodimerization of p65/p50 suppresses the promoter activity of Bax and p52/p52 homodimers prevent Bim transcription [151-152]. Therefore, this regulatory capacity of NF κ B may lead to decreased apoptotic response in most cancers. NF κ B is also involved in autophagy regulation. It is known that NF κ B pathway is activated following autophagy; however the role of NF κ B in autophagy regulation is still poorly understood as there are controversial studies reporting the inhibitor or the activator effect of NF κ B in the regulation of autophagy [153-158]. Importantly, Bax can cleave Beclin1 causing a reduction in the autophagy response [159].

1.6. Forkhead Family and FOXO3

Forkhead family which is characterized by a conserved DNA-binding domain (the Forkhead box, or FOX) comprises more than 100 members in humans. They are classified from FOXA to FOXR depending on their sequence similarity. Forkhead (FOXA), the first member and the founder of the family, was first identified in *Drosophila* as a gene whose mutation causes the development of fork-like head structure [160]. Forkhead proteins are also called as “winged helix” proteins because their DNA-binding domain consists of three α -helices flanked by two characteristic loops like butterfly wings.

Class “O”, FOXO transcription factors consist of FOXO1 (FoxO1a or FKHR), FOXO3 (FoxO3a/FKHRL1), FOXO4 (AFX) and FOXO6. They were all first identified as insulin/PI3K/Akt pathway-regulated transcription factors [161]. They contain a highly conserved winged-helix domain which mediates its binding to DNA.

Our main focus, FOXO3 (Figure 1. 18) has an important role in several cellular processes and acts as a tumor suppressor in various cancers. It is especially involved in the transcriptional regulation of cell death-related proteins Bim [162], Puma [163], Noxa [164], LC3 [165], Beclin 1 [166] and cell cycle arrest proteins such as p27KIP1 [167], cyclinD [168] and GADD45 α [169].

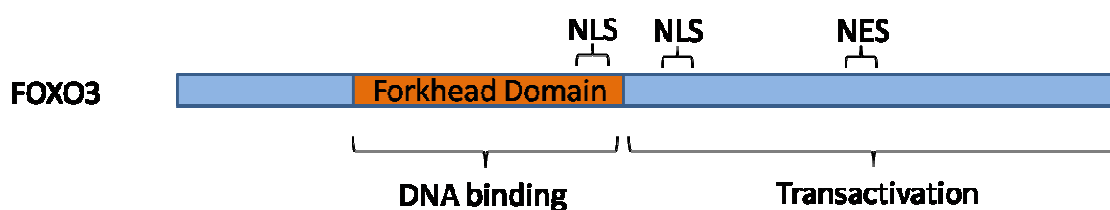


Figure 1. 18. Structure of FOXO3

In the absence of growth signals, FOXO3 is localized in the nucleus as a potent transcriptional activator and binds to the conserved DNA motif 5'-TTGTTTAC-3' [170-171]. The well known control mechanism of FOXO3 localization is especially

phosphorylation. External stimuli, such as growth factors or insulin, trigger FOXO3 phosphorylation at conserved serine/threonine residues in the nucleus. This phosphorylation creates a binding site for the chaperone protein 14-3-3. C-terminal alpha-helix of 14-3-3 binds to phosphorylated FOXO3 and triggers a conformational change in FOXO3 which dissociates FOXO3 from its DNA-binding site [172-174]. The binding of 14-3-3 leads to the exposure of nuclear export signal (NES) on 14-3-3 which enables the interaction between FOXO3 and nuclear exporters Crm1/Ran (Exportin-1/Ras-related nuclear protein) at the nuclear pore [175-178]. Following the export of FOXO3, phosphorylated FOXO3 is degraded by proteasome-dependent degradation in the cytoplasm (Figure 1. 19) [179].

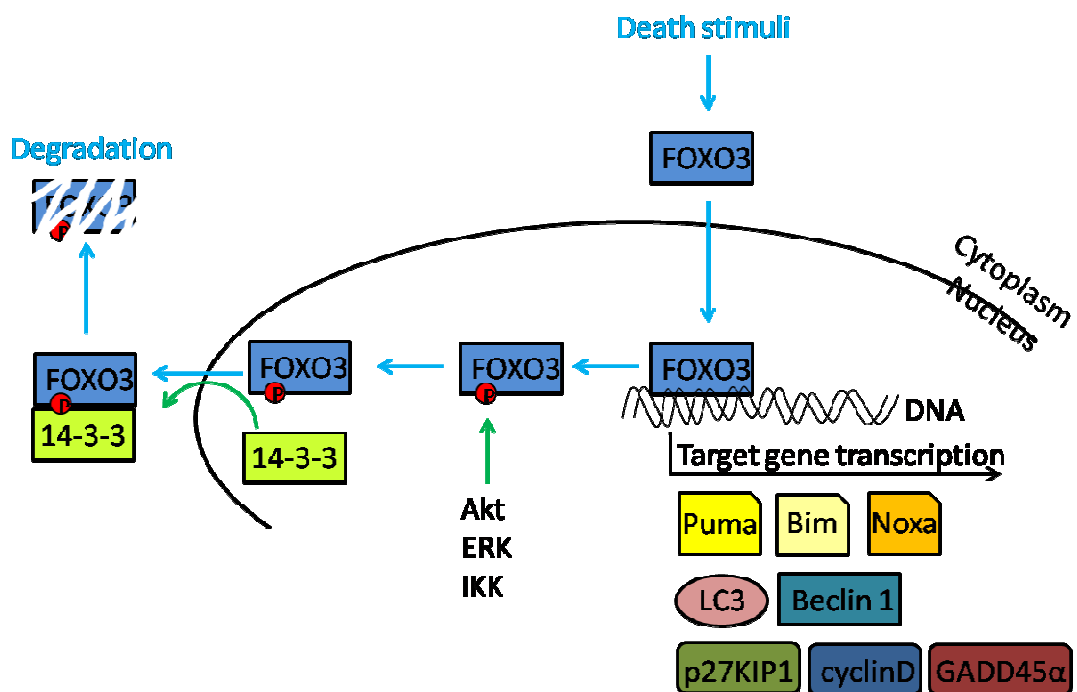


Figure 1. 19. Mechanism of FOXO3 action

It has been reported that the binding of 14-3-3 may alter the flexibility of NLS on FOXO3 for further preventing its re-entry [180]. However, studies showed that stress stimuli can also trigger the relocalization of FOXO members in the nucleus, even in the presence of growth factors [181-183].

Akt, AMPK, ERK1/2 and IKK β are thought to be the most potent upstream kinases that interfere with the function of FOXO3 in the nucleus [174, 184-186]. Although subcellular localization of FOXO3 is the main regulatory system, altering FOXO3 protein levels can also have dramatic effects. It was shown that overexpression of wild type FOXO in *C. Elegans* and *Drosophila* can extend lifespan [187-189], while loss of FOXO increases cancer in mammals [190-191].

Because FOXO3 upregulates several cell death proteins, inactivation of FOXO3 is directly related to chemoresistance and longevity [192-193]. It has been shown that active FOXO3 overcomes the resistance against various drugs such as Gefitinib/ZD1839 in breast cancer cells [194-195], Imatinib/STI571 and doxorubicin in chronic myelogenous leukemia [196-198], and cisplatin in colon cancer cells [199].

1.7. Aim of the Study

Approximately 30% of the women diagnosed with early-stage disease in turn progress to metastatic breast cancer, for which therapeutic options are limited due to the partial effectiveness of the drugs. Chemoresistance, resistance to the chemotherapeutic drugs, is the major obstacle to the effective treatment of many types of tumors including breast tumors. Paclitaxel and cisplatin are important agents in the treatment of malignant breast cancers and the first-line chemotherapy generally includes paclitaxel and/or cisplatin. Although those chemotherapeutics can alter the growth of tumors, in most cases their effect is limited and not long lasting as mentioned before. Therefore, there is a significant need for understanding the protein signaling mechanisms involved in chemoresistance in order to develop new therapy strategies to improve the response rates and potentially extend survival.

In the scientific literature, the major protein signaling pathways involved in cell death were mostly identified with their main elements; however, signaling pathways are not isolated systems and they can interact in a number of ways which forms sophisticated signaling networks. On this account, understanding the crosstalk

between those identified pathways is fundamental for designing molecularly targeted therapy against cancer.

The aim of this study was to investigate the potential crosstalk between FOXO3 and NF κ B pathway and to clarify the effect of this crosstalk on cell death response which is associated with chemoresistance. For that purpose, we focused on IKK-FOXO3 interaction and used two metastatic breast cancer cell lines as a model of chemoresistance: (1) MCF-7 which retains several characteristics of differentiated mammary epithelium and (2) MDA-MB-231 which shows highly dedifferentiated behavior. We first used paclitaxel or cisplatin as therapeutic agents to simulate the effect of first-line therapy in differentiated and dedifferentiated cells and then identified the physical interaction between IKK and FOXO3 which determines the cellular response to cisplatin resulting in chemoresistance or chemosensitivity.

Specifically, the aim was;

- a) to investigate cell cycle arrest or apoptosis upon chemotherapeutic drug treatment and to understand the role of Bcl-2 family proteins and DNA damage response by FACS and immunoblotting analyses,
- b) to understand NF κ B and FOXO pathways by using FOXO3 siRNA technology, enforced expression of FOXO3, immunoblotting and EMSA.
- c) to identify the role of IKK and its subunits on cell death response by chemical inhibition of IKK complex or enforced expression of IKK subunits.
- d) to identify the involvement of death response (autophagy or apoptosis) by fluorescent microscopy, FACS and immunoblotting analyses
- e) to understand the role of p53 on FOXO regulation by either ectopic expression of p53 in p53 knockout/p53 mutant cells or chemical inhibition of p53 in p53 wildtype colorectal and breast cancer cells.

2. MATERIALS AND METHODS

2.1. Materials

2.1.1. Chemicals and media

All chemicals and growth media used in this study are listed in Appendix A.

2.1.2. Antibodies and enzymes

All antibodies used in immunoblotting, FACS analysis and EMSA are listed in Appendix B.

2.1.3. Molecular biology kits and reagents

Molecular biology kits for gene transfection, plasmid isolation and protein analysis are listed in Appendix C.

2.1.4. Vectors

The maps of the expression vectors used are shown in Appendix D.

2.1.5. Oligonucleotides

FOXO3 consensus oligonucleotide for EMSA experiments, GADD45 α PCR primers and GAPDH PCR primers are listed in Appendix E.

2.1.6. Buffers and solutions

All buffers and solutions (manually prepared) are listed in Appendix F.

2.1.7. Equipment and computer software

Equipments and computer software used are listed in Appendix G.

2.2. Methods

2.2.1. Cell lines

MCF-7 (HTB-22, ATCC) and MDA-MB-231 (HTB-26, ATCC) breast adenocarcinoma cells were grown in DMEM with 2 mM L-glutamine, 10% FBS, 100 IU/ml penicillin and 100 μ g/ml streptomycin in a humidified incubator at 37°C and 5% CO₂; HCT-116 wild type (CCL-247, ATCC) and *p53*^{-/-} HCT116 colorectal carcinoma cells (kindly provided by B Vogelstein, Johns Hopkins University, Maryland) were grown in McCoy's 5A with 2 mM L-glutamine, 10% FBS, 100 IU/ml penicillin and 100 μ g/ml streptomycin in a humidified incubator at 37°C and 5% CO₂.

2.2.2. Cell cycle analysis

Cultured cells were harvested by trypsin (0.05% Trypsin/0.53 mM EDTA) and washed once with cold PBS (pH: 7,4). Pellets were fixed with 5ml of 70% ethanol (v/v) for 15 minutes and washed again with cold PBS (pH: 7,4) followed by incubation with propidium iodide staining buffer (see Appendix F) in the dark for 45 minutes. Then,

500µl of cold PBS (pH: 7,4) were added to the incubating cells to dilute the PI concentration and labeled cells were analyzed by FACS.

2.2.3. Cell death, viability and proliferation assays

Cell death response was assessed by FITC-conjugated Annexin-V. Briefly, cells to be analyzed were incubated with Annexin-V staining buffer for 15 minutes and quantified by FACS on FlowJo software. In order to detect cell viability or cell proliferation, the cells (7500 cells/well) were seeded in 96-well plates and analyzed by MTT (Cell Proliferation Kit I) according to the manufacturer's instructions. Results are expressed as percentage of cell viability, proliferation or cell death.

2.2.4. Cleaved caspase 3 staining

Cells were harvested and subjected to 3% formaldehyde (w/v) fixation for 10 minutes. Fixed cells were incubated with Methanol (15 minutes) for permeabilization and washed with %0.5 BSA (w/v) containing FACS incubation buffer (see Appendix F). Cells were incubated for 1 hour with 1:400 anti-cleaved caspase 3 monoclonal antibody and then with 1:800 FITC-anti-rabbit secondary antibody for 30 minutes. After two washes with PBS (pH: 7,4), cells were subjected to FACS analysis on FlowJo software.

2.2.5. Fluorescent Microscopy

Cells (50000 cells/well) were grown on sterile cover slides in cell culture conditions and fixed with cold Methanol:Acetone (1:1) for 15 minutes. Following three PBS (pH: 7,4) washes, cells were stained with DAPI by DAPI staining solution for 15 minutes and slides were analyzed with Olympus B60 fluorescent microscope using required filters.

2.2.6. Transfections

For the transfection experiments, cells were grown to 50% confluency and transiently transfected with pECE-HA-FOXO3(wt) (kindly provided by Gregory J. Gores), pEGFP-FOXO3(S644A) (kindly provided by Mien-Chie Hung), pCMV-flag-IKK β , pCMV-HA-IKK α , pCMV-flag-IKK γ (kindly provided by Richard B. Gaynor), pEGFP-LC3 (kindly provided by D Gozuacik), pCMV-p53(wt) (kindly provided by B Erman) or mock vectors using Fugene6 or Metafectene-easy transfection reagents. Briefly, 6 μ l Fugene6 were added to 100 μ l serum-free DMEM which contains 2 μ g of plasmid DNA. Then, the mixture was incubated for 30 minutes at room temperature and added dropwise to the cells. MCF-7 cells were transfected with FOXO3-specific siRNA or negative control (non-silencing) siRNA by Hiperfect transfection reagent. Briefly, 6 μ l Hiperfect reagent was added to 75ng siRNA containing 200 μ l serum-free DMEM and the mixture was briefly vortexed. Following 10-minute incubation at room temperature, the mixture was added dropwise to the cells. For FOXO3 silencing experiments, three sequential transfections were assessed to obtain a long term silencing effect. After the first transfection, the cells reached confluency in 2-3 days. Confluent cells were harvested; second and third transfections were performed during seeding. Transfected cells were verified by immunoblotting 48 hours after the transfection (after the third transfection in siRNA experiments).

2.2.7. RNA isolation

Cells in a 12-well plate were washed with cold PBS and scrapped off by 250 μ l Trizol, incubated in a 1,5 ml centrifuge tube for 5 minutes. Then, 100 μ l of chloroform was added and incubated at room temperature for another 5 minutes. The samples were centrifuged at max speed for 15 minutes (4°C) and upper phase of the mixture was separated to a new tube. After adding 250 μ l of isopropanol, tubes were incubated at room temperature for 10 minutes and centrifuged at max speed for 10 minutes (4°C). To wash the RNA pellet, supernatants were discarded and the pellets were washed first with 250 μ l 80% ethanol and centrifuged at 7500g/5 minutes (4°C). Pellets were dried on bench for 5 minutes and resuspended by 50 μ l DEPC-water.

2.2.8. Semi quantitative and quantitative PCR

The concentrations of isolated RNAs were quantified by spectrophotometric measurement using Nanodrop. For reverse transcriptase PCR, total RNA isolates (1µl) were incubated with Sensiscript RT kit for 1,5 hours at 37°C in the PCR machine. For semi quantitative PCR, the reaction mixture (100ng cDNA, 1µM forward and reverse primers and Taq PCR Master Mix) was run for 25 cycles and amplified cDNAs were analyzed by agarose gel (1%) electrophoresis in 1X TBE buffer. For quantitative realtime PCR analysis, 30-40 cycles were performed with quantitech SYBRgreen kit. 40 PCR cycles were run (each cycle contains 94°C for 1 minute, 51°C for 1 minute, 72°C for 30 seconds) with an additional 94°C 10-minute step in the beginning and a 72°C 10-minute for the final extension. The results were analyzed by Pfaffl equation method [200]. In both PCR experiments, GADD45α and GAPDH primers were used (see Appendix E).

2.2.9. Total protein isolation

Treated cells were washed with cold PBS (pH: 7,4), scraped off the surface of cell culture plates in 1ml PBS (pH: 7,4) and transferred to 1,5ml centrifuge tubes. Cells were cold centrifuged for 30 seconds at max speed. Pellets were resuspended in 50µl cold complete lysis buffer (see Appendix F), vortexed and kept on ice for 20 minutes. Samples were then cold centrifuged and supernatants containing total proteins were stored at -80°C.

2.2.10. Subcellular protein extraction

Following the cell scrapping and cold centrifugation, cell pellets were resuspended in 50µl hypotonic T1 buffer (see Appendix F) and kept on ice for 20 minutes. After the cold incubation, tubes were centrifuged at max speed for 1 minute and supernatants containing cytoplasmic proteins were stored at -80°C. Pellets were resuspended in 20µl saline T2 buffer (see Appendix F) and incubated on ice for another 20 minutes followed by cold centrifugation for 20 minutes at max speed. Supernatants containing nuclear proteins were stored at -80°C immediately.

2.2.11. Protein concentration determination

Protein concentrations of protein extracts were determined by Bradford reagent. Bovine serum albumin (BSA, stock solution: 1mg/ml) was used as the standard protein. Starting with 5µg BSA/well in 96-well plates, BSA was 1:1 diluted to constitute a standard graph, 1µl of samples were prepared simultaneously and 100µl of Bradford reagent were added to the wells. Absorbance was spectrophotometrically measured at 595nm by a microplate reader with the first standard set as blank. Protein concentrations in the samples were then determined by extrapolating their absorbance values against the standard curve. For every new assay a new standard curve was generated.

2.2.12. Immunoblotting

Total cell lysates were isolated with complete lysis buffer (see appendix F). Total cell lysates or subcellular fractions were separated on SDS-PAGE using running buffer and transferred onto PVDF membrane that has been activated in methanol for 30 seconds. For this transfer step, freshly prepared transfer buffer (see Appendix F) was used. Membranes were blocked with blocking solution and incubated with indicated primary antibodies and required HRP-conjugated secondary antibodies in the antibody incubation solution. Proteins were finally analyzed using ECL Advance and exposed to Hyperfilm ECL. All critical blots and immunoprecipitation experiments were repeated at least three times.

2.2.13. Densitometric analysis

Densitometric values for immunoblotting results were calculated by ImageJ software.

2.2.14. Preparation of radiolabeled oligonucleotides

Complementary oligonucleotides (FOXO3 consensus, IGF1P IRS site. See Appendix E) were obtained separately (stock solution: 3mg/ml) and 2µl of each oligonucleotides were mixed and incubated in 46µl annealing buffer (see Appendix F)

first 4 minutes at 95°C, then 10 minutes at 70°C. Oligonucleotides were then left at room temperature to cool down and stored at -20°C. Complementary oligonucleotide was labeled with γ -³²P-dATP (3000 Ci/mmol) by T₄ polynucleotide kinase in the oligonucleotide labeling reaction mix (see Appendix F) and then purified on a Sephadex G-25 column. Sephadex G-25 columns were washed completely off its buffer first by gravitation, then by centrifugation twice at 3500rpm (1650g) for 2 minutes. Total reaction mix (50 μ l) was applied to the center of the column in an upright position. The assembly was centrifuged twice at 2300rpm (1100g) for 4 minutes.

2.2.15. Electrophoretic Mobility Shift Assay (EMSA)

Cytoplasmic and nuclear proteins were separately isolated and nuclear extracts were subjected to EMSA as described before [201]. Briefly, 5 μ g of nuclear proteins were incubated 30 minutes at room temperature with ³²P-labelled oligonucleotide probes in the EMSA incubation buffer. DNA–protein complexes were resolved on 6% non-denaturing polyacrylamide gels (see Appendix F). The gels were then dried and autoradiographed on X-ray films. For supershift assay, 1 μ l anti-FOXO3 antibody was added 10 minutes before the binding incubation was finalized.

2.2.16. Co-immunoprecipitation

Cell lysates were isolated in complete lysis buffer (see Appendix F). 800-1000 μ g proteins were immunoprecipitated with 1 μ l (stock solution: 1mg/ml) anti-FOXO3 or anti-IKK β primary antibodies at 4°C for 2 hours and captured by 50% slurry of protein G-Sepharose beads (50 μ l) in complete lysis buffer at 4°C for another 2 hours. Immunoprecipitates were then washed four times with complete lysis buffer. Finally, the beads were resuspended with 20 μ l of Laemmli sample buffer, boiled at 95°C for 5 minutes and finally loaded into the wells of the polyacrylamide gel for immunoblotting analysis.

2.2.17. Statistical analysis

The statistical significance of the results was analyzed by Student's t-tail test and $*P<0.05$, $**P<0.01$ and $***P<0.001$ were considered statistically significant.

2.2.18. Illustrations

All illustrations shown in “Introduction”, “Results” and “Discussion and Conclusion” sections were designed by the thesis author using Adobe Photoshop CS5, Irfanview and MS Office 2007 softwares.

3. RESULTS

3.1. Effect of Cisplatin or Paclitaxel treatment on cell viability and cell death in

MCF-7 and MDA-MB-231 cells

In order to determine the cytotoxic effects of cisplatin and paclitaxel individually, we treated MCF-7 and MDA-MB-231 breast cancer cell lines with various concentrations of cisplatin or paclitaxel. Cell viability was then assessed by MTT assay (Figure 3. 1). At physiologically relevant concentrations of cisplatin (30 μ M) and paclitaxel (20nM), MTT results showed that MDA-MB-231 cells are more resistant to both chemotherapeutics (paclitaxel \rightarrow 73%, cisplatin \rightarrow 76% viability) than MCF-7 cells (paclitaxel \rightarrow 59%, cisplatin \rightarrow 64% viability).

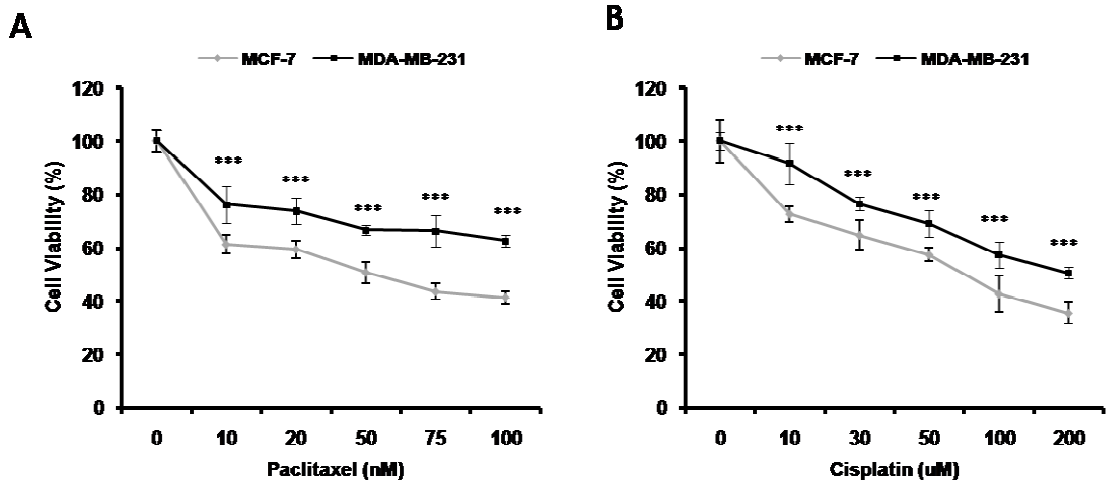


Figure 3. 1. The effect of paclitaxel/cisplatin on cell viability. MCF-7 and MDA-MB-231 cells were treated with different paclitaxel concentrations (**A**) or cisplatin concentrations (**B**) for 48 hours. Cytotoxicity was determined by MTT Assay and the results represent the mean (\pm SEM) values obtained from at least three different experiments with eight repeats (**= $p < 0.01$).

Because MTT assay works on the metabolic activity which can be variable in different cell lines, we also performed Annexin-V staining 48 hours after cisplatin or paclitaxel treatment to monitor drug-induced cell death (Figure 3. 2). For that purpose, we used FITC-conjugated Annexin-V protein which has a high affinity to PI on dying cells' surface. Especially in physiologically relevant concentrations, 30 μ M cisplatin or 20nM paclitaxel, 70% (for paclitaxel) and 36% (for cisplatin) of MCF-7 cells were analyzed as Annexin-V positive, indicating the cells undergoing cell death, whereas MDA-MB-231 cells showed only 46% and 23% cell death respectively, in response to paclitaxel or cisplatin treatment. Depending on the results obtained and previously published studies, 30 μ M cisplatin and 20nM paclitaxel were used for further experiments [202].

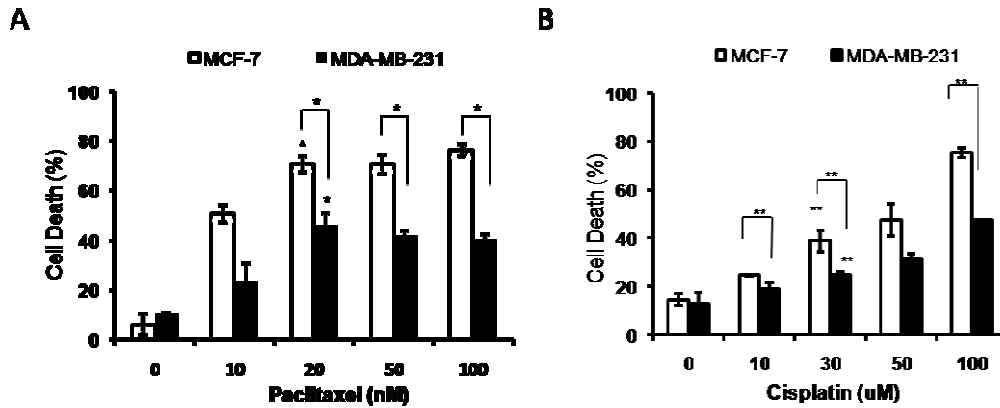


Figure 3. 2. The effect of paclitaxel/cisplatin on cell death. MCF-7 and MDA-MB-231 cells were treated with indicated concentrations of (A) paclitaxel or (B) cisplatin for 48 hours, stained with FITC-Annexin-V and subjected to FACS analysis (**= $p < 0.05$).

3.2. Effect of Cisplatin or Paclitaxel treatment on cell cycle arrest

The period of growth is referred to as interphase and comprises three phases of the cell cycle: a gap phase (G1), in which the cells resume the biosynthesis which has been dormant during mitosis; a synthesis phase (S), in which the DNA content of the cell is doubled and the chromosomes are replicated; and a second gap phase (G2) [203].

Paclitaxel is a potent inhibitor of cell division causing an arrest in the late G2/M phase of the cell cycle [204] and cisplatin induces the cell cycle arrest through G1 checkpoint [205]. To investigate the possible differences in MCF-7 and MDA-MB-231 cells regarding the cell cycle arrest, we treated the cells with cisplatin or paclitaxel for 12 and 24 hours and dyed with propidium iodide along with the untreated controls (Figure 3. 3). 85% of MCF-7 cells and 72% of MDA-MB-231 cells were detected in G2/M stage 24 hours after paclitaxel treatment. For both cell lines, the percentage of the cells that newly accumulated in the G2/M phase was approximately 35%. Prior to cisplatin treatment, while MCF-7 cells in the G1 stage constitute 41% of the whole population, cisplatin treatment caused additional 37% cell accumulation (78%). However, MDA-MB-231 cells showed only 8% additional cell accumulation in the G1 phase (46% \rightarrow 54%).

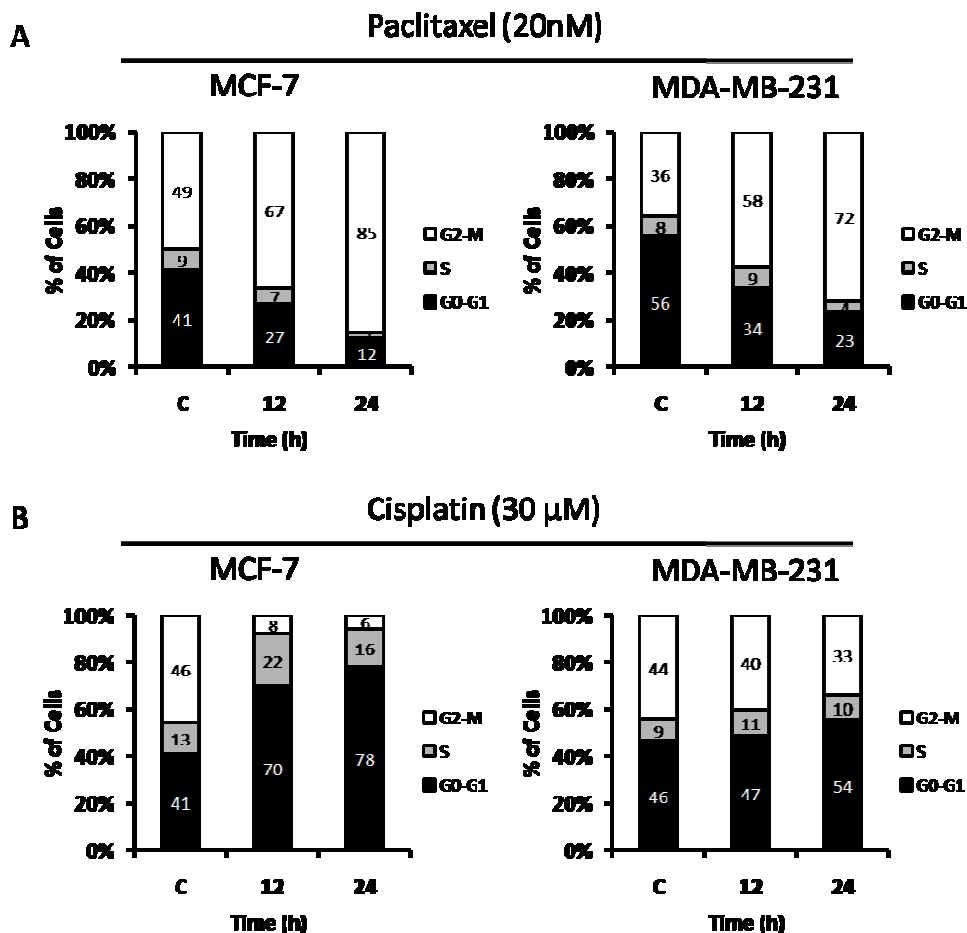


Figure 3. 3. Cell cycle analysis in response to paclitaxel/cisplatin treatment. MCF-7 and MDA-MB-231 cells were treated with (A) paclitaxel or (B) cisplatin for 0, 12 or 24 hours, then fixed and labeled with propidium iodide for FACS analysis.

3.3. Expression of Bcl-2 Family proteins in response to drug treatments

It was previously reported that paclitaxel treatment in myeloid leukemia cells and cisplatin treatment in thoracic cancer cells can induce both extrinsic and intrinsic apoptotic pathways [206-207]. Because the effects of chemotherapeutics are highly cell type-dependent, we checked the expression of Bcl-2 family proteins which compose the major intrinsic apoptosis regulators. To elucidate the expression pattern of Bcl-2 family proteins, MCF-7 and MDA-MB-231 cells were treated with paclitaxel or cisplatin, and then total cell lysates were subjected to immunoblotting using specific antibodies indicated (Figure 3. 4).

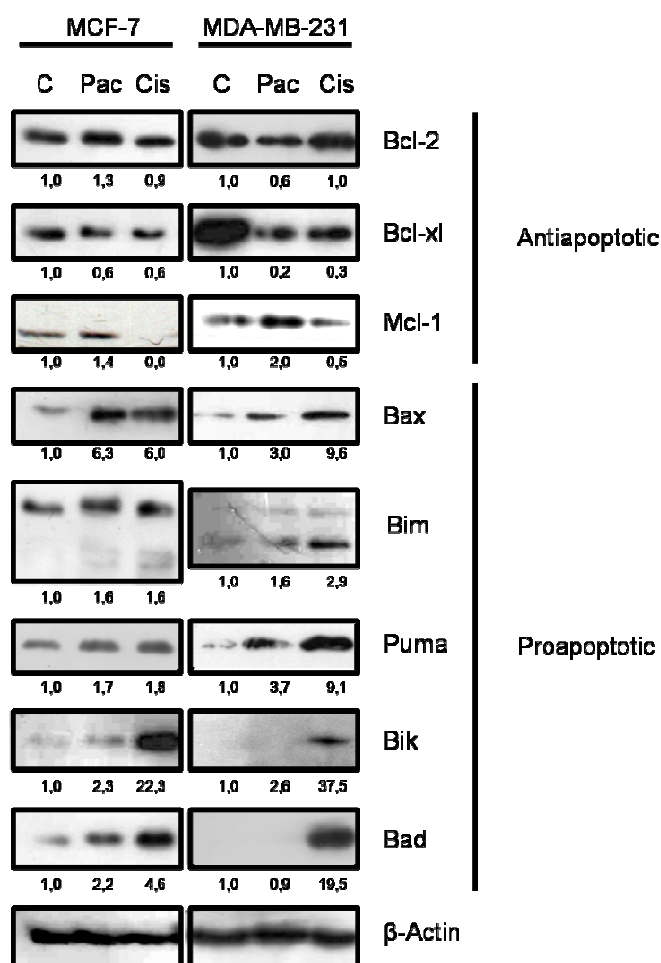


Figure 3. 4. The expression of Bcl-2 family members in response to paclitaxel/cisplatin.

MCF-7 and MDA-MB-231 cells were treated with paclitaxel or cisplatin for 48 hours and total cell lysates were subjected to immunoblotting. The results of the densitometric analysis were given as numbers below the related bands. β -Actin was used as a loading control.

The results showed that proapoptotic members, Bax, Bim, Puma, Bik and Bad, were upregulated in both cell lines and drug treatments. However, the increase in their expression was more prominent in cisplatin treated cells. Moreover, anti-apoptotic members, Bcl-2, Bcl-xl and Mcl-1, were all downregulated in chemosensitive MCF-7 cells following cisplatin treatment. In MDA-MB-231 cells, while Bcl-2 expression did not indicate a significant change, Bcl-xl and Mcl-1 were downregulated upon cisplatin

treatment. On the other hand, paclitaxel treatment did not demonstrate a pattern as distinct as in cisplatin treated cells according to densitometric analysis.

As mentioned before, FOXO3 is known as the transcriptional regulator of Puma and Bim. It was previously reported that MCF-7 cells express higher amount of FOXO3 than MDA-MB-231 cells which may influence the cell death response in response to several chemotherapeutics [162]. To check this differential expression pattern in our experimental setup, we obtained total cell lysates from MCF-7 and MDA-MB-231 cells for immunoblot analysis and detected at least 2-fold less amount of FOXO3 in MDA-MB-231 cells than MCF-7 cells (Figure 3. 5).

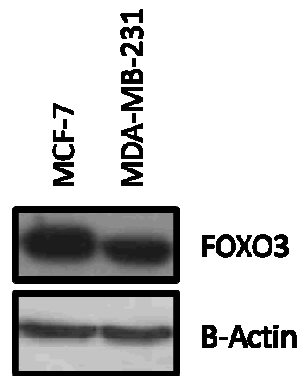


Figure 3. 5. Expression of FOXO3 in MCF-7 and MDA-MB-231 cells. Total proteins were isolated from the cells under normal conditions and immunoblotted with anti-FOXO3 antibody. β -Actin was used as a loading control.

Previously, a study with a special focus on FOXO3-paclitaxel relationship in breast cancer cells was published showing the upregulation of FOXO3 following 24-hour paclitaxel treatment [162]. The aim of our research was to investigate FOXO3 activation in early time points in order to study the effect of NF κ B pathway on FOXO3. Thus, according to our data and published other studies, we eliminated paclitaxel and used only cisplatin as a chemotherapeutic drug for further experiments.

3.4. Transcriptional upregulation of DNA damage protein GADD45 α

Cisplatin mainly induces the formation of DNA adducts which lead to activation of DNA repair mechanism. Although low concentrations of cisplatin can be compensated by this repair mechanism within the cells, the amount used in chemotherapy generally causes irreversible DNA damage triggering the cell death signaling. However, in chemoresistant cancer cells, sequential mutations occurred during carcinogenesis and uncontrolled cell divisions may cause a downregulation in DNA repair and cell cycle check point control. GADD45 α is a DNA damage response and growth arrest protein that can be induced by cisplatin [169, 208-209]. It is also directly activated by p53 and FOXO3 upon cisplatin exposure which then leads to cell cycle arrest through the G1 check point [210]. Because cisplatin treatment showed consistent data considering FOXO3 targets, to check the transcription of GADD45 α gene, we performed semiquantitative PCR and quantitative realtime PCR by using a specific set of primers to amplify GADD45 α mRNA (Figure 3. 6). According to semiquantitative PCR and realtime PCR results, cisplatin treatment clearly upregulated GADD45 α transcription in MCF-7 cells indicating FOXO3 activation. In MDA-MB-231 cells, GADD45 α transcription did not show a significant change in semiquantitative PCR results and showed a slight decrease in realtime PCR analysis.

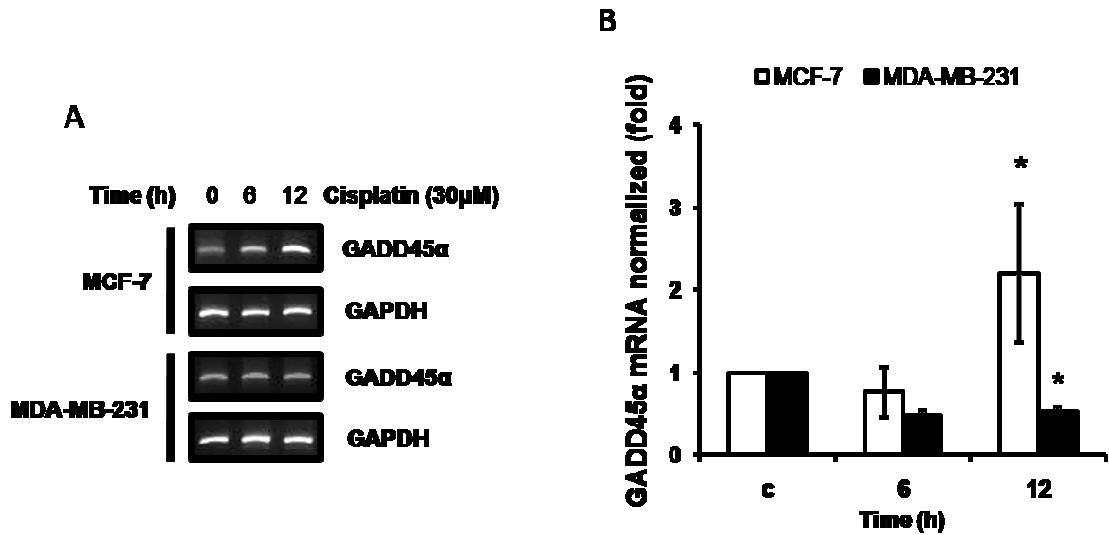


Figure 3. 6. The effect of cisplatin treatment on GADD45 α transcription. MCF-7 and MDA-MB-231 cells were treated with cisplatin and total mRNAs were isolated in indicated time points. **(A)** Semi quantitative PCR was performed using specific primers for GADD45 α mRNA. GAPDH was used for loading control. **(B)** Quantitative realtime PCR was performed with triplicates and the results were normalized with GAPDH.

3.5. Cisplatin induces apoptosis in MCF-7 and MDA-MB-231 cells.

To analyze the type of cell death induced by cisplatin, we interrogated the cellular levels of autophagy marker protein; LC3, apoptosis markers; cleaved caspase 9, cleaved caspase 3, cleaved caspase 7, cleaved PARP, BH3-only Bcl-2 family members; Bim, Puma and an important tumor suppressor; p53 by immunoblotting (Figure 3. 7).

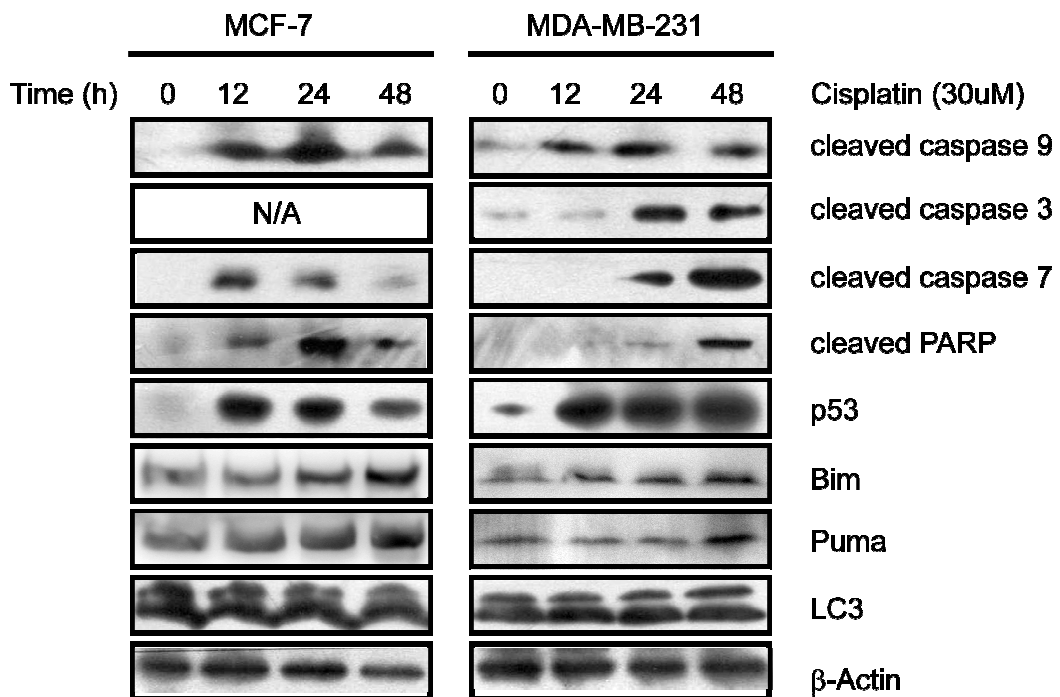


Figure 3. 7. Cisplatin-induced apoptosis in MCF-7 and MDA-MB-231 cells. Cells were treated with 30 μ M cisplatin for indicated time points. Total cell lysates were analyzed by immunoblotting with the antibodies specific to cell death-related proteins. β -Actin was used as a loading control.

According to the immunoblotting results, increases in the level of cleaved caspase 9, 3, 7 and cleaved PARP indicate that cisplatin treatment induced apoptosis in both MCF-7 and MDA-MB-231 cells. Additionally, pro-apoptotic FOXO3 target proteins Bim and Puma were upregulated and the level of LC3 forms (LC3-I and LC3-II) did not change significantly after cisplatin treatment. Interestingly, while MCF-7 cells harboring wild type p53 showed an increase in p53 expression after cisplatin treatment, p53 levels in MDA-MB-231 cells were also elevated even though MDA-MB-231 cells have a mutant form of p53 [211].

3.6. NF κ B pathway in response to cisplatin

To investigate the effect of cisplatin on NF κ B pathway, cells were treated with cisplatin in a time dependent manner and total proteins were analyzed by

immunoblotting (Figure 3. 8). While MCF-7 cells showed a decreased IKK activation even 30 min after cisplatin treatment, IKK activity in MDA-MB-231 cells was not affected as fast as in MCF-7 cells. Of note, total FOXO3 was slightly upregulated in both cell lines.

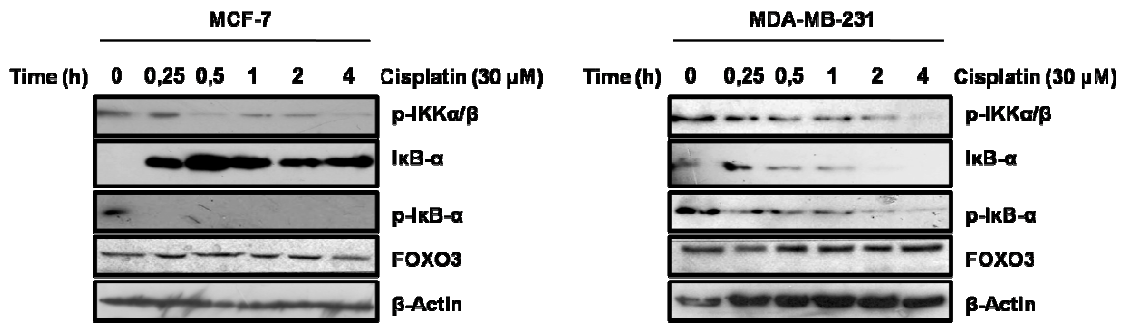


Figure 3. 8. Effect of cisplatin on NFκB pathway. MCF-7 and MDA-MB-231 cells were treated with cisplatin for indicated time points. Total cell lysates were then analyzed by immunoblotting using the antibodies against NFκB pathway proteins and FOXO3. β-Actin was used as a loading control.

3.7. Cisplatin induces nuclear translocation of FOXO3 in MCF-7 but not in MDA-MB-231 cells

The transcription activity of FOXO3 mainly depends on its nuclear shuttling upon a stimulus. Because the total protein level of FOXO3 shown in Figure 3. 5 cannot indicate its transcriptional activation, cytoplasmic and nuclear protein fractions were obtained separately at indicated time points to investigate the localization of FOXO3 in MCF-7 and MDA-MB-231 cells (Figure 3. 9). Immunoblotting results clearly showed that FOXO3 was translocated to the nucleus in MCF-7 cells after 1-hour cisplatin treatment. On the other hand, cisplatin treatment did not significantly change the localization of FOXO3 in MDA-MB-231 cells. Additionally, it was observed that the amount of cytoplasmic FOXO3 slightly increased after 15 minutes of cisplatin treatment in both cell lines. In our study, a substantial amount of FOXO3 had been always evident

in both nuclear and cytoplasmic fractions of MDA-MB-231 cells contrary to a reported study [212].

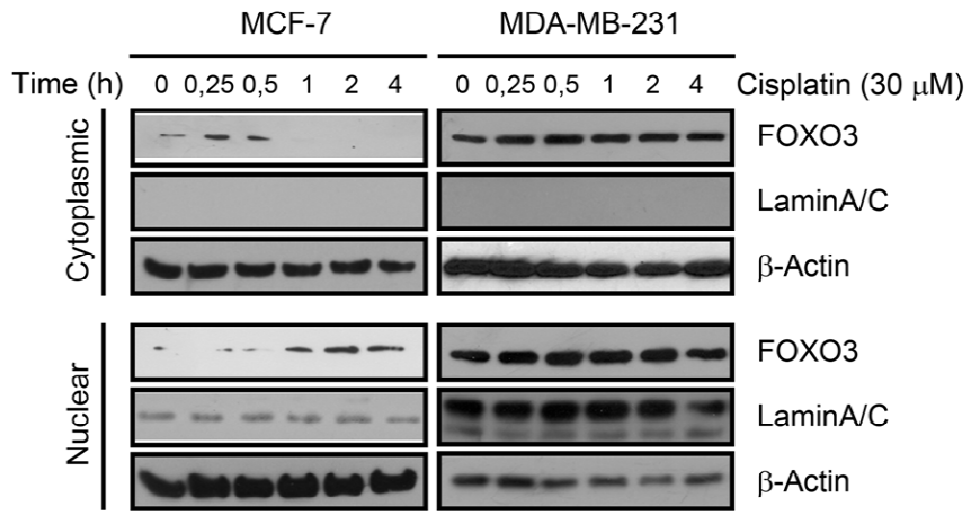


Figure 3. 9. Cisplatin-induced translocation of FOXO3. Following cisplatin treatment, cytoplasmic and nuclear proteins were separately extracted from breast cancer cells at early time points and subjected to immunoblotting. β -Actin and LaminA/C antibodies were used as controls.

Following the localization studies, to determine the DNA-binding ability of FOXO3 in MCF-7 cells, nuclear fractions were subjected to electrophoretic mobility shift assay (EMSA) by using radioactively labeled FOXO3 consensus oligonucleotides (Figure 3. 10). The results showed that nuclear FOXO3 bound to its consensus sequence in MCF-7 cells and consistent with localization results shown in Figure 3. 9, DNA binding ability of FOXO3 did not change in chemoresistant MDA-MB-231 cells.

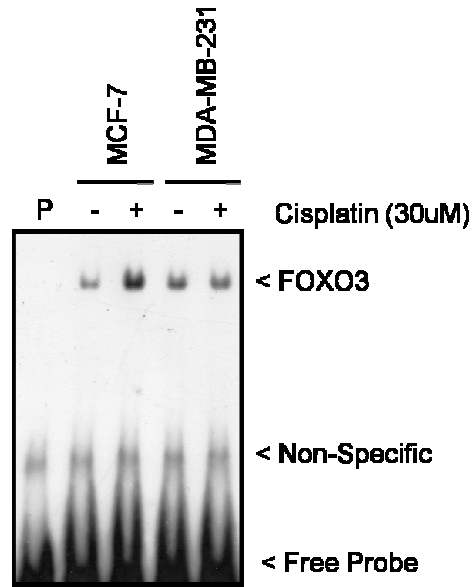


Figure 3. 10. Cisplatin-induced FOXO3 activation. Nuclear proteins were subjected to EMSA by incubation with radioactively labeled FOXO3 consensus oligonucleotide probes after 1-hour cisplatin treatment or without treatment (P; Probe only).

3.8. Transfection of siFOXO3 decreases FOXO3 target gene expression and induces the proliferative activity of MCF-7 cells.

The basal level of FOXO3 expression may vary in different cell types and the amount of FOXO3 in the cells may constitute diverse cellular characteristics [213]. Here, we proposed that high FOXO3 level in MCF-7 cells might be associated with cisplatin chemosensitivity. Thus, we performed RNA interference technique in MCF-7 cells by using siFOXO3 or non-silencing siRNA to mimic the low level of FOXO3 in MDA-MB-231 cells. After siRNA transfection, protein lysates were immunoblotted with the indicated antibodies to check FOXO3 expression (Figure 3. 11). Immunoblotting results showed a significant decrease in FOXO3 level after siRNA transfection as in its pro-apoptotic target proteins Bim and Puma. Additionally, MTT proliferation assay showed that silencing of FOXO3 promoted the proliferative activity of MCF-7 cells (137% proliferation) in agreement with another study on human bladder cancer cells [214].

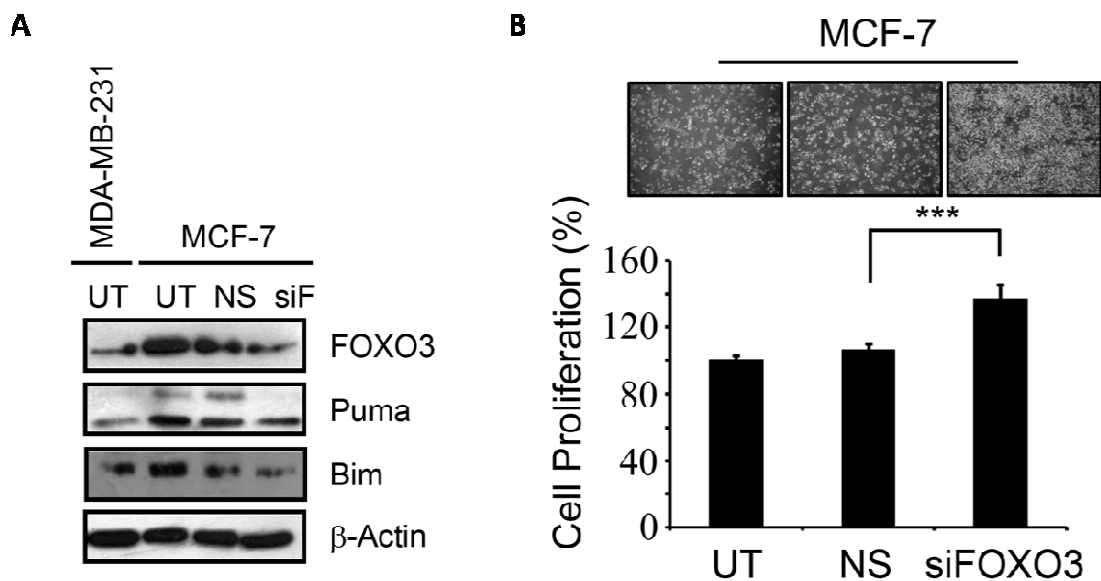


Figure 3. 11. Silencing of FOXO3 expression in MCF-7 cells. MCF-7 cells were transfected with FOXO3 silencing (siF) siRNA, non-silencing (NS) siRNA or left untransfected (UT). **(A)** Total cell lysates were analyzed by immunoblotting to confirm silencing effect and downregulation of FOXO3 target gene expression; Bim and Puma. Untransfected MDA-MB-231 cells were shown for the comparison of FOXO3 levels. β -Actin was used as a loading control. **(B)** MTT Cell Proliferation assay was performed after 48 hours following transfection. The results represent the mean (\pm SEM) values obtained from at least three independent experiments (**= $p < 0.001$).

3.9. FOXO3 silencing inhibits cisplatin-induced cell death in MCF-7 cells

To understand the role of FOXO3 in cisplatin-induced cell death, siFOXO3 transfected, non-silencing siRNA transfected and untransfected cells were treated with cisplatin. Cell death response was then assayed by immunoblotting and Annexin-V staining (Figure 3. 12). Data showed that silencing of FOXO3 not only caused a decrease in caspase 9 cleavage and p53 level, but also significantly diminished cisplatin-induced cell death in MCF-7 cells. These results further support the essential role of FOXO3 in cisplatin-induced apoptosis in MCF-7 cells.

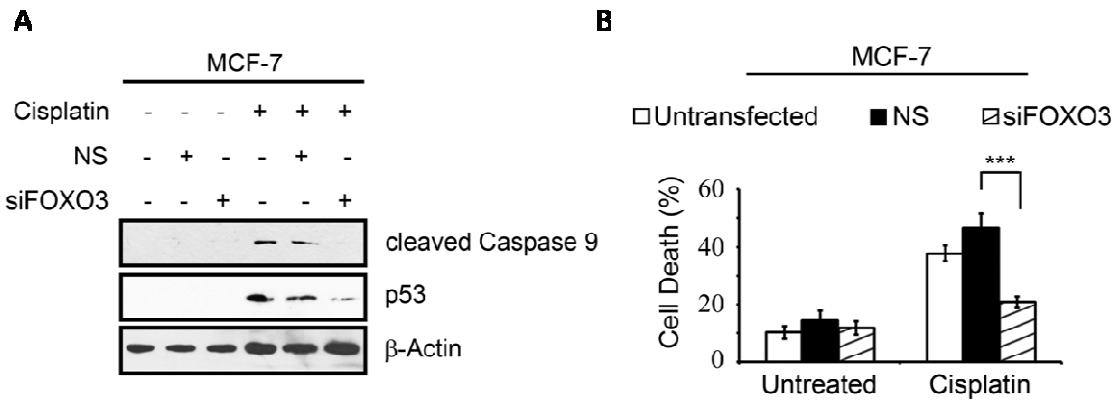


Figure 3. 12. Apoptotic response in siFOXO3 transfected MCF-7 cells. **(A)** siFOXO3 transfected or Non-silencing siRNA (NS) transfected MCF-7 cells were analyzed by immunoblotting using antibodies against cleaved caspase 9 and p53. β -Actin was used as a loading control. **(B)** Untransfected, siFOXO3 or non-silencing (NS) siRNA transfected MCF-7 cells were treated with cisplatin for 48 hours and incubated with FITC-Annexin-V, then analyzed by FACS (***= $p < 0.001$).

3.10. Overexpression of FOXO3 potentiates cisplatin-induced cell death in MDA-MB-231 cells

In order to further investigate the effect of FOXO3 expression level in cell death response, MDA-MB-231 cells that express relatively low FOXO3 were transfected with either wild type FOXO3 encoding expression plasmid or mock vector. Transfected MDA-MB-231 cells were then exposed to cisplatin for 48 hours and cell lysates were immunoblotted with the antibodies indicated (Figure 3. 13). Overexpression of FOXO3 increased the level of Bim and Puma concurrently with a rise in the cell death response in MDA-MB-231 cells. It was also observed in EMSA results that FOXO3 overexpression increased the amount of FOXO3 bound to DNA in nuclear extracts. The results indicate that FOXO3 level is critical for the modulation of cisplatin-induced cell death in MDA-MB-231 cells.

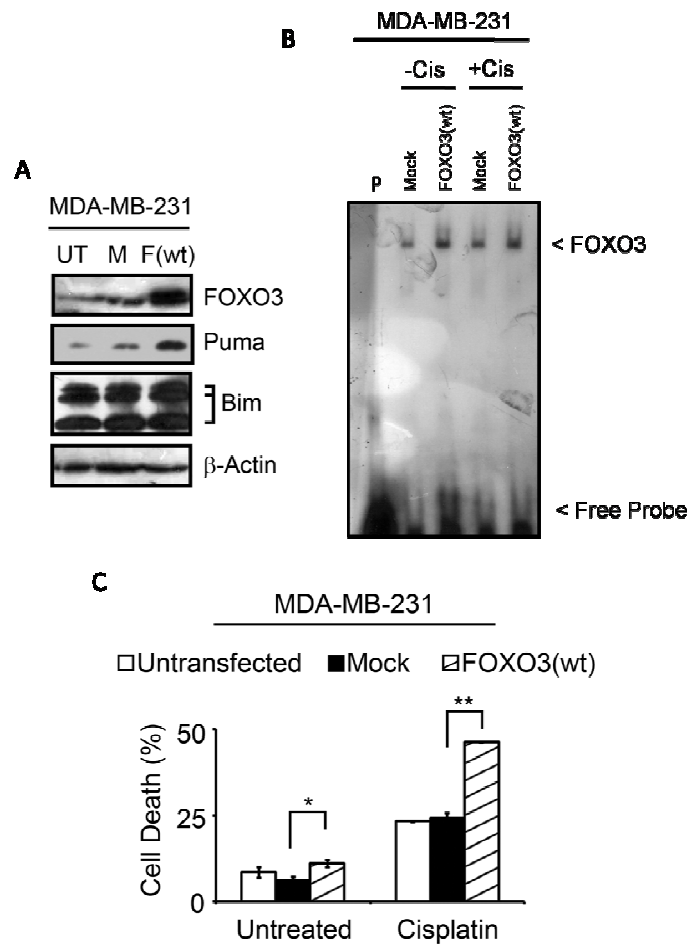


Figure 3. 13. Overexpression of FOXO3 in MDA-MB-231 cells. **(A)** MDA-MB-231 cells were transfected with pECE-HA-FOXO3(wt) expression plasmid (F(wt)), mock vector (M) or left untransfected (UT). The effect of the transfection was analyzed by immunoblotting. **(B)** Nuclear proteins isolated from transfected cells were subjected to EMSA by incubation with radioactively labeled FOXO3 consensus oligonucleotide probes after 1-hour cisplatin treatment or without treatment (P; Probe only). **(C)** pECE-HA-FOXO3(wt), mock vector (M) transfected of untransfected (UT) MDA-MB-231 cells were treated with cisplatin for 48 hours and cell death analysis with FITC-Annexin-V staining was determined by FACS (*= $p < 0.05$, **= $p < 0.01$).

3.11. Overexpression of IKK subunits and their effects on cell proliferation and viability

Activation of the IKK complex is a tightly regulated, highly stimulus-specific, and target-specific event that is essential for the functions attributed to NF κ B and other targets. While the reports revealing NF κ B-independent roles of IKK members are progressively increased in the scientific literature [215], understanding those complex relationships became more essential for the therapy strategies. As a starting point, we first transfected MCF-7 and MDA-MB-231 cells with the expression plasmids encoding the different subunits of IKK complex (IKK α , IKK β and IKK γ) along with the mock plasmid. Total cell lysates were immunoblotted with the specific antibodies (HA and Flag) to visualize the exogenous expression of the subunits in both cell lines (Figure 3. 14).

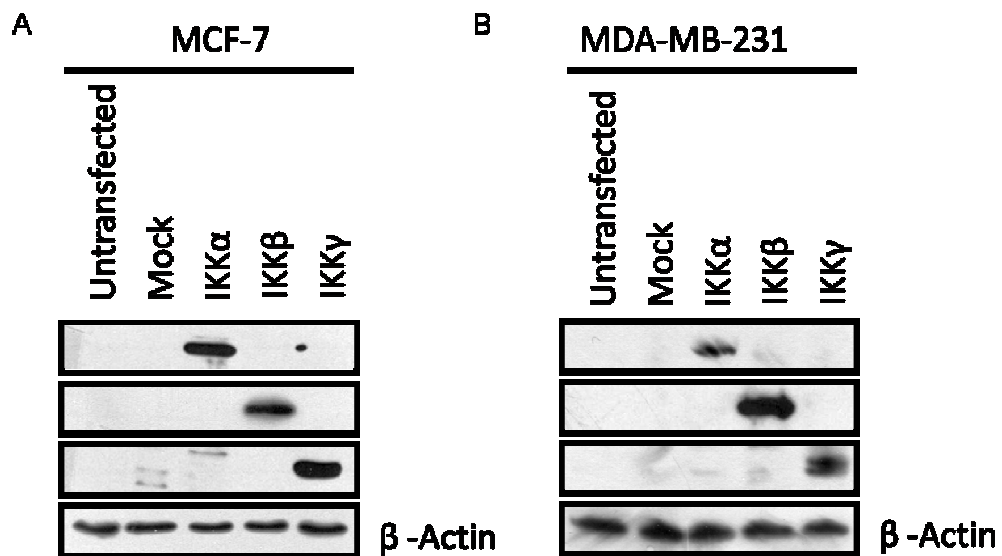


Figure 3. 14. Overexpression of IKK subunits. (A) MCF-7 and (B) MDA-MB-231 cells were transfected with IKK α , IKK β or IKK γ expression plasmids and total lysates were immunoblotted with Flag or HA specific antibodies. β -Actin was used as a loading control.

Following the successful transfection of IKK subunits, transfected cells were treated with cisplatin or left untreated for another 48 hours and subjected to MTT-based proliferation/cell viability assay (Figure 3. 15).

The results demonstrated that while overexpression of IKK β increases cell proliferation, IKK γ overexpression appears to inhibit proliferation in MCF-7 cells suggesting that IKK β somehow promotes proliferation and the regulatory subunit IKK γ has a role in growth inhibition. Apparently, transfection of IKK α did not alter proliferation, but caused a significant increase in cell viability after cisplatin treatment. On the other hand, overexpression of IKK subunits did not affect cell viability or proliferation in MDA-MB-231 cells.

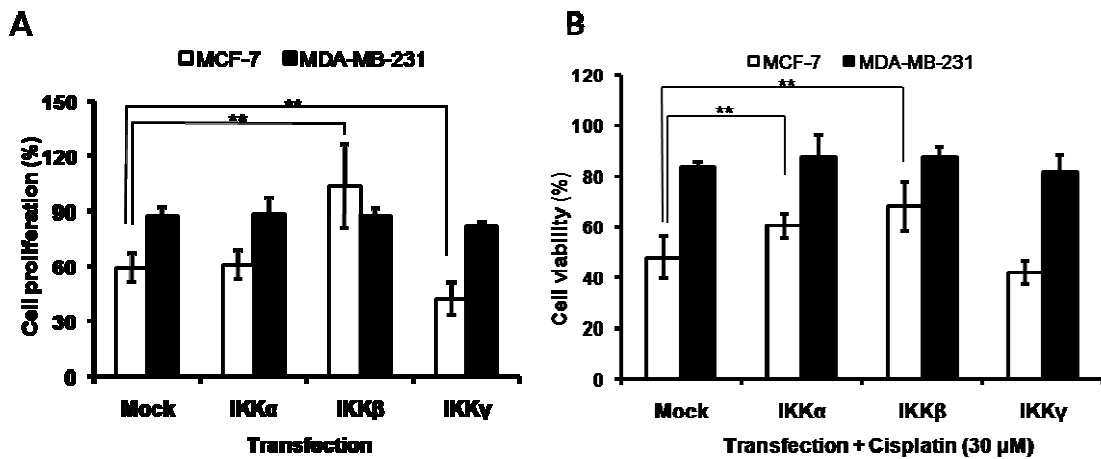


Figure 3. 15. Effect of IKK overexpression on cell proliferation and viability. MCF-7 and MDA-MB-231 cells were transfected with pCMV-IKK β , pCMV-IKK α , pCMV-IKK γ or mock plasmids. (A) The proliferative activity of transfected cells was determined by MTT proliferation assay. (B) Transfected cells were treated with cisplatin for 48 hours and cell viability was detected. The results represent the mean (\pm SEM) values obtained from at least three independent experiments (***)= $p < 0.001$)

3.12. Differential interaction between FOXO3 and IKK β

To identify the interaction between FOXO3 and IKK β , we co-immunoprecipitated endogenous FOXO3 and IKK β with indicated antibodies and the precipitates were subjected to immunoblotting (Figure 3. 16). The results showed that IKK β physically interacts with FOXO3 in MCF-7 cells under normal conditions; however, 1-hour cisplatin treatment appears to be adequate for the loss of FOXO3-IKK β interaction. Oppositely, this interaction takes place only after cisplatin treatment in MDA-MB-231 cells.

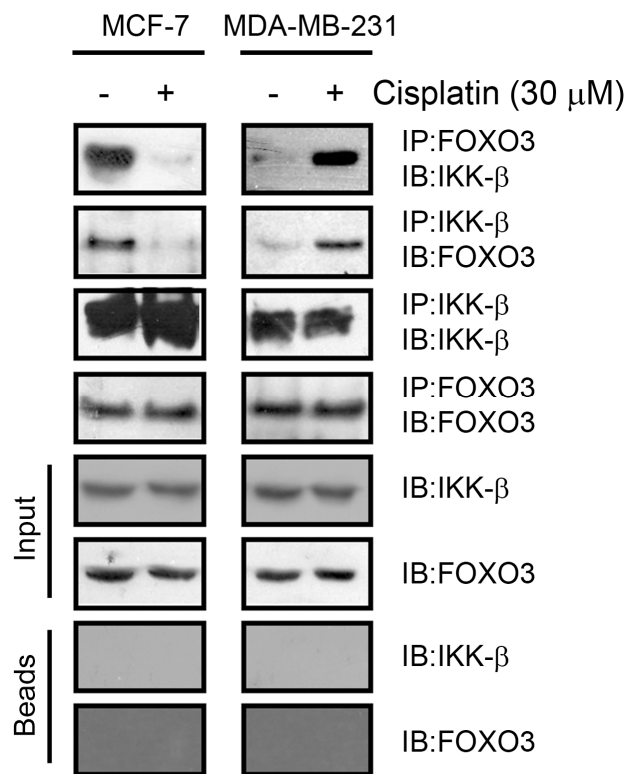


Figure 3. 16. IKK β interacts with FOXO3. MCF-7 and MDA-MB-231 cells were treated with cisplatin for 1 hour or left untreated. Total cell lysates were preincubated with G-protein coated beads to clear the cell lysates from proteins that unspecifically bind to sepharose beads. The beads alone were subjected to immunoblotting (shown as Beads). Cell lysates were pulled down (IP) with anti-FOXO3 or anti-IKK β antibodies.

Immunoprecipitates were then captured by sepharose beads and probed with the indicated antibody (IB) for the immunoblotting analysis.

3.13. IKK β sequesters FOXO3 in the cytoplasm

Since MCF-7 and MDA-MB-231 cells show different sensitivities to cisplatin treatment, we speculated that IKK β in MDA-MB-231 cells might have a role in inhibiting FOXO3 and accordingly decreasing cell death response. To elucidate the importance of the ratio between FOXO3 and IKK β , we transfected MCF-7 cells with IKK β expression plasmid and treated with cisplatin for 1 hour or left untreated. Nuclear and cytoplasmic protein fractions were then immunoblotted (Figure 3. 17). The results indicate that overexpression of IKK β induced the accumulation of endogenous FOXO3 in the cytoplasm; moreover, IKK β expressing MCF-7 cells seemed to promote FOXO3 degradation.

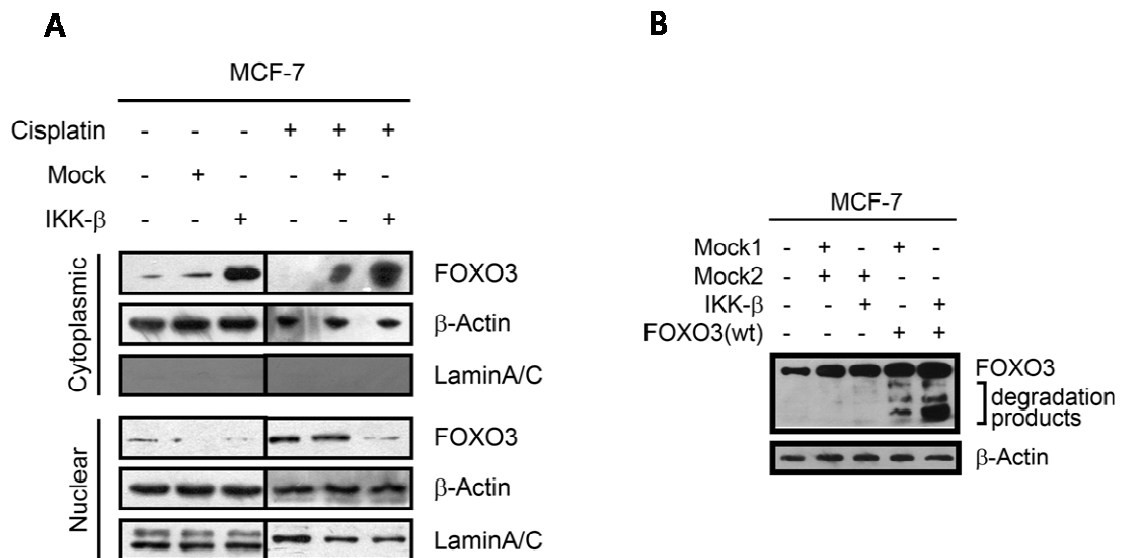


Figure 3. 17. IKK β sequesters FOXO3 in the cytoplasm. **(A)** MCF-7 cells were transfected with pCMV-flag-IKK β , mock plasmid or left untransfected and treated with cisplatin for 1 hour. Cytoplasmic and nuclear fractions were subjected to immunoblotting with the antibodies indicated. β -Actin and LaminA/C were used as controls. **(B)** MCF-7 cells were cotransfected with pCMV-flag-IKK β and pECE-HA-FOXO3(wt) vectors or with their mock vectors (Mock1; pCMV-flag empty vector, Mock2; pECE-HA empty vector). 48 hours after transfection, cell lysates were immunoblotted with anti-FOXO3 antibody to visualize the degradation products. β -Actin was used as a loading control.

We had found above that IKK β physically interacted and inhibited FOXO3, additionally, FOXO3 overexpressing MDA-MB-231 cells showed an increased cell death response in response to cisplatin. According to the data observed, we hypothesized that, after the balance between IKK β and FOXO3 were diminished because of FOXO3 overexpression, the endogenous level of IKK β might not achieve to inhibit all FOXO3 molecules in FOXO3 overexpressing MDA-MB-231 cells. Thus, to find out whether the excess amount of FOXO3 (unbound to IKK β) can be detected in immunoblotting, MDA-MB-231 cells were transfected with FOXO3(wt) expression plasmid, exposed to cisplatin for 1 hour and endogenous IKK β was immunoprecipitated. Supernatants were then subjected to immunoblotting along with precipitates using anti-FOXO3 polyclonal antibody (Figure 3. 18). The results indicate that FOXO3 overexpression causes an increase in cisplatin-induced cell death because of the fact that endogenous IKK β is unable to capture all FOXO3 proteins. Consequently, free FOXO3 molecules are able to translocate to the nucleus and regulate its target gene expression as previously shown in Figure 3. 13.

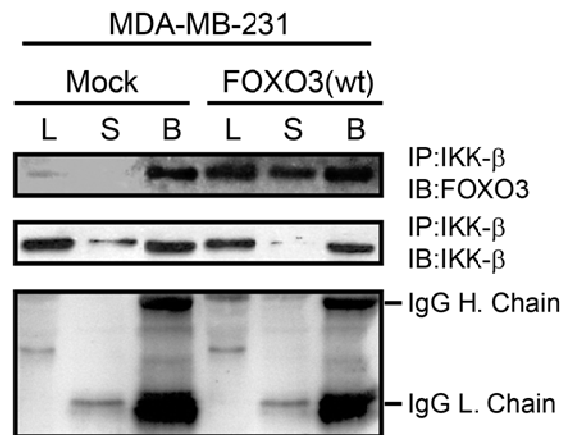


Figure 3. 18. Sequestering FOXO3 is limited to IKK β level. Total cell lysates of pECE-HA-FOXO3(wt) and mock vector transfected MDA-MB-231 cells were first incubated with anti-IKK β antibody and then G-protein coated beads. Fractions of immunoprecipitation (L; lysate, S; supernatant, B; beads) were analyzed by immunoblotting with the help of anti-FOXO3 and anti-IKK β antibodies. IgG fragments were shown as a control (H. Chain; Heavy Chain, L. Chain; Light Chain)

3.14. Chemical inhibition of IKK allows nuclear translocation of FOXO3 in MDA-MB-231 cells

Since the kinase activity of IKK α subunit can also influence FOXO3 inhibition and the effect of IKK γ on FOXO3 is not known yet, we have inhibited IKK complex by chemical means rather than silencing all subunits by RNA interference. We used IKK inhibitor-II which specifically inhibits IKK complex without effecting Akt pathway [216]. To find out whether chemical inhibition of IKK complex alters FOXO3 localization in MDA-MB-231 cells, we treated MDA-MB-231 cells with only IKK inhibitor-II and obtained subcellular protein fractions to be subjected to immunoblotting (Figure 3. 19. A). The results showed that IKK-II inhibitor promoted FOXO3 translocation into the nucleus after 1-hour treatment. While cisplatin treatment in MDA-MB-231 cells does not significantly change the level of active FOXO3 in the nucleus, it was increased by cisplatin together with IKK inhibitor-II pretreatment (Figure 3. 19. B). These results indicate that inhibition of IKK complex promotes the function of FOXO3 by inducing its nuclear translocation. The immunoblotting results obtained with the antibodies against FOXO3 targets also showed an increase in the expression of Bim and Puma after IKK inhibition (Figure 3. 19. C). Interestingly, although Bim and Puma levels were increased upon IKK inhibitor-II treatment only, pretreatment of IKK inhibitor-II followed by cisplatin downregulated Bim and Puma (data not shown). Conversely, the cells exposed to IKK inhibitor-II and cisplatin together showed an increased cell death compared to only cisplatin treated cells suggesting that a non-apoptotic or Bim/Puma-independent cell death process might be involved (Figure 3. 19. D).

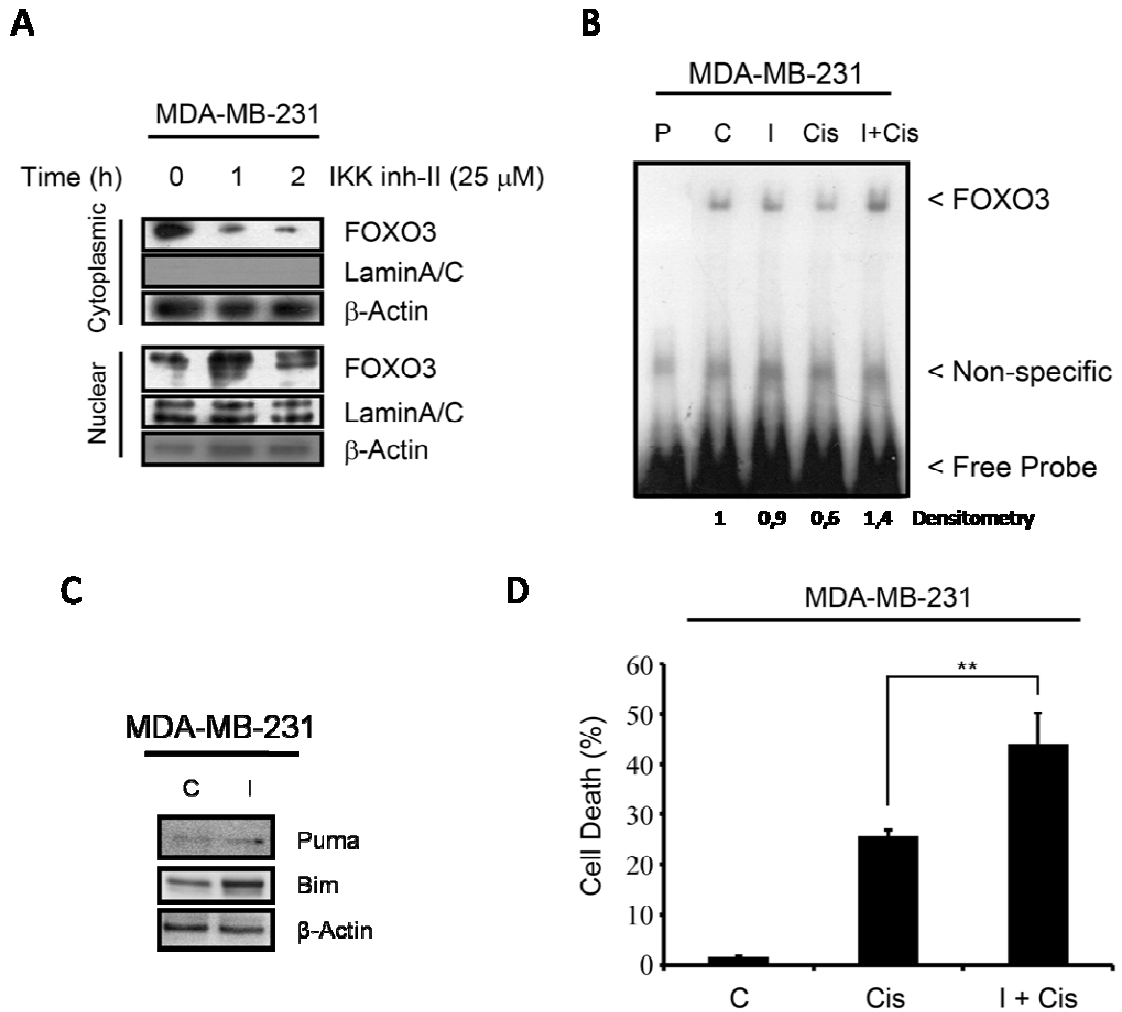


Figure 3. 19. Inhibition of IKK activates FOXO3. **(A)** MDA-MB-231 cells were treated with IKK inhibitor-II for indicated time points and subcellular fractions were subjected to immunoblotting. β -Actin and LaminA/C were used as controls. **(B)** MDA-MB-231 cells were pretreated with IKK inhibitor-II (30 minutes) and treated with cisplatin for 1 hour, and then nuclear lysates were analyzed by EMSA with radioactively labeled FOXO3 consensus oligonucleotides (P; Probe only, C; Control, I; IKK inhibitor-II, Cis; cisplatin). **(C)** Total lysates of untreated (shown as C), IKK inhibitor-II pretreated (shown as I) cells were appraised by immunoblotting using anti-Bim and anti-Puma antibodies. β -Actin was used as a loading control. **(D)** MDA-MB-231 cells were treated with only Cisplatin (Cis) or pretreated with IKK inhibitor-II and treated with Cisplatin (I+ Cis) for 48 hours, and then incubated with FITC-Annexin-V, along with untreated control (shown as C), to determine cell death response (**= $p < 0.01$).

3.15. Ser-644 residue on FOXO3 is essential for cisplatin resistance in MDA-MB-

231 cells

It was previously shown that IKK β is able to phosphorylate Ser-644 residue on FOXO3. To find out whether this phosphorylation site has a significant role on chemoresistance, we made use of a mutant FOXO3 plasmid encoding FOXO3(S644A) protein. This mutant protein product has alanine amino acid instead of serine on the residue 644 and cannot be phosphorylated by IKK β . MDA-MB-231 cells were transfected with mock, FOXO3(wt) or FOXO3(S644A) expression plasmids and subjected to MTT cell viability assay (Figure 3. 20). MTT results showed that MDA-MB-231 cells transfected with FOXO3(S644A) plasmid became significantly cisplatin-sensitive indicating the inability of IKK β for sequestering the mutant variant of FOXO3 due to the absent phosphorylation site. Here, we can specify IKK β as a regulator of chemoresistance in MDA-MB-231 cells which performs its function through phosphorylation and inhibition of FOXO3.

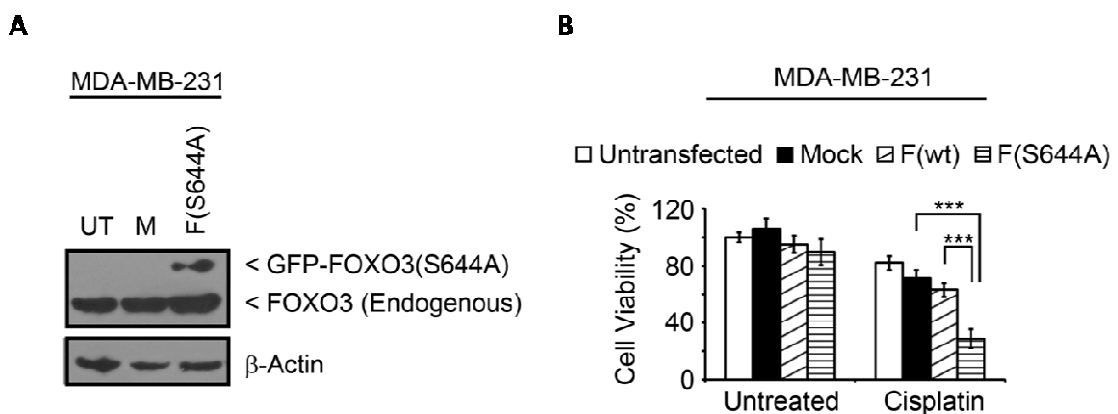


Figure 3. 20. Transfection of mutant FOXO3 decreases cell viability in response to cisplatin. MDA-MB-231 cells were transfected with either pEGFP-FOXO3(S644A) (F(S644A)) or mock (M) vector in addition to untransfected control (UT). (A) Total cell lysates were immunoblotted with anti-FOXO3 antibody to check the transfection. β -Actin was used as a loading control. (B) MDA-MB-231 cells were transfected with Mock, wild type FOXO3 encoding (F(wt)), mutant FOXO3 encoding (F(S644A)) vectors or left untransfected. Cells were analyzed by MTT cell viability assay 48 hours after cisplatin treatment (**= $p < 0.01$, ***= $p < 0.001$).

3.16. FOXO3 overexpression induces autophagy in MDA-MB-231 cells after cisplatin treatment

To investigate the type of cell death in FOXO3 overexpressing MDA-MB-231 cells, transfected cells were fixed, permeabilized and labeled with cleaved caspase 3 monoclonal antibody for FACS analysis (Figure 3. 21. A). While untransfected and mock transfections showed active caspase 3 positive cells (29% and 26% respectively), cells expressing high level of FOXO3 did not show a significant change in caspase 3 cleavage after cisplatin treatment (14%).

To monitor the aspect of caspase 9, the upstream protease of caspase 3, FOXO3(wt) plasmid transfected cells were subjected to immunoblotting for the detection of caspase 9 cleavage. Results showed a loss of caspase 9 cleavage following cisplatin treatment explaining the undetectable cleaved caspase 3. Moreover, cisplatin treatment also downregulated Bim and Puma expression indicating the suppression of pro-apoptotic signals in FOXO3 overexpressing MDA-MB-231 cells. On the other hand, an increase of cytosolic LC3 level (LC3-I) was detected in FOXO3(wt) transfected cells under normal conditions, whereas after cisplatin treatment LC3-I appeared to be converted to its autophagosome-associating form, LC3-II (Figure 3. 21. B).

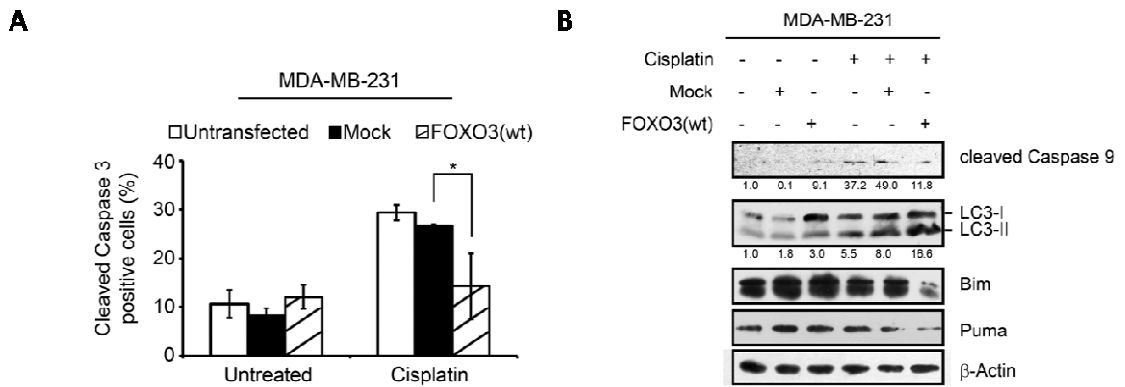


Figure 3. 21. FOXO3 overexpression diminishes cisplatin-induced apoptosis. **(A)** MDA-MB-231 cells were transfected with mock, pECE-HA-FOXO3(wt) plasmids or left untransfected. After 48 hours of transfection, cells were treated with cisplatin for 48 hours or left untreated and then incubated with a specific monoclonal antibody against cleaved caspase 3. Following required washes, cells were subjected to FITC-conjugated anti-rabbit antibody incubation. Stained cells were then analyzed by FACS. **(B)** Untransfected, mock vector or pECE-HA-FOXO3(wt) transfected cells were treated with cisplatin for 48 hours and total cell lysates were immunoblotted with the antibodies against LC3, cleaved caspase 9, Bim and Puma. Densitometry values for respective samples (indicated below the bands of cleaved caspase 9 and LC3-II) were normalized with respect to the control. β -Actin was used as a loading control.

To visualize autophagosome formation induced by cisplatin, we co-transfected MDA-MB-231 cells with FOXO3(wt) and LC3-GFP expression plasmids and treated with only cisplatin, cisplatin with 3MA (3-Methyladenine, an autophagy inhibitor) or left untreated. LC3-GFP dots were displayed by fluorescence microscopy (Figure 3. 22). Cells with autophagic dots were counted and autophagic cells were determined depending on the threshold value of the control. The results pointed that FOXO3 overexpression led to an increase in the number of autophagosomes in MDA-MB-231 cells upon cisplatin and this process can be reversed by autophagy inhibitor 3MA treatment. Additionally, it was found that neither cisplatin treatment nor excess amount of FOXO3 expression alone was adequate to trigger autophagosome formation in MDA-MB-231 cells. In this case, cisplatin acts as an autophagy inducer (43% autophagic cells) rather than a strong apoptotic agent when FOXO3 was overexpressed.

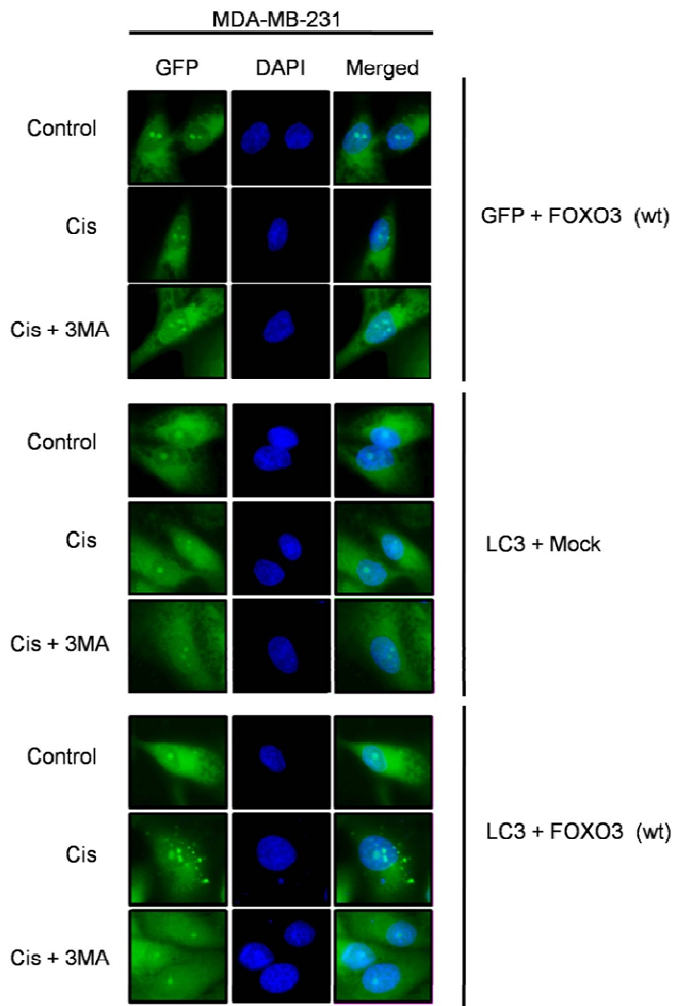
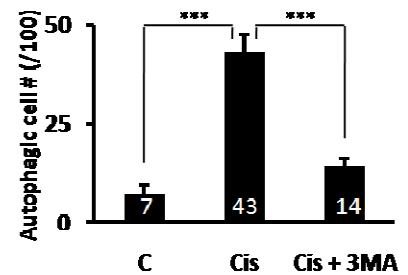
A**B**

Figure 3. 22. Cisplatin-induced autophagic cell death in FOXO3 overexpressing MDA-MB-231 cells. (A) MDA-MB-231 cells were grown on cover slides and transfected with pEGFP-LC3 and/or pECE-HA-FOXO3(wt) expression plasmids along with the required mock vectors (Mock; pECE-HA empty vector, GFP; pEGFP empty vector). Cisplatin treatment following 3MA pretreatment or only cisplatin treatment was carried out in MDA-MB-231 cells. Cover slides with fixed cells were dyed with DAPI and washed three times and then analyzed by fluorescence microscope with required filters. (B) Fluorescence dots of LC3-GFP in transfected cells, which represents autophagosomes, were counted in at least 100 cells and autophagic cell number was determined by the cells transcended the threshold value of the control.

3.17. Functional p53 is involved in sequestering FOXO3 in the cytoplasm

P53 is one of the most studied and important tumor suppressors that can induce cell death independent of its transcriptional activity [217]. Recently, several studies reported that p53 is one of the interacting partners of FOXO3 in the transcription machinery upon several cell death stimuli [218-221]. Interestingly, p53 was also shown as a FOXO3 inhibitor in response to DNA damage in mouse fibroblasts [222].

We already know the difference in p53 status of MCF-7 and MDA-MB-231 cells (MCF-7 has wild type p53, MDA-MB-231 has (R280K) p53 that cannot bind to DNA). To monitor the inhibitory effect of p53 on FOXO3, Pifithrin- α (a chemical inhibitor against the transcriptional activity of p53) [223], was used in MCF-7 cells. Cells were treated with pifithrin- α and/or cisplatin and subcellular localization of FOXO3 was analyzed (Figure 3. 23. A). In MCF-7 cells that have functional p53, pifithrin- α alone increased the level of FOXO3 in the nucleus after 3-hour treatment and cisplatin treatment combined with pifithrin- α resulted in nuclear import of FOXO3. Moreover, we transfected MDA-MB-231 cells with p53(wt) expression plasmid or mock plasmid and treated with cisplatin. Cellular fractions were again analyzed by immunoblotting for FOXO3 localization (Figure 3. 23. B). The results showed that when wild type p53 was ectopically expressed in MDA-MB-231 cells, cisplatin treatment facilitates cytoplasmic FOXO3 accumulation.

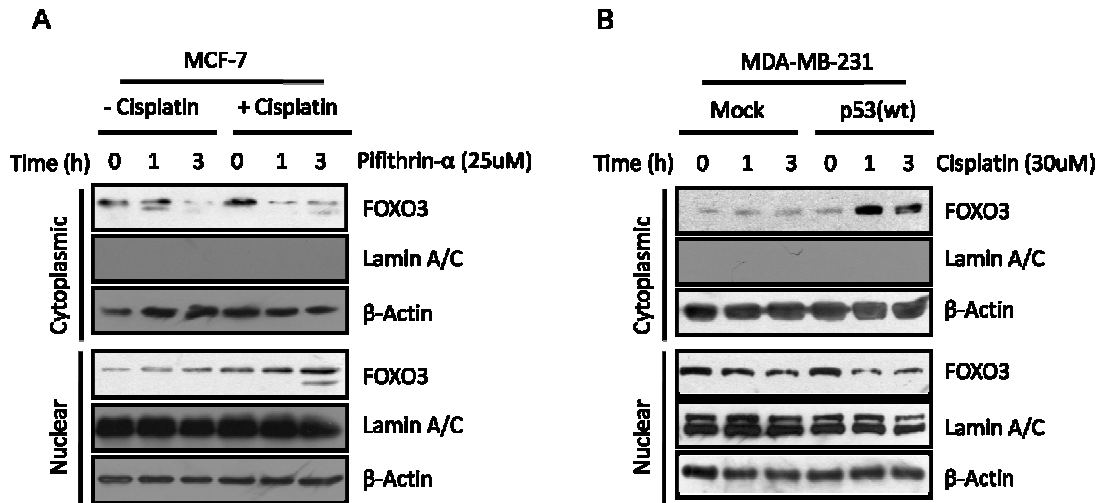


Figure 3. 23. The effect of functional p53 on FOXO3 subcellular localization in breast cancer cells. **(A)** MCF-7 cells were pretreated with 25 μM of Pifithrin-α and/or cisplatin and subcellular fractions were analyzed by immunoblotting. **(B)** MDA-MB-231 cells were transfected with pCMV-p53(wt) expression plasmid and treated with cisplatin. Then, subcellular fractions were analyzed by immunoblotting. LaminA/C and β-Actin were used as loading controls.

Needless to say, p53 status is not the only difference between MCF-7 and MDA-MB-231 cells as they have different genotypes. Thus, we tested the same experiment in wild type and $p53^{-/-}$ HCT116 colorectal cancer cells that have same genotypic background except p53 status. In wild type HCT116 cells, while only pifithrin-α treatment did not significantly change the localization of FOXO3, pifithrin-α and cisplatin combination promoted FOXO3 nuclear translocation as observed in MCF-7 cells (Figure 3. 24. A). These results suggest that cisplatin treatment following p53 inhibition causes the nuclear accumulation of FOXO3 in wild type HCT116 and MCF-7 cells. Additionally, p53(wt) expression plasmid transfected $p53^{-/-}$ HCT116 cells showed that cisplatin treatment facilitated cytoplasmic FOXO3 accumulation as in MDA-MB-231 cells while cisplatin treatment did not change FOXO3 profile before p53(wt) transfection (Figure 3. 24. B).

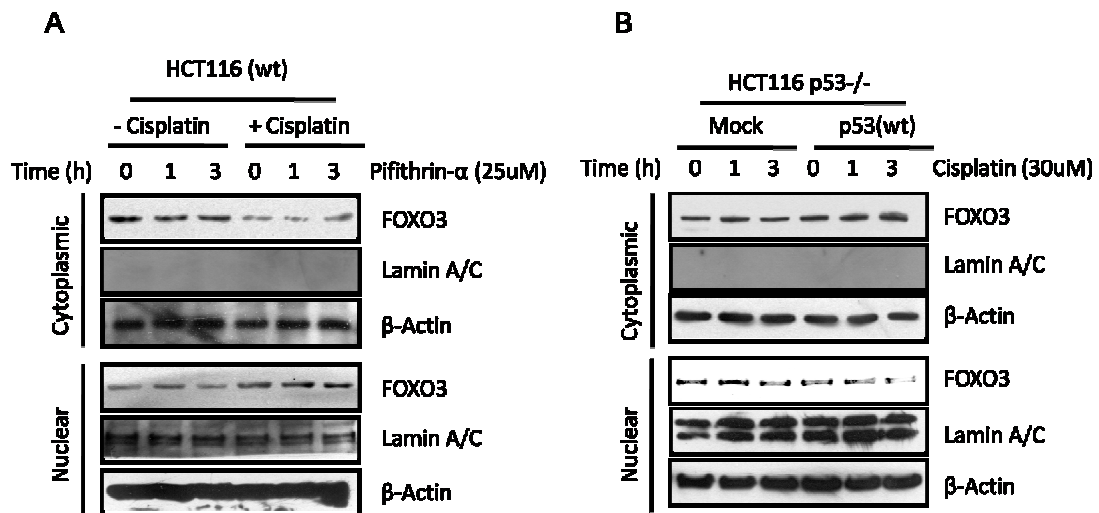


Figure 3. 24. The effect of functional p53 on FOXO3 subcellular localization in colorectal cancer cells. **(A)** Wild type HCT116 cells were pretreated with only Pifithrin- α or Pifithrin- α and cisplatin. Total cell lysates were extracted at indicated time points after treatment and subjected to immunoblotting. **(B)** $p53^{-/-}$ HCT116 cells were transfected with wild type p53 encoding expression plasmid (p53(wt)) or mock vector. Transfected cells were exposed to cisplatin for indicated time points. Cytoplasmic and nuclear lysates were obtained and subjected to immunoblotting. β -Actin and LaminA/C were used as controls.

To examine the effect of p53 status on FOXO3 localization, we also treated wild type and $p53^{-/-}$ HCT116 cells with cisplatin for 1 hour and extracted nuclear and cytoplasmic fractions to analyze FOXO3 localization without any further treatment (Figure 3. 25. A). Immunoblotting results showed that FOXO3 in $p53^{+/+}$ HCT116 cells translocated to the nucleus as in MCF-7 cells and subcellular localization of endogenous FOXO3 in $p53^{-/-}$ cells was also similar to MDA-MB-231 cells after cisplatin treatment. However, nuclear FOXO3 did not appear to bind its consensus site in wild type HCT116 cells according to EMSA results (Figure 3. 25. B). In contrast, nuclear FOXO3 in $p53^{-/-}$ cells dramatically showed an elevated DNA binding compared to wild type cells.

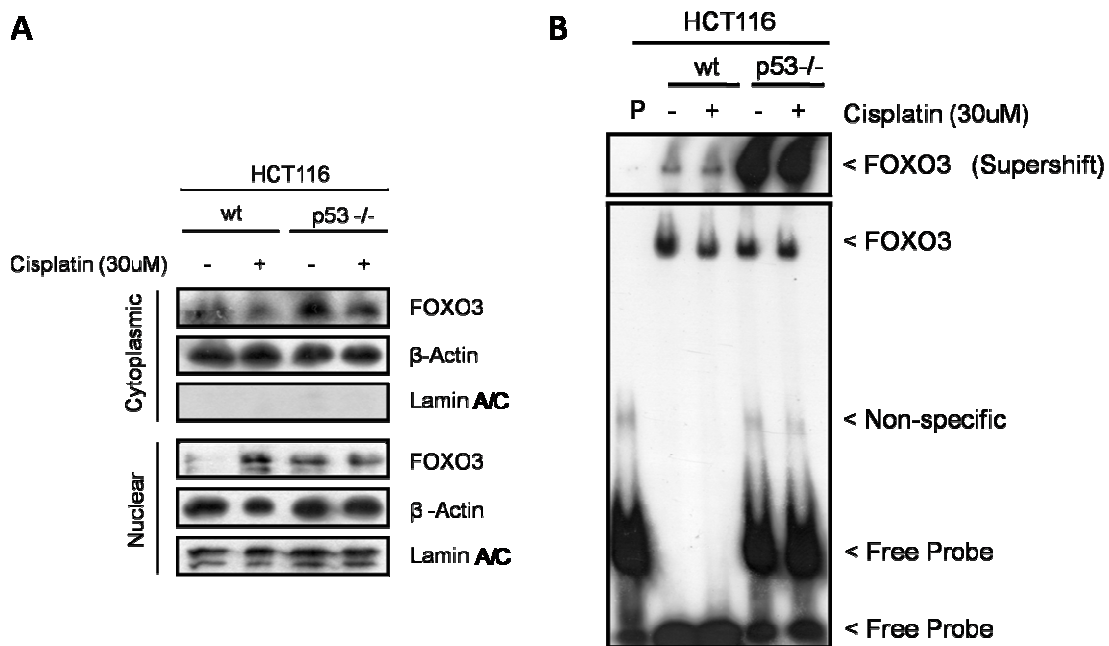


Figure 3. 25. Subcellular localization of FOXO3 in wild type and p53^{-/-} HCT116 cells. **(A)** HCT116 cells were treated with cisplatin for 1 hour and subcellular fractions were subjected to immunoblotting to determine the localization of FOXO3 in response to cisplatin. β-Actin and LaminA/C were used as controls. **(B)** Cisplatin treated and untreated cells were subjected to EMSA to analyze active FOXO3 (P; Probe only).

It has been previously demonstrated that IKK inhibitor-II sensitized MDA-MB-231 cells to cisplatin cytotoxicity (Figure 3. 19. D). Finally, we examined the effect of cisplatin and IKK inhibition on wt and p53^{-/-} colorectal cancer cells. The results demonstrated that loss of p53, differently than non-functional p53 in MDA-MB-231, enhanced the effect of cisplatin on cell death (Figure 3. 26).

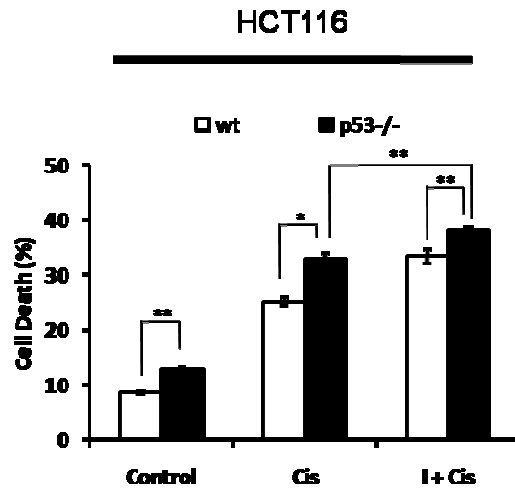


Figure 3. 26. Cell death response in HCT116 cells. HCT116 cells were treated with cisplatin (Cis) or cisplatin and IKK inhibitor-II together (I+Cis). Cells were stained with Annexin-V and death response was determined by FACS.

4. DISCUSSION AND CONCLUSION

In cancer tissues, each cell division might result in the formation of cells with aggressive behavior that show rigorous resistance to chemotherapeutics [224]. In this study, we intended to find a molecular target responsible for chemoresistance in breast cancer cells. We showed here that the direct inhibitory effect of IKK β on FOXO3 and established a signaling mechanism which has an important role in chemoresistance. By now, most of the targeted therapies were pointing out NF κ B inhibition by IKK; however, in this study, we propose that the inhibition of IKK might be a new therapy strategy against chemoresistant breast cancer cells.

Among other FOXO3-regulating kinases such as Akt, AMPK and ERK, IKK overcomes the regulatory effects of these kinases on FOXO3. The crosstalk between FOXO3 and IKK β appears to be essential for the final decision of cellular response to chemotherapeutics. We investigated that FOXO3 decides the cell fate by switching the signaling pathways towards a particular type of cell death: apoptosis or autophagy. FOXO3 acts both as a molecular mediator and a regulator of cell death by modulating the physiological consequences of activation/inactivation of both apoptosis- and autophagy-related genes.

IKK inhibitor-II is a potent inhibitor of IKK complex and blocks IKK-mediated FOXO3 inactivation. When it is used in combination with cisplatin, IKK inhibitor-II greatly potentiates the effect of cisplatin through FOXO3 activation on tumor cell growth (Figure 3. 19). Additionally, ectopic FOXO3 expression and cisplatin treatment together significantly induce cell death of chemoresistant MDA-MB-231 cells, suggesting that the dual therapy strategy involving exogenous FOXO3 gene expression with concurrent IKK inhibition may be a promising novel gene therapy modality to treat advanced breast cancers. Although cancer cells can choose either apoptosis for rapid self

execution or autophagy for generating energy and promoting survival, in each case, they ultimately undergo cellular death in response to dual therapy. In addition to cancer, identification of FOXO3 signaling may enable the development of specific and rationale therapies against pathologic conditions caused by dysregulation of apoptosis and autophagy such as neurodegenerative diseases.

4.1. FOXO3 Stability

Although FOXO3 has been studied as a substrate of Akt in most research articles, IKK β was shown to have a significant impact on FOXO3 inactivation in our study. Accordingly, inhibition of IKK complex by anti-nemo peptide has been shown to induce nuclear localization of FOXO3 in agreement with our results [138]. IKK complex not only phosphorylates FOXO3, but also regulates cellular localization and stabilization of FOXO3 (Figure 3. 17). Clearly, inhibition of FOXO3 phosphorylation at Ser-644 is sufficient to sensitize breast cancer cells to cisplatin cytotoxicity even though FOXO3 is a substrate of other potent kinases (Figure 3. 20). In this view, chemical inhibition of IKK complex might also promote FOXO3 stabilization independently of Akt activity (Figure 3. 19). Therefore, in breast cancer cells with cisplatin resistance, IKK inhibitor-II and other specific IKK inhibitors might be good candidates for combination therapy with cisplatin to enhance the tumor suppressor activity of FOXO3.

Besides the fact that the regulatory effect of IKK β on FOXO3, IKK α has been also shown to phosphorylate FOXO3 *in vitro* [186]. Overexpression studies we performed with IKK subunits (Figure 3. 14) had demonstrated the protective effect of IKK α in response to cisplatin. However, the activation of IKK complex is known to be directional. In unstimulated cells, IKK α inhibits the constitutive kinase activity of IKK β ; in stimulated cells, IKK α activity is required for the induction of IKK β [237-238]. For this reason, we speculated that IKK β might be activated by IKK α in the cells overexpressing IKK α in response to cisplatin which influenced the cell viability indirectly through IKK β activation. Additionally, statistically significant change was not observed in proliferation activity of those cells with elevated IKK α expression (Figure 3. 15).

Active ERK was demonstrated to phosphorylate FOXO3 at Ser-294, Ser-344 and Ser-425 residues and ERK-phosphorylated FOXO3 was shown to be subjected to proteosomal degradation leading to chemoresistance. ERK activation also appears to promote the cell survival by Bcl-2 upregulation and Bim degradation in cisplatin resistant ovarian cancers [239-240]. In this regard, the reason for the difference of basal FOXO3 levels in MDA-MB-231 and MCF-7 cells (Figure 3. 5) might arise from the high level of basal ERK activity observed in MDA-MB-231 cells compared to MCF-7 cells under normal conditions [241].

4.2. DNA Damage and p53

FOXO3, similar to other transcription factors, has also interacting partners which determine the gene specificity on transcription machinery. It is involved in the induction of GADD45 α transcription together with its well known partner p53 [169, 230]. It has been shown that the activation of GADD45 α transcription occurs only in cells having a wild type p53 according to the published studies [210, 231]. In our experiments, we demonstrate the absence of GADD45 α transcriptional upregulation in MDA-MB-231 cells harboring mutant p53, while MCF-7 cells show a distinct upregulation in GADD45 α mRNA level upon cisplatin exposure (Figure 3. 6). The findings suggest a mutual relationship between FOXO3 and p53 in GADD45 α gene regulation. However, the effectiveness of expressed GADD45 α protein in DNA repair mechanism is yet to be investigated.

Puma is another target gene for both FOXO3 and p53; however, transcription of Puma by FOXO3 is not necessarily p53-dependent as reported previously [232]. Although mutant p53, in theory, has a dominant negative (DN) effect on wild type p53; previous studies indicated the promoter selective DN effect of this mutant rather than acting as DN for all p53-regulated genes [233-235]. On this account, the direct or indirect regulatory effect of mutant p53 on FOXO3 remains uncertain. Moreover, a study has demonstrated that the loss of p53 enhances the catalytic activity of IKK β introducing the inhibitory effect of p53 on IKK β [236]. Hence, cellular response to

chemotherapeutic agents may also depend on this regulatory system (p53-IKK) rather than p53-FOXO3 partnership.

4.3. FOXO3 Expression

While the regulation of FOXO3 activity has been extensively studied, the control of FOXO3 gene expression is largely unknown. As examined in our study, the expression level of FOXO3 is likely to play a crucial role to determine the cellular response to cisplatin. A recently published report revealed that p53 transactivates FOXO3 by binding to the second intron of FoxO3 gene which is associated with extreme longevity in humans [242]. Plus, we observed p53 upregulation (Figure 3. 7) and a slight increase in FOXO3 expression in total lysates which is also detectable in the cytoplasmic fractions following cisplatin treatment (Figure 3. 9). In addition to the report mentioned above, our investigation shows that loss of FOXO3 impairs the stabilization of p53 protein (Figure 3. 12). In contravention of their genotypic differences, mutant p53-containing MDA-MB-231 cells and p53^{-/-} HCT116 cells have shown no difference on the localization of FOXO3 upon cisplatin treatment, on the other hand, the ectopic expression of functional p53 in these cell lines has induced the cytoplasmic accumulation of FOXO3 (Figure 3. 23 and Figure 3. 24). Accordingly, it seems conceivable that FOXO3 and p53 might regulate each others' stabilization as a feedback mechanism.

FOXO3 has also been shown to induce autophagy in muscle cells via LC3 and Bnip3 which displaces Beclin1 from Bcl-x1 [165]. In our study, it is apparent that FOXO3 level is a critical factor since deviations from IKK β -FOXO3 balance (Figure 3. 18 and Figure 3. 13) lead cells to either apoptotic or autophagic cell death (Figure 3. 21 and Figure 3. 22). FOXO3, being a key protein that can switch the stimuli to a specific type of cell death, is most likely regulated by other posttranslational modifications that can interfere its function in transcription. Acetylation, for instance, has also profound roles in nuclear shuttling and transcriptional activation/repression of FOXO transcription factors. SIRT1 is known to be responsible for FOXO3 deacetylation which promotes chemoresistance in most cases [243-244]. A previous study showed that

deacetylation of FOXO3 by SIRT1 induces cell cycle arrest proteins such as p27KIP1 and GADD45 α ; however, this deacetylation also decreases the level of proapoptotic FOXO3 target Bim [181]. These findings indicate that SIRT1 deacetylation of FOXO3 does not inevitably repress FOXO3 function, but in the end, gene selection of FOXO3 appears to support chemoresistance ultimately upon such a deacetylation. In our study, we show a rise in the LC3-I, Bim and Puma protein levels when FOXO3 is ectopically expressed. However, cisplatin treatment significantly decreases Bim and Puma protein levels while LC3-I is converted to its lipidated form for autophagosome formation (Figure 3. 21. B). These autophagic vesicles may be the reason of the decrease in Bim and Puma levels since the autophagic vesicles can contain organelles, such as mitochondria, in order to degrade the macromolecules within.

In chemoresistant cells, the absence of functional p53 may result in SIRT1 activation which enhances the resistance through survival or autophagic gene expression by FOXO3. Considering FOXO3 as a partner of p53 in the transcription machinery, upregulation of proapoptotic FOXO3 target proteins may also require p53 because functional p53 inhibits SIRT1 activity [245]. In our study, we mostly focused on expressed target proteins involved in apoptosis and autophagy. However, the extensive functionality of FOXO3 in the transcriptional regulation of autophagy-related genes needs to be further investigated to clarify how autophagy is initiated.

A delicate molecular network including p53, IKK β and FOXO3 seems to determine chemoresistance/chemosensitivity in breast cancer cells (Figure 4. 1). In sensitive cells, functional p53 and IKK β inhibits activity of FOXO3 under normal conditions. Cisplatin treatment causes nuclear translocation of FOXO3 leading to bim, puma upregulation and apoptosis. In resistant cells, on the other hand, cisplatin treatment induces IKK β which triggers FOXO3 phosphorylation on Ser-644 residue and its degradation. FOXO3 overexpression (excess FOXO3) in chemoresistant cells triggers autophagic cell death. Moreover, functional p53 seems to inhibit FOXO3 action in both cells.

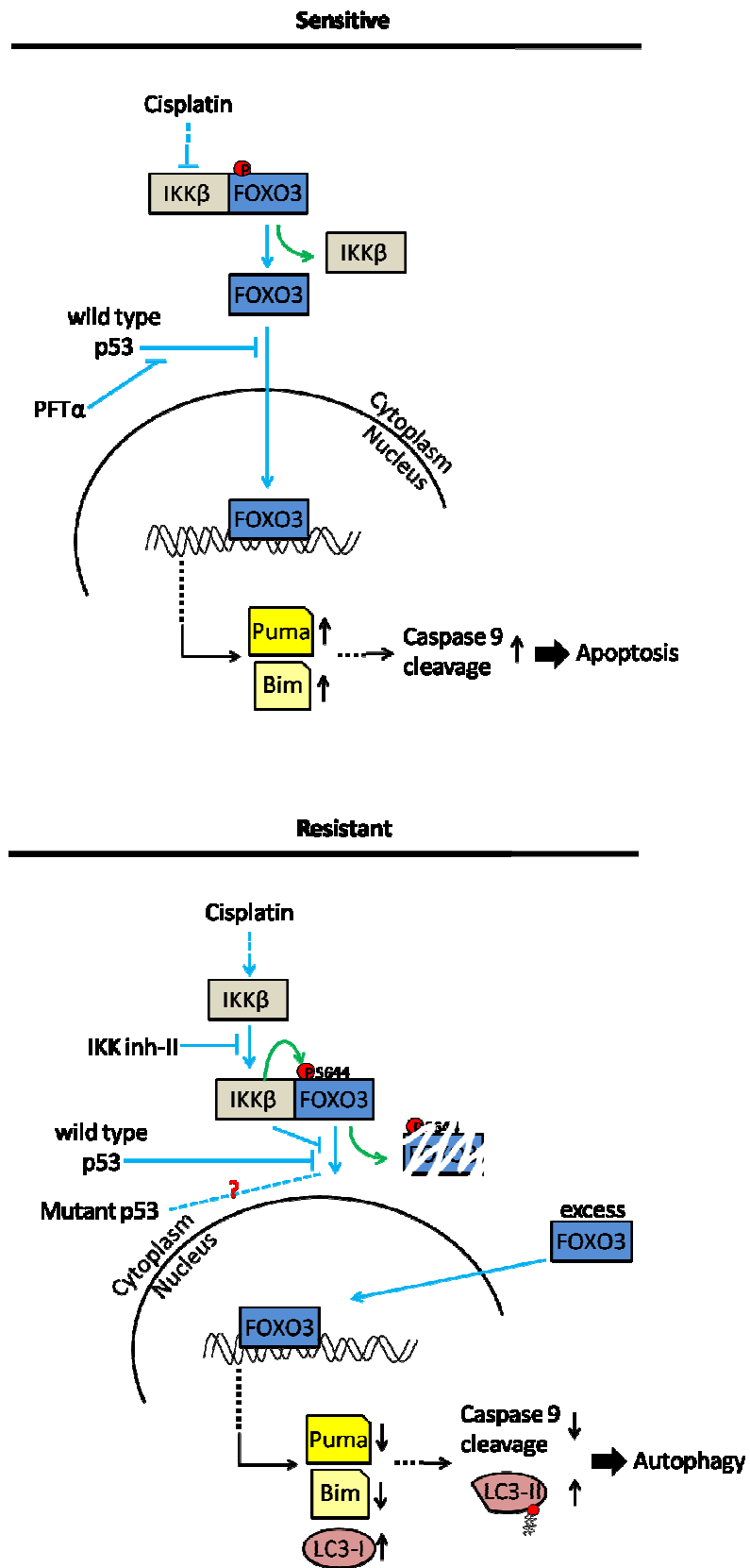


Figure 4. 1. The proposed mechanism with FOXO3-IKK β crosstalk.

4.4. Hormone Signalling

In chemoresistance, as well as in tumorigenesis, hormone signaling and associated receptors actively influence the cell fate. FOXO transcription factors were first identified as insulin-regulated factors and the important role of FOXOs in human longevity mainly takes the root from this insulin signaling pathways. Regarding its target proteins, FOXO3 also activates the genes responsible from anti-oxidative defense and eliminates the effects of oxidative stress, oxidative stress-related mutations and prevents tumorigenesis. In cancer cells, however, this defense system becomes an important element in chemoresistance by compensating drug-derived oxidative stress. In our study, we observed a reduced oxidative stress in siFOXO3 transfected cells following cisplatin treatment supporting the protective effect of FOXO3 in cancer cells (data not shown).

In a variety of animals including mice, rats and hamsters, administration of estrogen increases the incidence of cancers in a number of different organs [225]. Estrogen receptors are overexpressed in about 70% of breast cancer cases but the exact mechanism of its effect on tumor formation is still not fully understood [226]. Two hypotheses with evidence suggest that either **(1)** estrogens promote mammary cell proliferation through estrogen receptors and leads to DNA replication followed by mutations, or **(2)** increased activity in estrogen metabolism produces genotoxic compounds that cause mutations. In the end, both hypothetical processes result in tumor formation by disruption of cell cycle, apoptosis and DNA repair. Additionally, accumulating data in breast cancer studies indicate that silencing of FOXO3 promotes tumor progression and cisplatin resistance by repressing ER function [227-228]. MCF-7 cells have estrogen receptor and high FOXO3 expression; on the other hand, MDA-MB-231 cells have low FOXO3 with undetectable estrogen receptor expression. Thereby, in the present study, we show the increased rate of proliferation following FOXO3 silencing (Figure 3. 11) which further supports the involvement of FOXO3 in tumor formation and chemoresistance in addition to the other published reports [229].

4.5. Future Studies

The research presented in this thesis seems to have raised more questions than it has answered. There are several lines of research arising from this work which should be pursued.

In this thesis we mainly focused on the general outcome of FOXO3 and IKK interaction in cell death response; however, there are several potential key proteins in cell death regulation which might be actively involved in the switch mechanism between apoptosis and autophagy. Since FOXO3 regulates more metabolic genes than death-related genes in response to metabolic stress, it is also important to focus on physiologic conditions such as diabetic stress and starvation for investigating the consequences of changes in metabolic pathways regulated by FOXO3 [184].

Furthermore, the role of p53 on FOXO3 regulation should be investigated in detail. Although several studies on p53 function have been published, very limited number of studies exists on p53 and FOXO3 cooperation. Because most of the transcription factors are also involved in the gene regulation independently from their DNA binding ability -which determines the “fine-tune” in transcriptional regulation-, this line of research will allow us to understand the transcription machinery more accurately.

Finally, it is our intention to investigate thoroughly the crosstalk between FOXO3 and NF κ B pathway in other cancerous and healthy cell lines with a view of explaining how different physical interactions can affect proliferation and cell death signaling. Needless to say, mRNAs of FOXO3 and IKK β can be spliced alternatively in different cell lines (transcript variants) which might have an effect on protein-protein interactions in signaling pathways. After extensive studies incorporating numerous cell lines, the nature of this crosstalk and structural properties of the expressed proteins can be incorporated to chemotherapeutic design.

5. REFERENCES

- [1] Sondik EJ. Breast cancer trends. Incidence, mortality, and survival. *Cancer* 1994;74:995-9.
- [2] Launay L, Dejardin O, Pernet C, Morlais F, Guittet L, Launoy G, et al. Influence of socioeconomic environment on survival in patients diagnosed with esophageal cancer: a population-based study. *Dis Esophagus* 2012.
- [3] Landi MT, Consonni D, Rotunno M, Bergen AW, Goldstein AM, Lubin JH, et al. Environment And Genetics in Lung cancer Etiology (EAGLE) study: an integrative population-based case-control study of lung cancer. *BMC Public Health* 2008;8:203.
- [4] Park SK, Garcia-Closas M, Lissowska J, Sherman ME, McGlynn KA, Peplonska B, et al. Intrauterine environment and breast cancer risk in a population-based case-control study in Poland. *Int J Cancer* 2006;119:2136-41.
- [5] Desoubieux N, Herbert C, Launoy G, Maurel J, Gignoux M. Social environment and prognosis of colorectal cancer patients: a French population-based study. *Int J Cancer* 1997;73:317-22.
- [6] Engholm G, Palmgren F, Lynge E. Lung cancer, smoking, and environment: a cohort study of the Danish population. *BMJ* 1996;312:1259-63.
- [7] Anand P, Kunnumakkara AB, Sundaram C, Harikumar KB, Tharakan ST, Lai OS, et al. Cancer is a preventable disease that requires major lifestyle changes. *Pharm Res* 2008;25:2097-116.
- [8] Ingvarsson S. Molecular genetics of breast cancer progression. *Semin Cancer Biol* 1999;9:277-88.
- [9] Sengupta S, Jordan VC. Selective estrogen modulators as an anticancer tool: mechanisms of efficiency and resistance. *Adv Exp Med Biol* 2008;630:206-19.

- [10] Sunami E, Shinozaki M, Sim MS, Nguyen SL, Vu AT, Giuliano AE, et al. Estrogen receptor and HER2/neu status affect epigenetic differences of tumor-related genes in primary breast tumors. *Breast Cancer Res* 2008;10:R46.
- [11] Miller MA, Lippman ME, Katzenellenbogen BS. Antiestrogen binding in antiestrogen growth-resistant estrogen-responsive clonal variants of MCF-7 human breast cancer cells. *Cancer Res* 1984;44:5038-45.
- [12] Abu-Surrah AS, Kettunen M. Platinum group antitumor chemistry: design and development of new anticancer drugs complementary to cisplatin. *Curr Med Chem* 2006;13:1337-57.
- [13] Poklar N, Pilch DS, Lippard SJ, Redding EA, Dunham SU, Breslauer KJ. Influence of cisplatin intrastrand crosslinking on the conformation, thermal stability, and energetics of a 20-mer DNA duplex. *Proc Natl Acad Sci U S A* 1996;93:7606-11.
- [14] Eastman A. The formation, isolation and characterization of DNA adducts produced by anticancer platinum complexes. *Pharmacol Ther* 1987;34:155-66.
- [15] Chaney SG, Campbell SL, Bassett E, Wu Y. Recognition and processing of cisplatin- and oxaliplatin-DNA adducts. *Crit Rev Oncol Hematol* 2005;53:3-11.
- [16] Wang D, Lippard SJ. Cellular processing of platinum anticancer drugs. *Nat Rev Drug Discov* 2005;4:307-20.
- [17] Mymryk JS, Zaniewski E, Archer TK. Cisplatin inhibits chromatin remodeling, transcription factor binding, and transcription from the mouse mammary tumor virus promoter in vivo. *Proc Natl Acad Sci U S A* 1995;92:2076-80.
- [18] Brabec V, Kasparkova J. Modifications of DNA by platinum complexes. Relation to resistance of tumors to platinum antitumor drugs. *Drug Resist Updat* 2005;8:131-46.
- [19] Havrilesky LJ, Elbendary A, Hurteau JA, Whitaker RS, Rodriguez GC, Berchuck A. Chemotherapy-induced apoptosis in epithelial ovarian cancers. *Obstet Gynecol* 1995;85:1007-10.
- [20] Chang YF, Li LL, Wu CW, Liu TY, Lui WY, P'Eng F K, et al. Paclitaxel-induced apoptosis in human gastric carcinoma cell lines. *Cancer* 1996;77:14-8.
- [21] Gan Y, Wientjes MG, Schuller DE, Au JL. Pharmacodynamics of taxol in human head and neck tumors. *Cancer Res* 1996;56:2086-93.

- [22] Yen WC, Wientjes MG, Au JL. Differential effect of taxol in rat primary and metastatic prostate tumors: site-dependent pharmacodynamics. *Pharm Res* 1996;13:1305-12.
- [23] Ehrlichova M, Vaclavikova R, Ojima I, Pepe A, Kuznetsova LV, Chen J, et al. Transport and cytotoxicity of paclitaxel, docetaxel, and novel taxanes in human breast cancer cells. *Naunyn Schmiedebergs Arch Pharmacol* 2005;372:95-105.
- [24] Lowe J, Li H, Downing KH, Nogales E. Refined structure of alpha beta-tubulin at 3.5 A resolution. *J Mol Biol* 2001;313:1045-57.
- [25] Jordan MA, Wilson L. Microtubules as a target for anticancer drugs. *Nat Rev Cancer* 2004;4:253-65.
- [26] Bharadwaj R, Yu H. The spindle checkpoint, aneuploidy, and cancer. *Oncogene* 2004;23:2016-27.
- [27] Brito DA, Yang Z, Rieder CL. Microtubules do not promote mitotic slippage when the spindle assembly checkpoint cannot be satisfied. *J Cell Biol* 2008;182:623-9.
- [28] Ganguly A, Yang H, Cabral F. Paclitaxel-dependent cell lines reveal a novel drug activity. *Mol Cancer Ther* 2010;9:2914-23.
- [29] Belardo G, Piva R, Santoro MG. Heat stress triggers apoptosis by impairing NF-kappaB survival signaling in malignant B cells. *Leukemia* 2010;24:187-96.
- [30] Pustisek N, Situm M. UV-radiation, apoptosis and skin. *Coll Antropol* 2011;35 Suppl 2:339-41.
- [31] Goodkin ML, Morton ER, Blaho JA. Herpes simplex virus infection and apoptosis. *Int Rev Immunol* 2004;23:141-72.
- [32] Pogo BG, Melana SM, Blaho J. Poxvirus infection and apoptosis. *Int Rev Immunol* 2004;23:61-74.
- [33] Ho FY, Tsang WP, Kong SK, Kwok TT. The critical role of caspases activation in hypoxia/reoxygenation induced apoptosis. *Biochem Biophys Res Commun* 2006;345:1131-7.
- [34] Miller EA, Keku TO, Satia JA, Martin CF, Galanko JA, Sandler RS. Calcium, vitamin D, and apoptosis in the rectal epithelium. *Cancer Epidemiol Biomarkers Prev* 2005;14:525-8.
- [35] Mattson MP, Chan SL. Calcium orchestrates apoptosis. *Nat Cell Biol* 2003;5:1041-3.

- [36] MacFarlane M, Jones NA, Dive C, Cohen GM. DNA-damaging agents induce both p53-dependent and p53-independent apoptosis in immature thymocytes. *Mol Pharmacol* 1996;50:900-11.
- [37] Zamzami N, Susin SA, Marchetti P, Hirsch T, Gomez-Monterrey I, Castedo M, et al. Mitochondrial control of nuclear apoptosis. *J Exp Med* 1996;183:1533-44.
- [38] Kroemer G, Petit P, Zamzami N, Vayssiere JL, Mignotte B. The biochemistry of programmed cell death. *FASEB J* 1995;9:1277-87.
- [39] Liu X, Kim CN, Yang J, Jemmerson R, Wang X. Induction of apoptotic program in cell-free extracts: requirement for dATP and cytochrome c. *Cell* 1996;86:147-57.
- [40] Gonzalez F, Gottlieb E. Cardiolipin: setting the beat of apoptosis. *Apoptosis* 2007;12:877-85.
- [41] Kagan VE, Tyurin VA, Jiang J, Tyurina YY, Ritov VB, Amoscato AA, et al. Cytochrome c acts as a cardiolipin oxygenase required for release of proapoptotic factors. *Nat Chem Biol* 2005;1:223-32.
- [42] Sakurai K, Katoh M, Fujimoto Y. Alloxan-induced mitochondrial permeability transition triggered by calcium, thiol oxidation, and matrix ATP. *J Biol Chem* 2001;276:26942-6.
- [43] Gottlieb RA. Mitochondria: execution central. *FEBS Lett* 2000;482:6-12.
- [44] Szabo I, Zoratti M. The mitochondrial permeability transition pore may comprise VDAC molecules. I. Binary structure and voltage dependence of the pore. *FEBS Lett* 1993;330:201-5.
- [45] Jones A. Does the plant mitochondrion integrate cellular stress and regulate programmed cell death? *Trends Plant Sci* 2000;5:225-30.
- [46] Baines CP, Kaiser RA, Sheiko T, Craigen WJ, Molkenin JD. Voltage-dependent anion channels are dispensable for mitochondrial-dependent cell death. *Nat Cell Biol* 2007;9:550-5.
- [47] Kumarswamy R, Chandna S. Putative partners in Bax mediated cytochrome-c release: ANT, CypD, VDAC or none of them? *Mitochondrion* 2009;9:1-8.
- [48] Tsujimoto Y, Finger LR, Yunis J, Nowell PC, Croce CM. Cloning of the chromosome breakpoint of neoplastic B cells with the t(14;18) chromosome translocation. *Science* 1984;226:1097-9.

- [49] Cory S, Adams JM. The Bcl2 family: regulators of the cellular life-or-death switch. *Nat Rev Cancer* 2002;2:647-56.
- [50] Kutuk O, Basaga H. Bcl-2 protein family: implications in vascular apoptosis and atherosclerosis. *Apoptosis* 2006;11:1661-75.
- [51] Hsu YT, Wolter KG, Youle RJ. Cytosol-to-membrane redistribution of Bax and Bcl-X(L) during apoptosis. *Proc Natl Acad Sci U S A* 1997;94:3668-72.
- [52] Wolter KG, Hsu YT, Smith CL, Nechushtan A, Xi XG, Youle RJ. Movement of Bax from the cytosol to mitochondria during apoptosis. *J Cell Biol* 1997;139:1281-92.
- [53] Antonsson B, Montessuit S, Sanchez B, Martinou JC. Bax is present as a high molecular weight oligomer/complex in the mitochondrial membrane of apoptotic cells. *J Biol Chem* 2001;276:11615-23.
- [54] Griffiths GJ, Dubrez L, Morgan CP, Jones NA, Whitehouse J, Corfe BM, et al. Cell damage-induced conformational changes of the pro-apoptotic protein Bak in vivo precede the onset of apoptosis. *J Cell Biol* 1999;144:903-14.
- [55] Bellosillo B, Villamor N, Lopez-Guillermo A, Marce S, Bosch F, Campo E, et al. Spontaneous and drug-induced apoptosis is mediated by conformational changes of Bax and Bak in B-cell chronic lymphocytic leukemia. *Blood* 2002;100:1810-6.
- [56] Pang YP, Dai H, Smith A, Meng XW, Schneider PA, Kaufmann SH. Bak Conformational Changes Induced by Ligand Binding: Insight into BH3 Domain Binding and Bak Homo-Oligomerization. *Sci Rep* 2012;2:257.
- [57] Walensky LD, Gavathiotis E. BAX unleashed: the biochemical transformation of an inactive cytosolic monomer into a toxic mitochondrial pore. *Trends Biochem Sci* 2011;36:642-52.
- [58] Nouraini S, Six E, Matsuyama S, Krajewski S, Reed JC. The putative pore-forming domain of Bax regulates mitochondrial localization and interaction with Bcl-X(L). *Mol Cell Biol* 2000;20:1604-15.
- [59] Mikhailov V, Mikhailova M, Degenhardt K, Venkatachalam MA, White E, Saikumar P. Association of Bax and Bak homo-oligomers in mitochondria. Bax requirement for Bak reorganization and cytochrome c release. *J Biol Chem* 2003;278:5367-76.

- [60] Mikhailov V, Mikhailova M, Pulkrabek DJ, Dong Z, Venkatachalam MA, Saikumar P. Bcl-2 prevents Bax oligomerization in the mitochondrial outer membrane. *J Biol Chem* 2001;276:18361-74.
- [61] Goldstein JC, Waterhouse NJ, Juin P, Evan GI, Green DR. The coordinate release of cytochrome c during apoptosis is rapid, complete and kinetically invariant. *Nat Cell Biol* 2000;2:156-62.
- [62] Rehm M, Dussmann H, Prehn JH. Real-time single cell analysis of Smac/DIABLO release during apoptosis. *J Cell Biol* 2003;162:1031-43.
- [63] Kim H, Rafiuddin-Shah M, Tu HC, Jeffers JR, Zambetti GP, Hsieh JJ, et al. Hierarchical regulation of mitochondrion-dependent apoptosis by BCL-2 subfamilies. *Nat Cell Biol* 2006;8:1348-58.
- [64] Willis SN, Fletcher JI, Kaufmann T, van Delft MF, Chen L, Czabotar PE, et al. Apoptosis initiated when BH3 ligands engage multiple Bcl-2 homologs, not Bax or Bak. *Science* 2007;315:856-9.
- [65] Riedl SJ, Salvesen GS. The apoptosome: signalling platform of cell death. *Nat Rev Mol Cell Biol* 2007;8:405-13.
- [66] Acehan D, Jiang X, Morgan DG, Heuser JE, Wang X, Akey CW. Three-dimensional structure of the apoptosome: implications for assembly, procaspase-9 binding, and activation. *Mol Cell* 2002;9:423-32.
- [67] Yuan S, Yu X, Topf M, Ludtke SJ, Wang X, Akey CW. Structure of an apoptosome-procaspase-9 CARD complex. *Structure* 2010;18:571-83.
- [68] Hu Y, Ding L, Spencer DM, Nunez G. WD-40 repeat region regulates Apaf-1 self-association and procaspase-9 activation. *J Biol Chem* 1998;273:33489-94.
- [69] Yuan S, Yu X, Asara JM, Heuser JE, Ludtke SJ, Akey CW. The holo-apoptosome: activation of procaspase-9 and interactions with caspase-3. *Structure* 2011;19:1084-96.
- [70] McGrath LB, Onnis V, Campiani G, Williams DC, Zisterer DM, Mc Gee MM. Caspase-activated DNase (CAD)-independent oligonucleosomal DNA fragmentation in chronic myeloid leukaemia cells; a requirement for serine protease and Mn²⁺-dependent acidic endonuclease activity. *Apoptosis* 2006;11:1473-87.

- [71] Lu H, Hou Q, Zhao T, Zhang H, Zhang Q, Wu L, et al. Granzyme M directly cleaves inhibitor of caspase-activated DNase (CAD) to unleash CAD leading to DNA fragmentation. *J Immunol* 2006;177:1171-8.
- [72] Sakahira H, Enari M, Nagata S. Cleavage of CAD inhibitor in CAD activation and DNA degradation during apoptosis. *Nature* 1998;391:96-9.
- [73] Chan KT, Cortesio CL, Huttenlocher A. FAK alters invadopodia and focal adhesion composition and dynamics to regulate breast cancer invasion. *J Cell Biol* 2009;185:357-70.
- [74] Bokoch GM. Caspase-mediated activation of PAK2 during apoptosis: proteolytic kinase activation as a general mechanism of apoptotic signal transduction? *Cell Death Differ* 1998;5:637-45.
- [75] Verhoven B, Schlegel RA, Williamson P. Mechanisms of phosphatidylserine exposure, a phagocyte recognition signal, on apoptotic T lymphocytes. *J Exp Med* 1995;182:1597-601.
- [76] Yang Z, Klionsky DJ. An overview of the molecular mechanism of autophagy. *Curr Top Microbiol Immunol* 2009;335:1-32.
- [77] Cuervo AM. Autophagy: in sickness and in health. *Trends Cell Biol* 2004;14:70-7.
- [78] Levine B, Klionsky DJ. Development by self-digestion: molecular mechanisms and biological functions of autophagy. *Dev Cell* 2004;6:463-77.
- [79] Orenstein SJ, Cuervo AM. Chaperone-mediated autophagy: molecular mechanisms and physiological relevance. *Semin Cell Dev Biol* 2010;21:719-26.
- [80] Hay N, Sonenberg N. Upstream and downstream of mTOR. *Genes Dev* 2004;18:1926-45.
- [81] Beevers CS, Li F, Liu L, Huang S. Curcumin inhibits the mammalian target of rapamycin-mediated signaling pathways in cancer cells. *Int J Cancer* 2006;119:757-64.
- [82] Nobukuni T, Joaquin M, Roccio M, Dann SG, Kim SY, Gulati P, et al. Amino acids mediate mTOR/raptor signaling through activation of class 3 phosphatidylinositol 3OH-kinase. *Proc Natl Acad Sci U S A* 2005;102:14238-43.

- [83] Wang L, Harris TE, Roth RA, Lawrence JC, Jr. PRAS40 regulates mTORC1 kinase activity by functioning as a direct inhibitor of substrate binding. *J Biol Chem* 2007;282:20036-44.
- [84] Sancak Y, Thoreen CC, Peterson TR, Lindquist RA, Kang SA, Spooner E, et al. PRAS40 is an insulin-regulated inhibitor of the mTORC1 protein kinase. *Mol Cell* 2007;25:903-15.
- [85] Kim DH, Sarbassov DD, Ali SM, King JE, Latek RR, Erdjument-Bromage H, et al. mTOR interacts with raptor to form a nutrient-sensitive complex that signals to the cell growth machinery. *Cell* 2002;110:163-75.
- [86] Kim DH, Sarbassov DD, Ali SM, Latek RR, Guntur KV, Erdjument-Bromage H, et al. GbetaL, a positive regulator of the rapamycin-sensitive pathway required for the nutrient-sensitive interaction between raptor and mTOR. *Mol Cell* 2003;11:895-904.
- [87] Wullschleger S, Loewith R, Hall MN. TOR signaling in growth and metabolism. *Cell* 2006;124:471-84.
- [88] Sancak Y, Bar-Peled L, Zoncu R, Markhard AL, Nada S, Sabatini DM. Ragulator-Rag complex targets mTORC1 to the lysosomal surface and is necessary for its activation by amino acids. *Cell* 2010;141:290-303.
- [89] Levine B, Sinha S, Kroemer G. Bcl-2 family members: dual regulators of apoptosis and autophagy. *Autophagy* 2008;4:600-6.
- [90] Botti J, Djavaheri-Mergny M, Pilatte Y, Codogno P. Autophagy signaling and the cogwheels of cancer. *Autophagy* 2006;2:67-73.
- [91] Green DR, Wang R. Calcium and energy: making the cake and eating it too? *Cell* 2010;142:200-2.
- [92] Tracy K, Dibling BC, Spike BT, Knabb JR, Schumacker P, Macleod KF. BNIP3 is an RB/E2F target gene required for hypoxia-induced autophagy. *Mol Cell Biol* 2007;27:6229-42.
- [93] Gwinn DM, Shackelford DB, Egan DF, Mihaylova MM, Mery A, Vasquez DS, et al. AMPK phosphorylation of raptor mediates a metabolic checkpoint. *Mol Cell* 2008;30:214-26.
- [94] Egan D, Kim J, Shaw RJ, Guan KL. The autophagy initiating kinase ULK1 is regulated via opposing phosphorylation by AMPK and mTOR. *Autophagy* 2011;7:643-4.

- [95] Mizushima N. The role of the Atg1/ULK1 complex in autophagy regulation. *Curr Opin Cell Biol* 2010;22:132-9.
- [96] Cheong H, Lindsten T, Wu J, Lu C, Thompson CB. Ammonia-induced autophagy is independent of ULK1/ULK2 kinases. *Proc Natl Acad Sci U S A* 2011;108:11121-6.
- [97] Alers S, Löffler AS, Paasch F, Dieterle AM, Keppeler H, Lauber K, et al. Atg13 and FIP200 act independently of Ulk1 and Ulk2 in autophagy induction. *Autophagy* 2011;7:1423-33.
- [98] Pattingre S, Tassa A, Qu X, Garuti R, Liang XH, Mizushima N, et al. Bcl-2 antiapoptotic proteins inhibit Beclin 1-dependent autophagy. *Cell* 2005;122:927-39.
- [99] Park KJ, Lee SH, Lee CH, Jang JY, Chung J, Kwon MH, et al. Upregulation of Beclin-1 expression and phosphorylation of Bcl-2 and p53 are involved in the JNK-mediated autophagic cell death. *Biochem Biophys Res Commun* 2009;382:726-9.
- [100] Fan W, Nassiri A, Zhong Q. Autophagosome targeting and membrane curvature sensing by Barkor/Atg14(L). *Proc Natl Acad Sci U S A* 2011;108:7769-74.
- [101] Itakura E, Mizushima N. Characterization of autophagosome formation site by a hierarchical analysis of mammalian Atg proteins. *Autophagy* 2010;6:764-76.
- [102] Polson HE, de Lartigue J, Rigden DJ, Reedijk M, Urbe S, Clague MJ, et al. Mammalian Atg18 (WIPI2) localizes to omegasome-anchored phagophores and positively regulates LC3 lipidation. *Autophagy* 2010;6.
- [103] Nobel Prize in Chemistry, 2004. Aaron Ciechanover, Avram Hershko and Irwin Rose. *Indian J Physiol Pharmacol* 2005;49:121.
- [104] Mizushima N, Noda T, Yoshimori T, Tanaka Y, Ishii T, George MD, et al. A protein conjugation system essential for autophagy. *Nature* 1998;395:395-8.
- [105] Shintani T, Mizushima N, Ogawa Y, Matsuura A, Noda T, Ohsumi Y. Apg10p, a novel protein-conjugating enzyme essential for autophagy in yeast. *EMBO J* 1999;18:5234-41.
- [106] Mizushima N, Noda T, Ohsumi Y. Apg16p is required for the function of the Apg12p-Apg5p conjugate in the yeast autophagy pathway. *EMBO J* 1999;18:3888-96.

- [107] Kuma A, Mizushima N, Ishihara N, Ohsumi Y. Formation of the approximately 350-kDa Apg12-Apg5-Apg16 multimeric complex, mediated by Apg16 oligomerization, is essential for autophagy in yeast. *J Biol Chem* 2002;277:18619-25.
- [108] Zhang J, Randall MS, Loyd MR, Dorsey FC, Kundu M, Cleveland JL, et al. Mitochondrial clearance is regulated by Atg7-dependent and -independent mechanisms during reticulocyte maturation. *Blood* 2009;114:157-64.
- [109] Zhao Z, Fux B, Goodwin M, Dunay IR, Strong D, Miller BC, et al. Autophagosome-independent essential function for the autophagy protein Atg5 in cellular immunity to intracellular pathogens. *Cell Host Microbe* 2008;4:458-69.
- [110] Nishida Y, Arakawa S, Fujitani K, Yamaguchi H, Mizuta T, Kanaseki T, et al. Discovery of Atg5/Atg7-independent alternative macroautophagy. *Nature* 2009;461:654-8.
- [111] Fujita N, Itoh T, Omori H, Fukuda M, Noda T, Yoshimori T. The Atg16L complex specifies the site of LC3 lipidation for membrane biogenesis in autophagy. *Mol Biol Cell* 2008;19:2092-100.
- [112] Geng J, Baba M, Nair U, Klionsky DJ. Quantitative analysis of autophagy-related protein stoichiometry by fluorescence microscopy. *J Cell Biol* 2008;182:129-40.
- [113] Kabeya Y, Mizushima N, Yamamoto A, Oshitani-Okamoto S, Ohsumi Y, Yoshimori T. LC3, GABARAP and GATE16 localize to autophagosomal membrane depending on form-II formation. *J Cell Sci* 2004;117:2805-12.
- [114] Ichimura Y, Kirisako T, Takao T, Satomi Y, Shimonishi Y, Ishihara N, et al. A ubiquitin-like system mediates protein lipidation. *Nature* 2000;408:488-92.
- [115] Hanada T, Noda NN, Satomi Y, Ichimura Y, Fujioka Y, Takao T, et al. The Atg12-Atg5 conjugate has a novel E3-like activity for protein lipidation in autophagy. *J Biol Chem* 2007;282:37298-302.
- [116] Kabeya Y, Mizushima N, Ueno T, Yamamoto A, Kirisako T, Noda T, et al. LC3, a mammalian homologue of yeast Apg8p, is localized in autophagosomal membranes after processing. *EMBO J* 2000;19:5720-8.
- [117] Geng J, Klionsky DJ. The Golgi as a potential membrane source for autophagy. *Autophagy* 2010;6:950-1.

- [118] Hailey DW, Rambold AS, Satpute-Krishnan P, Mitra K, Sougrat R, Kim PK, et al. Mitochondria supply membranes for autophagosome biogenesis during starvation. *Cell* 2010;141:656-67.
- [119] Ravikumar B, Moreau K, Rubinsztein DC. Plasma membrane helps autophagosomes grow. *Autophagy* 2010;6:1184-6.
- [120] Tabata K, Matsunaga K, Sakane A, Sasaki T, Noda T, Yoshimori T. Rubicon and PLEKHM1 negatively regulate the endocytic/autophagic pathway via a novel Rab7-binding domain. *Mol Biol Cell* 2010;21:4162-72.
- [121] Militello RD, Colombo MI. A membrane is born: origin of the autophagosomal compartment. *Curr Mol Med* 2011;11:197-203.
- [122] Tooze SA, Yoshimori T. The origin of the autophagosomal membrane. *Nat Cell Biol* 2010;12:831-5.
- [123] Axe EL, Walker SA, Manifava M, Chandra P, Roderick HL, Habermann A, et al. Autophagosome formation from membrane compartments enriched in phosphatidylinositol 3-phosphate and dynamically connected to the endoplasmic reticulum. *J Cell Biol* 2008;182:685-701.
- [124] Ravikumar B, Acevedo-Arozena A, Imarisio S, Berger Z, Vacher C, O'Kane CJ, et al. Dynein mutations impair autophagic clearance of aggregate-prone proteins. *Nat Genet* 2005;37:771-6.
- [125] Mann SS, Hammarback JA. Molecular characterization of light chain 3. A microtubule binding subunit of MAP1A and MAP1B. *J Biol Chem* 1994;269:11492-7.
- [126] Kouno T, Mizuguchi M, Tanida I, Ueno T, Kanematsu T, Mori Y, et al. Solution structure of microtubule-associated protein light chain 3 and identification of its functional subdomains. *J Biol Chem* 2005;280:24610-7.
- [127] Pankiv S, Alemu EA, Brech A, Bruun JA, Lamark T, Overvatn A, et al. FYCO1 is a Rab7 effector that binds to LC3 and PI3P to mediate microtubule plus end-directed vesicle transport. *J Cell Biol* 2010;188:253-69.
- [128] Cai H, Reinisch K, Ferro-Novick S. Coats, tethers, Rabs, and SNAREs work together to mediate the intracellular destination of a transport vesicle. *Dev Cell* 2007;12:671-82.

- [129] Aita VM, Liang XH, Murty VV, Pincus DL, Yu W, Cayanis E, et al. Cloning and genomic organization of beclin 1, a candidate tumor suppressor gene on chromosome 17q21. *Genomics* 1999;59:59-65.
- [130] Liang XH, Jackson S, Seaman M, Brown K, Kempkes B, Hibshoosh H, et al. Induction of autophagy and inhibition of tumorigenesis by beclin 1. *Nature* 1999;402:672-6.
- [131] Karin M, Lin A. NF-kappaB at the crossroads of life and death. *Nat Immunol* 2002;3:221-7.
- [132] Hayden MS, Ghosh S. Signaling to NF-kappaB. *Genes Dev* 2004;18:2195-224.
- [133] Kapahi P, Takahashi T, Natoli G, Adams SR, Chen Y, Tsien RY, et al. Inhibition of NF-kappa B activation by arsenite through reaction with a critical cysteine in the activation loop of Ikappa B kinase. *J Biol Chem* 2000;275:36062-6.
- [134] Scheibel M, Klein B, Merkle H, Schulz M, Fritsch R, Greten FR, et al. IkappaBbeta is an essential co-activator for LPS-induced IL-1beta transcription in vivo. *J Exp Med* 2010;207:2621-30.
- [135] Bourke E, Kennedy EJ, Moynagh PN. Loss of Ikappa B-beta is associated with prolonged NF-kappa B activity in human glial cells. *J Biol Chem* 2000;275:39996-40002.
- [136] Sun Z, Andersson R. NF-kappaB activation and inhibition: a review. *Shock* 2002;18:99-106.
- [137] Rothwarf DM, Zandi E, Natoli G, Karin M. IKK-gamma is an essential regulatory subunit of the IkappaB kinase complex. *Nature* 1998;395:297-300.
- [138] Chapuis N, Park S, Leotoing L, Tamburini J, Verdier F, Bardet V, et al. IkappaB kinase overcomes PI3K/Akt and ERK/MAPK to control FOXO3a activity in acute myeloid leukemia. *Blood* 2010;116:4240-50.
- [139] Thompson LM, Aiken CT, Kaltenbach LS, Agrawal N, Illes K, Khoshnan A, et al. IKK phosphorylates Huntingtin and targets it for degradation by the proteasome and lysosome. *J Cell Biol* 2009;187:1083-99.
- [140] Hacker H, Karin M. Regulation and function of IKK and IKK-related kinases. *Sci STKE* 2006;2006:re13.
- [141] Karin M, Cao Y, Greten FR, Li ZW. NF-kappaB in cancer: from innocent bystander to major culprit. *Nat Rev Cancer* 2002;2:301-10.

- [142] Habib AA, Chatterjee S, Park SK, Ratan RR, Lefebvre S, Vartanian T. The epidermal growth factor receptor engages receptor interacting protein and nuclear factor-kappa B (NF-kappa B)-inducing kinase to activate NF-kappa B. Identification of a novel receptor-tyrosine kinase signalosome. *J Biol Chem* 2001;276:8865-74.
- [143] Fagerlund R, Kinnunen L, Kohler M, Julkunen I, Melen K. NF- κ B is transported into the nucleus by importin α 3 and importin α 4. *J Biol Chem* 2005;280:15942-51.
- [144] Shrum CK, Defrancisco D, Meffert MK. Stimulated nuclear translocation of NF-kappaB and shuttling differentially depend on dynein and the dynactin complex. *Proc Natl Acad Sci U S A* 2009;106:2647-52.
- [145] Sen R, Baltimore D. Inducibility of kappa immunoglobulin enhancer-binding protein NF-kappa B by a posttranslational mechanism. *Cell* 1986;47:921-8.
- [146] Chen FE, Ghosh G. Regulation of DNA binding by Rel/NF-kappaB transcription factors: structural views. *Oncogene* 1999;18:6845-52.
- [147] Huang DB, Phelps CB, Fusco AJ, Ghosh G. Crystal structure of a free kappaB DNA: insights into DNA recognition by transcription factor NF-kappaB. *J Mol Biol* 2005;346:147-60.
- [148] Hoffmann A, Natoli G, Ghosh G. Transcriptional regulation via the NF-kappaB signaling module. *Oncogene* 2006;25:6706-16.
- [149] Chen-Park FE, Huang DB, Noro B, Thanos D, Ghosh G. The kappa B DNA sequence from the HIV long terminal repeat functions as an allosteric regulator of HIV transcription. *J Biol Chem* 2002;277:24701-8.
- [150] Hayden MS, Ghosh S. Shared principles in NF-kappaB signaling. *Cell* 2008;132:344-62.
- [151] Grimm T, Schneider S, Naschberger E, Huber J, Guenzi E, Kieser A, et al. EBV latent membrane protein-1 protects B cells from apoptosis by inhibition of BAX. *Blood* 2005;105:3263-9.
- [152] Wang Z, Zhang B, Yang L, Ding J, Ding HF. Constitutive production of NF-kappaB2 p52 is not tumorigenic but predisposes mice to inflammatory autoimmune disease by repressing Bim expression. *J Biol Chem* 2008;283:10698-706.

- [153] Sommermann TG, Mack HI, Cahir-McFarland E. Autophagy prolongs survival after NFkappaB inhibition in B-cell lymphomas. *Autophagy* 2012;8:265-7.
- [154] Nivon M, Richet E, Codogno P, Arrigo AP, Kretz-Remy C. Autophagy activation by NFkappaB is essential for cell survival after heat shock. *Autophagy* 2009;5:766-83.
- [155] Djavaheri-Mergny M, Amelotti M, Mathieu J, Besancon F, Bauvy C, Codogno P. Regulation of autophagy by NFkappaB transcription factor and reactive oxygen species. *Autophagy* 2007;3:390-2.
- [156] Copetti T, Bertoli C, Dalla E, Demarchi F, Schneider C. p65/RelA modulates BECN1 transcription and autophagy. *Mol Cell Biol* 2009;29:2594-608.
- [157] Schlottmann S, Buback F, Stahl B, Meierhenrich R, Walter P, Georgieff M, et al. Prolonged classical NF-kappaB activation prevents autophagy upon E. coli stimulation in vitro: a potential resolving mechanism of inflammation. *Mediators Inflamm* 2008;2008:725854.
- [158] Djavaheri-Mergny M, Amelotti M, Mathieu J, Besancon F, Bauvy C, Souquere S, et al. NF-kappaB activation represses tumor necrosis factor-alpha-induced autophagy. *J Biol Chem* 2006;281:30373-82.
- [159] Luo S, Rubinsztein DC. Apoptosis blocks Beclin 1-dependent autophagosome synthesis: an effect rescued by Bcl-xL. *Cell Death Differ* 2010;17:268-77.
- [160] Weigel D, Jurgens G, Kuttner F, Seifert E, Jackle H. The homeotic gene fork head encodes a nuclear protein and is expressed in the terminal regions of the Drosophila embryo. *Cell* 1989;57:645-58.
- [161] Calnan DR, Brunet A. The FoxO code. *Oncogene* 2008;27:2276-88.
- [162] Gilley J, Coffey PJ, Ham J. FOXO transcription factors directly activate bim gene expression and promote apoptosis in sympathetic neurons. *J Cell Biol* 2003;162:613-22.
- [163] Dudgeon C, Wang P, Sun X, Peng R, Sun Q, Yu J, et al. PUMA induction by FoxO3a mediates the anticancer activities of the broad-range kinase inhibitor UCN-01. *Mol Cancer Ther* 2010;9:2893-902.
- [164] Obexer P, Geiger K, Ambros PF, Meister B, Ausserlechner MJ. FKHRL1-mediated expression of Noxa and Bim induces apoptosis via the mitochondria in neuroblastoma cells. *Cell Death Differ* 2007;14:534-47.

- [165] Mammucari C, Milan G, Romanello V, Masiero E, Rudolf R, Del Piccolo P, et al. FoxO3 controls autophagy in skeletal muscle in vivo. *Cell Metab* 2007;6:458-71.
- [166] Sanchez AM, Csibi A, Raibon A, Cornille K, Gay S, Bernardi H, et al. AMPK promotes skeletal muscle autophagy through activation of forkhead FoxO3a and interaction with Ulk1. *J Cell Biochem* 2012;113:695-710.
- [167] Chandramohan V, Mineva ND, Burke B, Jeay S, Wu M, Shen J, et al. c-Myc represses FOXO3a-mediated transcription of the gene encoding the p27(Kip1) cyclin dependent kinase inhibitor. *J Cell Biochem* 2008;104:2091-106.
- [168] Schmidt M, Fernandez de Mattos S, van der Horst A, Klompaker R, Kops GJ, Lam EW, et al. Cell cycle inhibition by FoxO forkhead transcription factors involves downregulation of cyclin D. *Mol Cell Biol* 2002;22:7842-52.
- [169] Tran H, Brunet A, Grenier JM, Datta SR, Fornace AJ, Jr., DiStefano PS, et al. DNA repair pathway stimulated by the forkhead transcription factor FOXO3a through the Gadd45 protein. *Science* 2002;296:530-4.
- [170] Furuyama T, Nakazawa T, Nakano I, Mori N. Identification of the differential distribution patterns of mRNAs and consensus binding sequences for mouse DAF-16 homologues. *Biochem J* 2000;349:629-34.
- [171] Xuan Z, Zhang MQ. From worm to human: bioinformatics approaches to identify FOXO target genes. *Mech Ageing Dev* 2005;126:209-15.
- [172] Rinner O, Mueller LN, Hubalek M, Muller M, Gstaiger M, Aebersold R. An integrated mass spectrometric and computational framework for the analysis of protein interaction networks. *Nat Biotechnol* 2007;25:345-52.
- [173] Li J, Tewari M, Vidal M, Lee SS. The 14-3-3 protein FTT-2 regulates DAF-16 in *Caenorhabditis elegans*. *Dev Biol* 2007;301:82-91.
- [174] Brunet A, Bonni A, Zigmond MJ, Lin MZ, Juo P, Hu LS, et al. Akt promotes cell survival by phosphorylating and inhibiting a Forkhead transcription factor. *Cell* 1999;96:857-68.
- [175] Brunet A, Kanai F, Stehn J, Xu J, Sarbassova D, Frangioni JV, et al. 14-3-3 transits to the nucleus and participates in dynamic nucleocytoplasmic transport. *J Cell Biol* 2002;156:817-28.

- [176] Schwab TS, Madison BB, Grauman AR, Feldman EL. Insulin-like growth factor-I induces the phosphorylation and nuclear exclusion of forkhead transcription factors in human neuroblastoma cells. *Apoptosis* 2005;10:831-40.
- [177] Clavel S, Siffroi-Fernandez S, Coldefy AS, Boulukos K, Pisani DF, Derijard B. Regulation of the intracellular localization of Foxo3a by stress-activated protein kinase signaling pathways in skeletal muscle cells. *Mol Cell Biol* 2010;30:470-80.
- [178] Latre de Late P, Pepin A, Assaf-Vandecasteele H, Espinasse C, Nicolas V, Asselin-Labat ML, et al. Glucocorticoid-induced leucine zipper (GILZ) promotes the nuclear exclusion of FOXO3 in a Crm1-dependent manner. *J Biol Chem* 2010;285:5594-605.
- [179] Attaix D, Combaret L, Bechet D, Taillandier D. Role of the ubiquitin-proteasome pathway in muscle atrophy in cachexia. *Curr Opin Support Palliat Care* 2008;2:262-6.
- [180] Obsilova V, Vecer J, Herman P, Pabianova A, Sulc M, Teisinger J, et al. 14-3-3 Protein interacts with nuclear localization sequence of forkhead transcription factor FoxO4. *Biochemistry* 2005;44:11608-17.
- [181] Brunet A, Sweeney LB, Sturgill JF, Chua KF, Greer PL, Lin Y, et al. Stress-dependent regulation of FOXO transcription factors by the SIRT1 deacetylase. *Science* 2004;303:2011-5.
- [182] Kitamura YI, Kitamura T, Kruse JP, Raum JC, Stein R, Gu W, et al. FoxO1 protects against pancreatic beta cell failure through NeuroD and MafA induction. *Cell Metab* 2005;2:153-63.
- [183] Frescas D, Valenti L, Accili D. Nuclear trapping of the forkhead transcription factor FoxO1 via Sirt-dependent deacetylation promotes expression of glucogenetic genes. *J Biol Chem* 2005;280:20589-95.
- [184] Chiacchiera F, Simone C. Inhibition of p38alpha unveils an AMPK-FoxO3A axis linking autophagy to cancer-specific metabolism. *Autophagy* 2009;5:1030-3.
- [185] Yang JY, Zong CS, Xia W, Yamaguchi H, Ding Q, Xie X, et al. ERK promotes tumorigenesis by inhibiting FOXO3a via MDM2-mediated degradation. *Nat Cell Biol* 2008;10:138-48.

- [186] Hu MC, Lee DF, Xia W, Golfman LS, Ou-Yang F, Yang JY, et al. IkkappaB kinase promotes tumorigenesis through inhibition of forkhead FOXO3a. *Cell* 2004;117:225-37.
- [187] Henderson ST, Johnson TE. daf-16 integrates developmental and environmental inputs to mediate aging in the nematode *Caenorhabditis elegans*. *Curr Biol* 2001;11:1975-80.
- [188] Giannakou ME, Goss M, Junger MA, Hafen E, Leivers SJ, Partridge L. Long-lived *Drosophila* with overexpressed dFOXO in adult fat body. *Science* 2004;305:361.
- [189] Hwangbo DS, Gershman B, Tu MP, Palmer M, Tatar M. *Drosophila* dFOXO controls lifespan and regulates insulin signalling in brain and fat body. *Nature* 2004;429:562-6.
- [190] Borkhardt A, Repp R, Haas OA, Leis T, Harbott J, Kreuder J, et al. Cloning and characterization of AFX, the gene that fuses to MLL in acute leukemias with a t(X;11)(q13;q23). *Oncogene* 1997;14:195-202.
- [191] Paik JH, Kollipara R, Chu G, Ji H, Xiao Y, Ding Z, et al. FoxOs are lineage-restricted redundant tumor suppressors and regulate endothelial cell homeostasis. *Cell* 2007;128:309-23.
- [192] Liu JW, Chandra D, Rudd MD, Butler AP, Pallotta V, Brown D, et al. Induction of prosurvival molecules by apoptotic stimuli: involvement of FOXO3a and ROS. *Oncogene* 2005;24:2020-31.
- [193] Willcox BJ, Donlon TA, He Q, Chen R, Grove JS, Yano K, et al. FOXO3A genotype is strongly associated with human longevity. *Proc Natl Acad Sci U S A* 2008;105:13987-92.
- [194] Krol J, Francis RE, Albergaria A, Sunters A, Polychronis A, Coombes RC, et al. The transcription factor FOXO3a is a crucial cellular target of gefitinib (Iressa) in breast cancer cells. *Mol Cancer Ther* 2007;6:3169-79.
- [195] McGovern UB, Francis RE, Peck B, Guest SK, Wang J, Myatt SS, et al. Gefitinib (Iressa) represses FOXM1 expression via FOXO3a in breast cancer. *Mol Cancer Ther* 2009;8:582-91.
- [196] Hui RC, Francis RE, Guest SK, Costa JR, Gomes AR, Myatt SS, et al. Doxorubicin activates FOXO3a to induce the expression of multidrug resistance gene ABCB1 (MDR1) in K562 leukemic cells. *Mol Cancer Ther* 2008;7:670-8.

- [197] Hui RC, Gomes AR, Constantinidou D, Costa JR, Karadedou CT, Fernandez de Mattos S, et al. The forkhead transcription factor FOXO3a increases phosphoinositide-3 kinase/Akt activity in drug-resistant leukemic cells through induction of PIK3CA expression. *Mol Cell Biol* 2008;28:5886-98.
- [198] Kikuchi S, Nagai T, Kunitama M, Kirito K, Ozawa K, Komatsu N. Active FKHL1 overcomes imatinib resistance in chronic myelogenous leukemia-derived cell lines via the production of tumor necrosis factor-related apoptosis-inducing ligand. *Cancer Sci* 2007;98:1949-58.
- [199] Fernandez de Mattos S, Villalonga P, Clardy J, Lam EW. FOXO3a mediates the cytotoxic effects of cisplatin in colon cancer cells. *Mol Cancer Ther* 2008;7:3237-46.
- [200] Pfaffl MW, Tichopad A, Prgomet C, Neuvians TP. Determination of stable housekeeping genes, differentially regulated target genes and sample integrity: BestKeeper--Excel-based tool using pair-wise correlations. *Biotechnol Lett* 2004;26:509-15.
- [201] Legrand-Poels S, Schoonbroodt S, Piette J. Regulation of interleukin-6 gene expression by pro-inflammatory cytokines in a colon cancer cell line. *Biochem J* 2000;349 Pt 3:765-73.
- [202] Chen XP, Liu S, Tang WX, Chen ZW. Nuclear thioredoxin-1 is required to suppress cisplatin-mediated apoptosis of MCF-7 cells. *Biochem Biophys Res Commun* 2007;361:362-6.
- [203] Marx J. How cells cycle toward cancer. *Science* 1994;263:319-21.
- [204] Gupta N, Hu LJ, Deen DF. Cytotoxicity and cell-cycle effects of paclitaxel when used as a single agent and in combination with ionizing radiation. *Int J Radiat Oncol Biol Phys* 1997;37:885-95.
- [205] Sigdestad CP, Grdina DJ. In vivo cell cycle phase-preferential killing of murine fibrosarcoma cells by cisplatin. *Cancer Treat Rep* 1981;65:845-51.
- [206] Wang S, Wang Z, Dent P, Grant S. Induction of tumor necrosis factor by bryostatin 1 is involved in synergistic interactions with paclitaxel in human myeloid leukemia cells. *Blood* 2003;101:3648-57.
- [207] Shamimi-Noori S, Yeow WS, Ziauddin MF, Xin H, Tran TL, Xie J, et al. Cisplatin enhances the antitumor effect of tumor necrosis factor-related

- apoptosis-inducing ligand gene therapy via recruitment of the mitochondria-dependent death signaling pathway. *Cancer Gene Ther* 2008;15:356-70.
- [208] Smith ML, Kontny HU, Bortnick R, Fornace AJ, Jr. The p53-regulated cyclin G gene promotes cell growth: p53 downstream effectors cyclin G and Gadd45 exert different effects on cisplatin chemosensitivity. *Exp Cell Res* 1997;230:61-8.
- [209] Smith ML, Kontny HU, Zhan Q, Sreenath A, O'Connor PM, Fornace AJ, Jr. Antisense GADD45 expression results in decreased DNA repair and sensitizes cells to u.v.-irradiation or cisplatin. *Oncogene* 1996;13:2255-63.
- [210] Kastan MB, Zhan Q, el-Deiry WS, Carrier F, Jacks T, Walsh WV, et al. A mammalian cell cycle checkpoint pathway utilizing p53 and GADD45 is defective in ataxia-telangiectasia. *Cell* 1992;71:587-97.
- [211] Olivier M, Eeles R, Hollstein M, Khan MA, Harris CC, Hainaut P. The IARC TP53 database: new online mutation analysis and recommendations to users. *Hum Mutat* 2002;19:607-14.
- [212] Guo S, Sonenshein GE. Forkhead box transcription factor FOXO3a regulates estrogen receptor alpha expression and is repressed by the Her-2/neu/phosphatidylinositol 3-kinase/Akt signaling pathway. *Mol Cell Biol* 2004;24:8681-90.
- [213] Weng SC, Kashida Y, Kulp SK, Wang D, Brueggemeier RW, Shapiro CL, et al. Sensitizing estrogen receptor-negative breast cancer cells to tamoxifen with OSU-03012, a novel celecoxib-derived phosphoinositide-dependent protein kinase-1/Akt signaling inhibitor. *Mol Cancer Ther* 2008;7:800-8.
- [214] Shiota M, Yokomizo A, Kashiwagi E, Tada Y, Inokuchi J, Tatsugami K, et al. Foxo3a expression and acetylation regulate cancer cell growth and sensitivity to cisplatin. *Cancer Sci* 2010;101:1177-85.
- [215] Liu F, Xia Y, Parker AS, Verma IM. IKK biology. *Immunol Rev* 2012;246:239-53.
- [216] Kobori M, Yang Z, Gong D, Heissmeyer V, Zhu H, Jung YK, et al. Wedelolactone suppresses LPS-induced caspase-11 expression by directly inhibiting the IKK complex. *Cell Death Differ* 2004;11:123-30.

- [217] Geng Y, Akhtar RS, Shacka JJ, Klocke BJ, Zhang J, Chen X, et al. p53 transcription-dependent and -independent regulation of cerebellar neural precursor cell apoptosis. *J Neuropathol Exp Neurol* 2007;66:66-74.
- [218] Miyaguchi Y, Tsuchiya K, Sakamoto K. P53 negatively regulates the transcriptional activity of FOXO3a under oxidative stress. *Cell Biol Int* 2009;33:853-60.
- [219] Aranha MM, Sola S, Low WC, Steer CJ, Rodrigues CM. Caspases and p53 modulate FOXO3A/Id1 signaling during mouse neural stem cell differentiation. *J Cell Biochem* 2009;107:748-58.
- [220] Wang F, Marshall CB, Yamamoto K, Li GY, Plevin MJ, You H, et al. Biochemical and structural characterization of an intramolecular interaction in FOXO3a and its binding with p53. *J Mol Biol* 2008;384:590-603.
- [221] You H, Yamamoto K, Mak TW. Regulation of transactivation-independent proapoptotic activity of p53 by FOXO3a. *Proc Natl Acad Sci U S A* 2006;103:9051-6.
- [222] You H, Jang Y, You-Ten AI, Okada H, Liepa J, Wakeham A, et al. p53-dependent inhibition of FKHL1 in response to DNA damage through protein kinase SGK1. *Proc Natl Acad Sci U S A* 2004;101:14057-62.
- [223] Murphy PJ, Galigniana MD, Morishima Y, Harrell JM, Kwok RP, Ljungman M, et al. Pifithrin-alpha inhibits p53 signaling after interaction of the tumor suppressor protein with hsp90 and its nuclear translocation. *J Biol Chem* 2004;279:30195-201.
- [224] Schulze-Osthoff K, Ferrari D, Los M, Wesselborg S, Peter ME. Apoptosis signaling by death receptors. *Eur J Biochem* 1998;254:439-59.
- [225] Liehr JG. Genotoxicity of the steroidal oestrogens oestrone and oestradiol: possible mechanism of uterine and mammary cancer development. *Hum Reprod Update* 2001;7:273-81.
- [226] Duffy MJ. Estrogen receptors: role in breast cancer. *Crit Rev Clin Lab Sci* 2006;43:325-47.
- [227] Belguise K, Guo S, Sonenshein GE. Activation of FOXO3a by the green tea polyphenol epigallocatechin-3-gallate induces estrogen receptor alpha expression reversing invasive phenotype of breast cancer cells. *Cancer Res* 2007;67:5763-70.

- [228] Morelli C, Lanzino M, Garofalo C, Maris P, Brunelli E, Casaburi I, et al. Akt2 inhibition enables the forkhead transcription factor FoxO3a to have a repressive role in estrogen receptor alpha transcriptional activity in breast cancer cells. *Mol Cell Biol* 2010;30:857-70.
- [229] Lazennec G, Bresson D, Lucas A, Chauveau C, Vignon F. ER beta inhibits proliferation and invasion of breast cancer cells. *Endocrinology* 2001;142:4120-30.
- [230] Carrier F, Smith ML, Bae I, Kilpatrick KE, Lansing TJ, Chen CY, et al. Characterization of human Gadd45, a p53-regulated protein. *J Biol Chem* 1994;269:32672-7.
- [231] Kuerbitz SJ, Plunkett BS, Walsh WV, Kastan MB. Wild-type p53 is a cell cycle checkpoint determinant following irradiation. *Proc Natl Acad Sci U S A* 1992;89:7491-5.
- [232] You H, Pellegrini M, Tsuchihara K, Yamamoto K, Hacker G, Erlacher M, et al. FOXO3a-dependent regulation of Puma in response to cytokine/growth factor withdrawal. *J Exp Med* 2006;203:1657-63.
- [233] Blagosklonny MV, Giannakakou P, Romanova LY, Ryan KM, Vousden KH, Fojo T. Inhibition of HIF-1- and wild-type p53-stimulated transcription by codon Arg175 p53 mutants with selective loss of functions. *Carcinogenesis* 2001;22:861-7.
- [234] Aurelio ON, Kong XT, Gupta S, Stanbridge EJ. p53 mutants have selective dominant-negative effects on apoptosis but not growth arrest in human cancer cell lines. *Mol Cell Biol* 2000;20:770-8.
- [235] Blagosklonny MV. p53 from complexity to simplicity: mutant p53 stabilization, gain-of-function, and dominant-negative effect. *FASEB J* 2000;14:1901-7.
- [236] Kawauchi K, Araki K, Tobiume K, Tanaka N. Loss of p53 enhances catalytic activity of IKKbeta through O-linked beta-N-acetyl glucosamine modification. *Proc Natl Acad Sci U S A* 2009;106:3431-6.
- [237] O'Mahony A, Lin X, Geleziunas R, Greene WC. Activation of the heterodimeric IkkappaB kinase alpha (IKKalpha)-IKKbeta complex is directional: IKKalpha regulates IKKbeta under both basal and stimulated conditions. *Mol Cell Biol* 2000;20:1170-8.

- [238] Yamamoto Y, Yin MJ, Gaynor RB. IkappaB kinase alpha (IKKalpha) regulation of IKKbeta kinase activity. *Mol Cell Biol* 2000;20:3655-66.
- [239] Wang J, Zhou JY, Wu GS. ERK-dependent MKP-1-mediated cisplatin resistance in human ovarian cancer cells. *Cancer Res* 2007;67:11933-41.
- [240] Wang J, Zhou JY, Wu GS. Bim protein degradation contributes to Cisplatin resistance. *J Biol Chem* 2011;286:22384-92.
- [241] Chen H, Zhu G, Li Y, Padia RN, Dong Z, Pan ZK, et al. Extracellular signal-regulated kinase signaling pathway regulates breast cancer cell migration by maintaining slug expression. *Cancer Res* 2009;69:9228-35.
- [242] Renault VM, Thekkat PU, Hoang KL, White JL, Brady CA, Kenzelmann Broz D, et al. The pro-longevity gene FoxO3 is a direct target of the p53 tumor suppressor. *Oncogene* 2011;30:3207-21.
- [243] Motta MC, Divecha N, Lemieux M, Kamel C, Chen D, Gu W, et al. Mammalian SIRT1 represses forkhead transcription factors. *Cell* 2004;116:551-63.
- [244] Liang XJ, Finkel T, Shen DW, Yin JJ, Aszalos A, Gottesman MM. SIRT1 contributes in part to cisplatin resistance in cancer cells by altering mitochondrial metabolism. *Mol Cancer Res* 2008;6:1499-506.
- [245] Nemoto S, Fergusson MM, Finkel T. Nutrient availability regulates SIRT1 through a forkhead-dependent pathway. *Science* 2004;306:2105-8.

APPENDIX A

Chemicals and media (in alphabetical order)

Name of Chemical	Supplier Company	Catalog #
2-Mercaptoethanol	Fluka, Switzerland	63700
Acetic acid	Sigma, Germany	27225
Acetone	Sigma, Germany	179124
Acrylamide/Bis-acrylamide	Sigma, Germany	A3699
Acrylamide/Bis-acrylamide	Biorad, USA	161-0146
Agarose	Sigma, Germany,	A5093
Ammonium persulfate	Sigma, Germany	A3678
Ampicillin-Na salt	Serva, Germany	13399
Antibiotic solution	Sigma, Germany	P3539
ATP (Gamma-32P)	Izotop, Hungary	SBP301
Boric acid	Sigma, Germany	B6768
Bradford solution	Biorad, USA	500-0006
BSA	Amresco, USA	0332
BSA	Promega, USA	R396D
Chloroform	Sigma, Germany	C2432
Cisplatin (3,3M)	Bristol Myers Squibb, USA	
Coomassie Brilliant Blue	Merck, Germany	115444
DAPI	Roche, Germany	10236276001
Developer/Replenisher	Agfa, Belgium	G150
Dulbecco's MEM (DMEM)	Pan, Germany	P04-04510
DMSO	Sigma, Germany	D2650
DTT	Sigma, Germany	D9779
EDTA	Riedel-de Haén, Germany	27248
Ethanol	Riedel-de Haén, Germany	32221
Ethidium Bromide	Merck, Germany	OCO28942
Fixer E.O.S.	Agfa, Belgium	EKSSH
Foetal Bovine Serum	Pan, Germany	P30-1902
L-glutamine	Sigma, Germany	G7513

(Appendix A continued)

Name of Chemical	Supplier Company	Catalog #
G-25 sephadex quick spin column	Roche, Germany	11273949001
Glycerol	Riedel-de Haén, Germany	15523
Glycine	Molekula, UK	M10795755
HCl	Merck, Germany	100314
HEPES	Molekula, UK	M55704197
Hyperfilm ECL	Amersham, UK	RPN2114K
IKK inhibitor-II	Calbiochem, USA	401474
Isopropanol	Riedel-de Haén, Germany	24137
Kanamycin-sulfate	Applichem, Germany	A1493
KCl	Amresco, USA	0395
KH ₂ PO ₄	Riedel-de Haén, Germany	04243
KOH	Riedel-de Haén, Germany	06005
Liquid nitrogen	Karbogaz, Turkey	
Luria Agar	Sigma, Germany	L-3147
Luria Broth	Sigma, Germany	L-3022
Methanol	Riedel-de Haén, Germany	24229
3-Methyladenine	Sigma, Germany	M9281
McCoy's 5A	Pan Biotech, Germany	P04-05500
MgCl ₂	Sigma, Germany	M9272
Milk Diluent concentrate	KPL, USA	50-82-00
Na ₂ HPO ₄	Merck, Germany	7558-79-4
NaCl	Duchefa Biochemie, Natherlands	S05205000
NaO ₂ C ₂ H ₃ .3H ₂ O	Riedel-de Haén, Germany	25022
NaOH	Merck, Germany	106462
NaPO ₄ H ₂	Riedel-de Haén, Germany	04269
NP-40	Sigma, Germany	I3021
Paclitaxel/Taxol (7,2mM)	Bristol Myers Squibb, USA	
Paraformaldehyde	Aldrich, Germany	15,812-7
Penicilin/Streptomycin	PAN, Germany	P06-07100

(Appendix A continued)

Name of Chemical	Supplier Company	Catalog #
Phenol	Applichem, Germany	A1153
phoSTOP phosphatase inhibitor	Roche, Germany	4906837001
Pifithrin- α	Sigma, Germany	P4359
PMSF	Sigma, Germany	P7629
Poly dI/dC	Sigma, Germany	P4929
Propidium iodide	Sigma, Germany	P4170
Protease inhibitor cocktail tablet	Roche, Germany	4693124001
Protein G sepharose beads	Sigma, Germany	P3296
PVDF membrane	Roche, Germany	03010040001
Sodium Dodecyl Sulphate	Sigma, Germany	L4390
TEMED	Sigma, Germany	T7024-100ml
Triton X-100	Applichem, Germany	A1388
Tris	Molekula, UK	M11946779
Tween® 20	Molekula, UK	18945167
X-ray Film Biomax MS-1	Sigma, Germany	Z36,305-7
X-ray film	Sigma, Germany	F5388

APPENDIX B

Antibodies and enzymes (in alphabetical order)

Name	Supplier Company	Catalog #
Anti- β -Actin	Sigma, Germany	A1978
Anti-Bad	Cell Signaling, USA	9292
Anti-Bax	Cell Signaling, USA	2772
Anti-Bcl2	Cell Signaling, USA	2872
Anti-Bcl-xl	Cell Signaling, USA	2762
Anti-Bik	Cell Signaling, USA	4592
Anti-Bim	Cell Signaling, USA	2819
Anti-Cleaved Caspase 3	Cell Signaling, USA	9664
Anti-Cleaved Caspase 7	Cell Signaling, USA	9491
Anti-Cleaved Caspase 9	Cell Signaling, USA	9501
Anti-Cleaved PARP	Cell Signaling, USA	5625
Anti-Flag	Sigma, Germany	F3165
Anti-FOXO3	Cell Signaling, USA	9467
Anti-HA	Sigma, Germany	H3663
Anti-p-IKK α/β	Cell Signaling, USA	2678
Anti-I κ B- α	Santa Cruz, USA	sc847
Anti-p- I κ B- α	Santa Cruz, USA	sc8404
Anti-IKK- β	Cell Signaling, USA	2684
Anti-Lamin A/C	Cell Signaling, USA	2032
Anti-LC3	Cell Signaling, USA	4108
Anti-Mcl-1	Cell Signaling, USA	4572
Anti-mouse HRP	Cell Signaling, USA	7076
Anti-p53	Cell Signaling, USA	9282
Anti-Puma	Cell Signaling, USA	4976
Anti-rabbit HRP	Cell Signaling, USA	7074
Anti-rabbit FITC	Abcam, UK	ab6717
RNase A	Roche, Germany	119915
T4 polynucleotide kinase	Promega, USA	C131A
Trypsin-EDTA	Pan, Germany	P10-0231SP

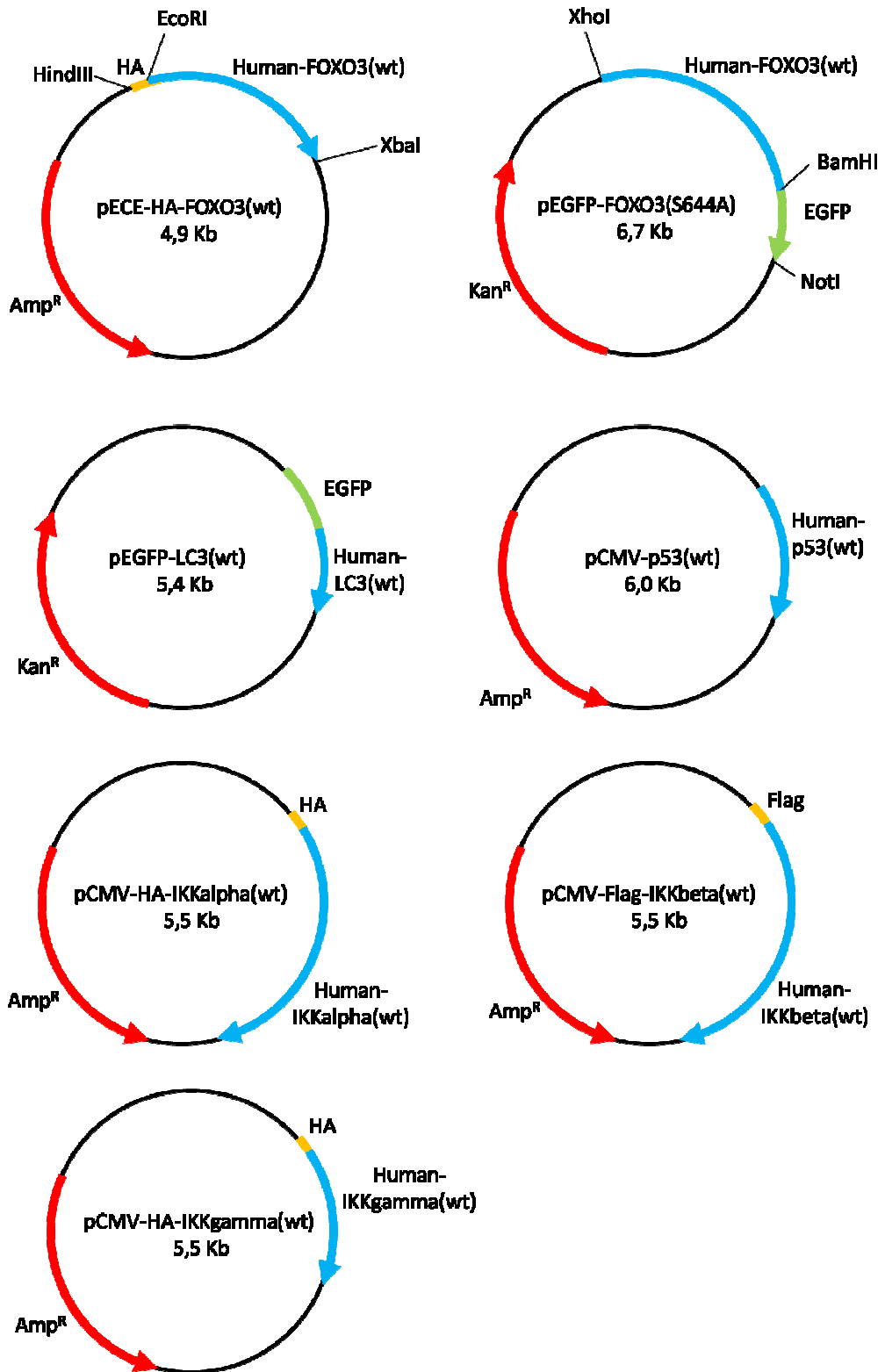
APPENDIX C

Molecular biology kits and reagents (in alphabetical order)

Name	Supplier Company	Catalog #
AnnexinV-FITC	Alexis, USA	ALX-209-250
ECL Advance	Amersham,UK	RPN2209
Fugene6 Transfection reagent	Roche, Germany	11814443001
Genopure plasmid midi kit	Roche, Germany	03143414001
Hiperfect transfection reagent	Qiagen, Netherlands	301705
Hs_FOXO3A_1_HP siRNA	Qiagen, Netherlands	SI00421092
Laemmli 2X sample buffer	Sigma, Germany	S3401-10VL
Metafectene-easy	Biontex, Germany	T090
MTT (Cell Proliferation Kit I)	Roche, Germany	11485007001
Negative Control siRNA	Qiagen, Netherlands	1027280
PageRuller plus, protein ladder	Fermentas, Lithuania	SM1812
Quantitech RT Kit	Qiagen, Netherlands	205311
Quantitech SYBRgreen Kit	Qiagen, Netherlands	204143
Sensiscript RT	Qiagen, Netherlands	1010892
T4 DNA kinase Kit	Promega, USA	M4103
Taq PCR Master Mix Kit	Qiagen, Netherlands	201443
Trizol	Invitrogen, USA	15596-018

APPENDIX D

Expression vectors



APPENDIX E

Oligonucleotides (Synthesized in IDT, Belgium)

GADD45 α F: 5'-ATA ACT GTC GGC GTG TAC GAG G

GADD45 α R: 5'-GTT TCT GTA ATC CTT GCA TCA GCG

GAPDH F: 5'-CAC CCA TGG CAA ATT CCA TG

GAPDH R: 5'-TCT AGA CGG CAG GTC AGG T

IGFBP1 F: 5'-ATT GCT AGC AAG CAA AAC AAA CCG CTA GCT TA

IGFBP2 R: 5'-TAA GCT AGC GGT TTG TTT TGC TTG CTA GCA AT

APPENDIX F

Buffers and solutions (in alphabetical order)

Annealing buffer

100mM KAcetate
30mM HEPES (pH: 7,4)
2mM MgAcetate

Annexin-V staining buffer

100µl cell suspension in FACS incubation buffer
2µl Annexin-V (Alexis)

Blocking solution

5g nonfat dried milk
100ml washing solution

Complete lysis buffer

20 mM Tris-HCl (pH 7.5)
150mM NaCl
NP-40 0.5% (v/v)
1 mM EDTA
0.5 mM PMSF
1 mM DTT
Protease and phosphatase inhibitor mix

DAPI stock solution (1000X)

10mg DAPI
10ml ddH₂O
Store at -20°C

DAPI working solution (1X)

1µl DAPI stock solution (1000X)
1ml Methanol (Store at +4°C up to 6 months)

(Appendix F continued)

EMSA binding buffer (5X)

100mM HEPES-KOH (pH: 7,9)

5mM EDTA (pH 7,9)

25% (v/v) glycerol

25mM MgCl₂

0,5M KCl

10mM DTT (Freshly added)

EMSA incubation buffer (20µl/sample)

4µl EMSA binding buffer

1 µl NP-40

3,45 µl Glycerol (87%)

1 µl BSA (stock: 1mg/ml)

1,5 µl poly dI-dC-poly dI-dC (stock: 1µg/µl)

1 µl radiolabelled oligonucleotide (from 1:20 dilution of column-purified 50 µl elute)

Add 5-8 µg nuclear protein and adjust to 20 µl

FACS incubation buffer

10mM HEPES

140mM NaCl

2,5mM CaCl₂

pH: 7,4

Immunoblotting washing solution

100ml PBS (10X)

900ml ddH₂O

2ml Tween20 (final: 0,2%)

(Appendix F continued)

Non-denaturing 6% polyacrylamide gel

24 ml of H₂O

10ml of 1x TBE

6ml of 40%acrylamide:1% bisacrylamide

280 µl of 10% APS (w/v)

36 µl TEMED

Oligonucleotide labeling reaction mix

10,25 µl of dH₂O

15 µl of oligonucleotide (final: 26,25pmol, stock: 1,75pmol/µl)

5 µl of T₄ kinase buffer (10X)

15,75 µl of γ -³²P-dATP (3000 Ci/mmol) (final: 52,5 pmol 170 µCi)

4 µl of T₄ polynucleotide kinase (final: 20U, stock: 5U/µl)

10 minutes at 37°C

Paraformaldehyde fixation (stock solution)

0,4 g of paraformaldehyde

8 ml of ddH₂O

5 µl of 1M NaOH

Heat to 70°C mix frequently until complete solubilization (~10 min at 70°C)

Cool down to room temperature (on ice)

Adjust volume to 9 ml with ddH₂O

Add 1 ml of PBS 10X and mix.

Filter solution using a 0.2 µm filter.

Paraformaldehyde fixation (working solution)

Prepare a 2% paraformaldehyde solution by diluting 4% paraformaldehyde solution in PBS. Use the fixative at room temperature

Primary antibody incubation solution

2ml 5% (w/v) milk blocking solution and 1µg primary antibody

(Appendix F continued)

Propidium iodide staining buffer

1mg Propidium iodide

60 µl Triton-X100

Adjust volume to 10 ml with PBS

Add 10µl Rnase A (stock: 10mG/ml) for each 1ml

Running buffer (10X)

144,1g glycine

30,3g Tris

10g SDS

Adjust to 1000ml with ddH₂O

Secondary antibody incubation solution

5ml 5% (w/v) milk blocking solution

1µg secondary antibody

T1 Buffer

10 mM HEPES-KOH (pH: 7,9)

2 mM MgCl₂.6H₂O

0,1 mM EDTA

10 mM KCl

1% NP-40

1 mM DTT (freshly added)

0,5 mM PMSF (freshly added)

Complete protease inhibitors (freshly added)

T2 Buffer

50 mM HEPES-KOH (pH: 7,9)

2 mM MgCl₂.6H₂O

0,1 mM EDTA

50 mM KCl

(Appendix F continued)

400mM NaCl

10% (v/v) Glycerol

1 mM DTT (freshly added)

0,5 mM PMSF (freshly added)

Complete protease inhibitors (freshly added)

TBE (10X)

108g Tris

55g Boric acid

40ml EDTA (pH:8.0)

Transfer buffer (stock: 10X)

144 g glycine

30.3 g Tris

Adjust to 1000ml with ddH₂O

Transfer buffer (working: 1X)

100ml Transfer buffer (10X)

700ml ddH₂O

200ml Methanol

APPENDIX G

Equipments

<i>Autoclave:</i>	Hirayama, Hiclave HV-110, Japan Certoclav, Table Top Autoclave CV -EL-12L, Austria
<i>Balance:</i>	Sartorius, BP211D, Germany Sartorius, BP221S, Germany Sartorius, BP610, Germany Schimadzu, Libror EB-3200 HU, Japan
<i>Centrifuge:</i>	Eppendorf, 5415C, Germany Eppendorf, 5415D, Germany Eppendorf, 5415R, Germany Kendro Lab. Prod., Heraeus Multifuge 3L, Germany Hitachi, Sorvall RC5C Plus, USA Hitachi, Sorvall Discovery 100 SE, USA
<i>Computer Software:</i>	FlowJo 7.2.5 Image J 1.42q Photoshop CS5 Irfanview 4.20 Quantity One 4.6.1 MS Office 2007
<i>Deepfreezer:</i>	-80°C, Kendro Lab. Prod., Heraeus Hfu486 Basic, Germany -20°C, Bosch, Turkey
<i>Distilled water:</i>	Millipore, MilliQ Academic, France
<i>Electrophoresis:</i>	Biogen Inc., USA V20-CDC Scie-plas, UK
<i>Flow cytometer:</i>	BD FACS Conto, USA
<i>Geiger counter:</i>	TAEK, Turkey
<i>Gel Drier:</i>	EC355, E-C Aparatus, USA
<i>Gel Analyzer:</i>	Las-4000 mini, Luminescent image analyzer, Fujifilm, Tokyo Universal Hood II, Gel Imager, Biorad, USA
<i>Ice Machine:</i>	Scotsman Inc., AF20, USA

(Appendix G continued)

<i>Incubator:</i>	Memmert Modell 300 and 600, Germany
<i>Laminar Flow:</i>	Kendro Lab. Prod., Heraeus, HeraSafe HS12, Germany
<i>Magnetic Stirrer:</i>	VELP Scientifica, ARE Heating Magnetic Stirrer, Italy
<i>Microliter Pipette:</i>	Gilson, Pipetman, France Mettler Toledo Volumate, USA Eppendorf, Germany
<i>Microscope:</i>	Olympus BX60 Olympus IX70
<i>pH meter:</i>	WTW, pH540 GLP MultiCal, Germany
<i>Power supply:</i>	Biorad, PowerPac 300, USA Wealtec, Elite 300, USA
<i>Refrigerator:</i>	4°C, Bosch, Turkey
<i>Shakers/ mixers:</i>	Forma Scientific, Orbital Shaker 4520, USA GFL Shaker 3011, USA New Brunswick Sci., Innova 4330, USA C25HC Incubator shaker, New Brunswick Scientific, USA Gyro rocker SSL3, Stuart, UK Thermomixer comfort, Eppendorf, Germany
<i>Spectrophotometer:</i>	Schimidzu UV-1208, Japan Scimidzu UV-3510, Japan ND-1000, Nanodrop, USA
<i>Thermocycler:</i>	iCycler Thermal cycler, Biorad, USA Eppendorf, Mastercycler Gradient, Germany
<i>Water bath:</i>	Huber, Polystat cc1, Germany